UNIVERSITY OF GENOVA

POLYTECHNIC SCHOOL
DIME
Department of Mechanical, Energy, Management and Transportation Engineering

MASTER OF SCIENCE THESIS
IN
MECHANICAL ENGINEERING

Study of the behaviour of ozone for Gasoline Compression Ignition Engine application

Supervisors:

Prof. Alessandro Bottaro
Prof. Fabrice Foucher

Co-supervisor:

Ing. Pietro Pinazzi

Candidates:

Stefano Macrì
Andrea Canevello

October 2016

Dedico questo lavoro
alla memoria di mia madre
nella speranza che possa gioirne con me,
Stefano

Contents

Sommario **viii**

Introduction **1**

1 Theoretical Background **3**
1.1 Internal combustion engines 3
1.2 Overview of the main engine parameters 7

2 Study of GCI Engine with UA=120°C Injector **8**
2.1 Experimental Set-up 8
2.2 Results 13
2.2.1 Single injection 13
2.2.2 Double injection 17
2.2.3 Comparison between single injection and double injection 21
2.3 GCI engines challenges 26

3 Study of ozone decomposition **27**
3.1 Ozone Theoretical Background 27
3.1.1 Definition and applications 27
3.1.2 Ozone Production 28
3.2 Objectives 30
3.3 Experimental set-up 31
3.3.1 O3-Injector Configuration 35
3.3.2 Test section insulation 40
3.3.3 Nitric oxide addition 41
3.4 Results and discussion 43
3.4.1 Experimental Results 43
3.4.2 Simulation Results 47
3.4.3 Simulation vs. Experimental 51

4 Ozone seeding in a GCI engine **54**
4.1 Experimenal set-up 54
4.2 Low Load Operation 56
4.3 Idle condition 62

5 Conclusions **64**

Bibliography **67**

Glossary **71**

List of Tables **72**

List of Figures **75**

Studio del comportamento dell'ozono per l'applicazione in motori ad accensione per compressione alimentati a benzina

Sommario

Questo lavoro si propone di studiare un approccio innovativo alla riduzione del consumo di carburante e conseguentemente delle emissioni di CO_2 nei motori a combustione interna. La strategia adottata per perseguire questo obiettivo è l'applicazione di ozono nel condotto di aspirazione di un motore ad accensione per compressione alimentato a benzina. Nella prima parte sono state investigate le potenzialità ed i limiti di questo tipo di motori, dopodiché l'attenzione si è spostata sullo studio, sia sperimentale che simulativo, del comportamento dell'ozono e della sua interazione con il monossido di azoto ed infine, sono stati verificati gli effetti dell'ozono sulla combustione in un motore GCI. L'ozono si è dimostrato un forte agente ossidante e promotore della combustione e per questo può considerarsi una soluzione interessante al fine di ridurre il consumo di combustibile dei tradizionali motori a combustione interna. Questa tesi ha inoltre evidenziato la presenza di alcuni aspetti tecnici tuttora da risolvere, riguardanti la compattezza dei produttori di ozono, la sua interazione con altre specie presenti nell'EGR, la produzione a partire dall'aria e l'ottimizzazione di vari parametri motoristici.

Study of the behaviour of ozone for gasoline compression igniton engines application

Abstract

This work aimed to study an innovative approach to reduce fuel consumption in internal combustion engines and consequently reduce CO_2 emissions. The strategy chosen to pursue this goal was the application ozone at the intake manifold of a gasoline compression ignition engine. At first the potential and limits of a GCI engine were investigated, after that the focus moved to the study, both experimental and simulative, of ozone behaviour and interaction with nitric oxide and lastly ozone seeding was applied to the intake manifold of a GCI engine in order to verify its effect. Ozone was proved to be a strong oxidizing agent and combustion promoter and thus it could be a interesting solution to reduce the fuel consumption of traditional internal combustion engines. This work also highlighted the presence of some technical issues that need to be solved, such as the compactness of ozone generators, the interaction of other EGR species with ozone, the production of this oxidizing specie from air and the optimization of various engine parameters.

Ringraziamenti

Ringraziamo innanzitutto i nostri relatori, il professor Alessandro Bottaro e il professor Fabrice Foucher. Il primo per averci offerto l'opportunità di effettuare questo tirocinio presso il *Laboratoire PRISME* e per il costante e proficuo sostegno umano e accademico, il secondo per l'accoglienza riservataci e le competenze trasmesse. Un sentito ringraziamento va inoltre a tutti i membri del laboratorio, in primis il nostro correlatore Ing. P. Pinazzi, i tecnici del gruppo *ECM*: Bruno Moreau, Julien Lemaire, Yahia Haidous; infine, ultimi ma non per importanza: Ida, Florian, Marco, Francesco, Jean-Baptiste, Ton, Ob, Medhi, Ricardo. Ricorderemo con molto piacere i sette mesi trascorsi assieme.

Stefano
Desidero ringraziare per primo il mio compagno di avventura (e tesi) Andrea per aver superato insieme i, non cosi rari, momenti di pressione e tensione dovuti alla grossa mole di lavoro svolta e all'ambientazione in un contesto nuovo. Tengo particolarmente a ringraziare la mia famiglia per essermi stata accanto in questi anni turbolenti sotto molti aspetti e, in particolar modo, per aver vissuto in maniera positiva e propositiva il periodo di lontananza per la tesi. Un grazie molto sentito va a Marta per aver affrontato questi anni assieme a me e per essere stata di grande aiuto e supporto durante il periodo a Orléans. La sua positività ha contribuito, e non poco, a farmi vivere appieno la bella esperienza in Francia. Un grazie sincero va anche a Simone per esserci sempre stato nonostante l'evolvere degli eventi l'abbia talvolta reso più difficile. Impossibile infine dimenticarsi di: Davide, Geo (l'unico coraggioso venuto a Orléans), Marco, Picca, Scusa, Giugno, Filippo, Ianneo e tutti quelli che ho tralasciato per i bei momenti trascorsi insieme in questi anni.

Andrea
Questa è per me forse la parte pi difficile della tesi, nonostante ci penso non sarebbe giusto saltarla poichè sono davvero grato a tutte le persone che sto per citare. Per prima cosa desidero ringraziare Stefano, per aver deciso di imbarcarsi in questa avventura con me e per la sincerità che mi ha sempre dimostrato in questi anni di amicizia. Un enorme grazie va a Martina, per avermi sostenuto ed aiutato durante questi mesi lontani, questa esperienza ci ha reso pi forti che mai e ciò mi rende davvero molto felice. Desidero inoltre ringraziare la mia famiglia che mi ha sempre sostenuto, incoraggiato e trasmettendomi i suoi valori mi ha aiutato ad essere la persona che sono. Infine voglio esprimere la mia gratitudine verso tutti gli amici che mi hanno accompagnato lungo il mio percorso: Greg, Virtu, Ali, Miki, Marco, Matte, Picca, Geo e Quelli della Domenica. Grazie per tutti i momenti, positivi o difficili, che abbiamo passato insieme.

Acknowledgements

First of all we would like to thank our supervisors, Professor Alessandro Bottaro and Professor Fabrice Foucher. The former for having offered us the opportunity to attend this traineeship at the *Laboratoire PRISME*, and for the constant and profitable human and academic support, the latter for the kind welcome and the transmitted knowledges. An heartfelt thank you goes to the members of the Lab., firstly our co-supervisor Eng. P. Pinazzi, the technical staff of the *ECM* group: Bruno Moreau, Julien Lemaire, Yahia Haidous; last but not least, we want to thank: Ida, Florian, Marco, Francesco, Jean-Baptiste, Ton, Ob, Medhi, Ricardo. We'll remember with pleasure the seven month spent together.

Stefano
First of all I would like to thank my wingman and co-worker Andrea for having faced together the, not so uncommon, pressure and tension moments due to the high amount of work and to the setting in a new contest. I want particularly to thank my family to be there during this turbulent, under several side, years and for having passed these months of distance in a profitable and proactive way. An heartfelt thank you goes to Marta for having faced these year next to me and for having been a great help and support during the period in Orléans. Her positivity concurred, and not few, to fully enjoy my good experience in France. A sincere thanks goes to Simone to be always there despite the turn of events has sometimes made it more difficult. It's impossible at the end forget of: Davide, Geo (the brave one who came to Orléans), Marco, Picca, Scusa, Giugno, Filippo, Ianneo and all the one I left out, for the good time spent together in these years.

Andrea
For me this is perhaps the most difficult part of this work, nevertheless I think it would be unfair to skip it because I am really grateful to the people I am about to mention. First off, I would like to thank Stefano, for deciding to dive into this adventure with me and for the honesty he has always shown during our friendship. A huge thank you goes to Martina, she supported and helped me during this months apart. This experience strengthen us and this makes me truly happy. I also wish to thank my family that has always supported me, encouraged me and helped me become who I am by transmitting its values. In the end, I want to express my gratitude towards every friend that shared my path: Greg, Virtu, Ali, Miki, Marco, Matte, Picca, Geo e Quelli della Domenica. Thank you all for every moment, both positive and difficult, that we spent together.

Sommario

L'obiettivo più importante, in materia di sostenibilità ambientale è sicuramente la riduzione delle emissioni di CO_2 su scala mondiale. Ovviamente questo proposito coinvolge ogni aspetto dell'attività umana, concentrandosi sul settore dei trasporti ed in particolare sull'industria dell'autoveicolo, è possibile fare dei passi avanti in questo senso migliorando l'aerodinamica dei veicoli, riducendo le loro masse, abbattendo gli attriti tra manto stradale e pneumatici ed infine elevando l'efficienza dei motori.
Al giorno d'oggi sul mercato coesistono principalmente due tipi di motori a combustione interna: motori ad accensione comandata e motori ad accensione per compressione; questi ultimi presentano efficienze sicuramente maggiori ma anche costi più elevati ed hanno lo svantaggio di essere alimentati a gasolio o suoi surrogati, che risultano essere decisamente meno diffusi a livello globale rispetto alla benzina. Sarebbe quindi molto vantaggioso sviluppare un motore in grado di possedere le elevate efficienze tipiche del motore ad accensione per compressione ma con alimentazione a benzina; in questo senso la ricerca si è mossa in varie direzioni, tra cui quella del motore GCI (gasoline compression ignition) dove appunto la miscela aria-benzina non viene più accesa con l'ausilio della scintilla fornita dalla candela, ma bensì attraverso il raggiungimento di condizioni termodinamiche tali da permetterne l'autoaccensione.
Non si tratta di un compito facile in quanto questo combustibile presenta fra le sue caratteristiche principali un'elevata resistenza all'autoaccensione. Per sormontare questo ostacolo sono state sviluppate diverse soluzioni, ad esempio l'adozione di sistemi di distribuzione avanzati con fasatura variabile accoppiati a sistemi di sovralimentazione a geometria variabile. Tale soluzione comporta però un livello di complessità molto elevato, come si può evincere dalla letteratura [31] [33] [30] [32] [4], ed inoltre un costo notevole.
Un'altra soluzione percorribile potrebbe essere un motore GCI con combustione assistita da ozono, per questo motivo il presente studio sperimentale è composto da una prima parte dove il motore GCI viene testato senza l'ausilio di alcun sistema (VVT, turbosovralimentazione, ozono) al fine di comprenderne i limiti, successivamente si passa ad un'indagine sul comportamento dell'ozono al di fuori del motore, per poi infine applicare un generatore di ozono al condotto di aspirazione di un motore GCI allo scopo di studiarne gli effetti sulla combustione.

La prima parte del lavoro è stata dedicata alla sperimentazione al banco motore ed in particolar modo allo studio della combustione in un motore GCI. Poiché altri esperimenti portati avanti nel *Laboratiore PRISME* [28] mostrano un confronto tra due iniettori con diverso "angolo di ombrello" (UA), 90° e 156°, al fine di valutare la miglior soluzione per il funzionamento GCI, si è deciso di studiare un terzo iniettore con UA 120°.

Viene presentato per prima cosa il setup sperimentale adottato per lo studio della combustione GCI con iniettore con UA 120°, la descrizione del motore impiegato, del sistema di controllo e di quello di raccolta dei dati.

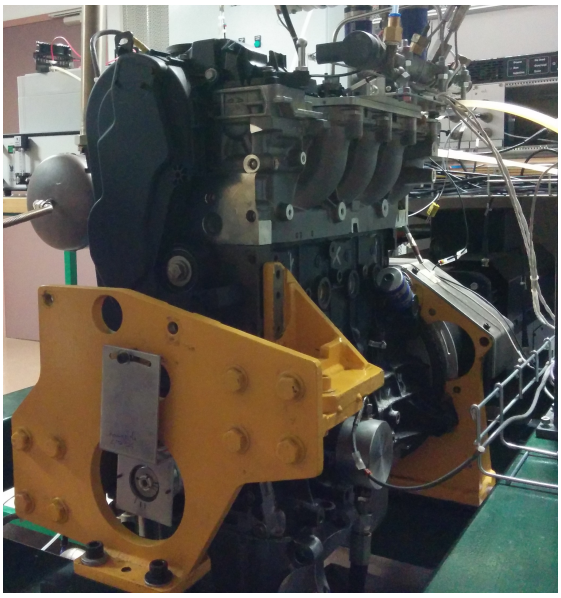

Figure 1: *Peugeot DW-10.*

Successivamente si passa all'analisi dei risultati ottenuti attuando una panoramica dei possibili momenti di iniezione, con una strategia a singola iniezione e portata di combustibile costante, in particolare le condizioni sono riportate nella tabella sottostante.

Table 1: *Condizioni operative con singola iniezione.*

	Media	Deviazione Standard	RSD
Velocità	1500[rpm]		
P ammissione	1[bar]		
Portata Combustibile	0.3403$[kg/h]$	0.0023	0.67
Ricchezza Brettsinger	0.291	0.0085	2.92%
T ammissione	206.12°C	0.3182	0.154%

Nello specifico, osservando il grafico relativo all'efficienza di combustione in funzione del momento di iniezione (SOI), si può notare l'esistenza di un intervallo di SOI nel quale si ottiene un'elevata efficienza di combustione. L'estremo inferiore di questo intervallo probabilmente legato all'Umbrella Angle ed è anche per questo motivo che la scelta è ricaduta sull'iniettore con 120° di UA che risulta essere un buon compromesso tra le due soluzioni precedentemente citate. Per quanto riguarda l'estremo superiore invece, il limite è dato dal sopraggiungere della condizione di misfire dovuta principalmente alle caratteristiche di propensità all'accensione del combustibile, avendo mantenuto costante il rapporto di compressione.

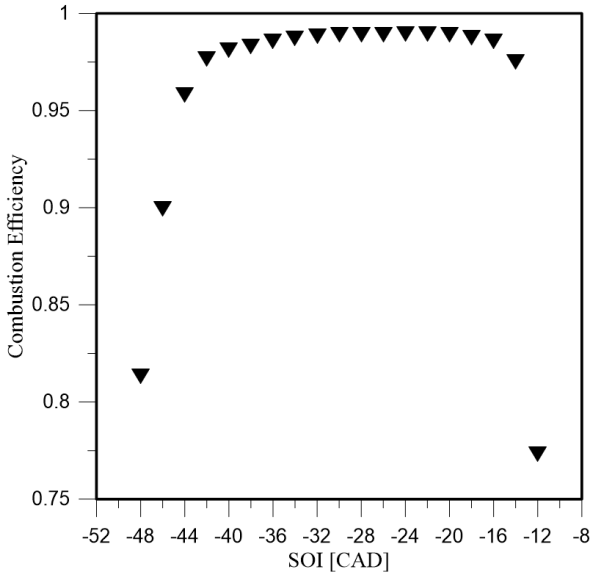

Figure 2: *Efficienza di combustione con singola iniezione.*

Un altro importante parametro da considerare è il massimo gradiente di pressione all'interno del cilindro, infatti, come si può vedere dalla figura sottostante, si raggiungono livelli tali da superare gli standard commerciali in termini di comfort di bordo e vibrazioni.

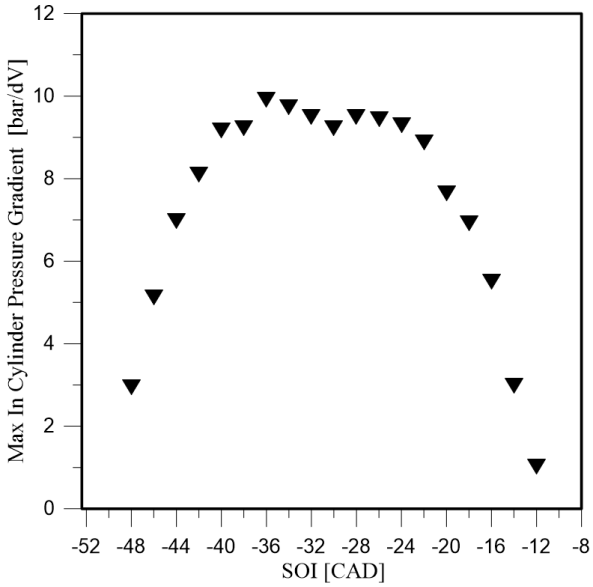

Figure 3: *Massimo gradiente di pressione all'interno del cilindro con singola iniezione.*

All'interno del Capitolo 2 si può trovare l'analisi di altri importanti parametri, come il CA50, la durata di combustione e le emissioni inquinanti, tuttavia già dai parametri elencati in questo breve sommario, si evince la necessità di passare allo studio di una strategia con doppia iniezione. In questo modo è possibile ridurre i gradienti di pressione all'interno del cilindro ottenendo quindi una combustione più graduale.

Per svolgere l'indagine sulla doppia iniezione è stata adottata la strategia riportata in Tab. 2, con un'equa ripartizione della massa di combustibile iniettata nei due momenti di iniezione.

Table 2: *Condizioni operative con doppia iniezione.*

	Mean	Standard deviation	RSD
Speed	1500[rpm]		
P admission	1[bar]		
Fuel mass (50%SOI1 - 50%SOI2)	0.344$[kg/h]$	0.001629	0.47%
Brettsinger Equivalence ratio	0.2996	0.002918	0.97%
T admission	204.6°C	0.2545	0.12%

Anche in questo caso è stata eseguita una panoramica dei vari momenti di iniezione seguendo la mappa riportata in Tab.3; fissato l'istante di inizio della prima iniezione, si è valutata l'influenza dell'istante della seconda iniezione sui vari parametri operativi.

Table 3: *Mappa della strategia di iniezione.*

SOI2 [CAD]

SOI1 [CAD]	-35	-30	-25	-20	-15	-10	-5	0
-45	•	•	•	•	•	•	•	•
-40	•	•	•	•	•	•	•	•
-35		•	•	•	•	•	•	•
-30			•	•	•	•	•	•
-25				•	•	•	•	•
-20					•	•	•	•

Adottando questa strategia l'efficienza di combustione rimane elevata ed in particolare cresce ritardando la prima iniezione, questo fenomeno può essere dovuto all'interazione tra spray di combustibile e cielo del pistone, infatti anticipando eccessivamente la prima iniezione si rischia di colpire le pareti del cilindro.

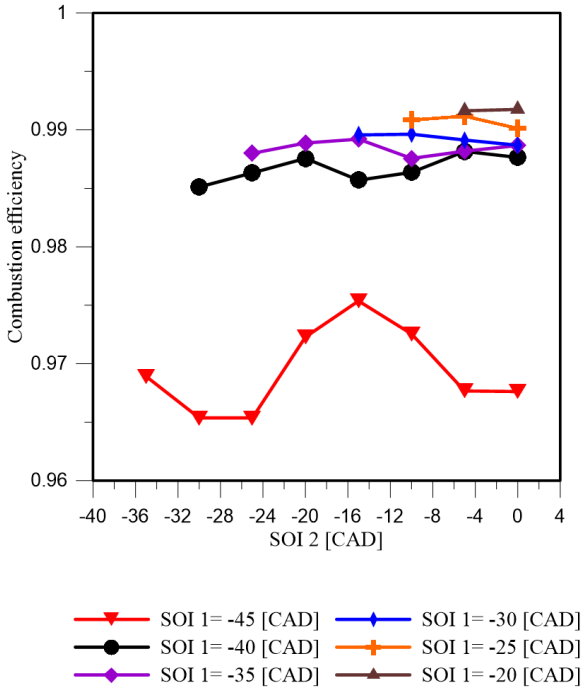

Figure 4: *Efficienza di combustione con doppia iniezione.*

Sebbene i risultati ottenuti in questa fase siano promettenti, si sono evidenziati alcuni limiti da superare per una futura applicazione di questa tecnologia. Uno di questi è rappresentato dalla necessità, ai bassi carichi, di creare le condizioni per l'autoaccensione del combustibile, ciò può essere perseguito attraverso le soluzioni citate nella parte iniziale. In questo lavoro viene approfondita la metodologia che si avvale dell'ozono come promotore della combustione. È stato quindi deciso di sviluppare un setup sperimentale che permettesse lo studio del comportamento dell'ozono in condizioni tali da replicare quelle del condotto di aspirazione del motore. Si è scelto di utilizzare come sezione di prova un tubo di acciaio munito di otto predisposizioni per la misura della concentrazione di ozono, lo si è dotato di un sistema di riscaldamento elettrico e di coibentazione per mantenere constante la temperatura inoltre, per evitare problemi di parziale miscelazione tra il flusso proveniente dal produttore di ozono ed il flusso principale, è stato progettato un apposito iniettore, Fig 5.

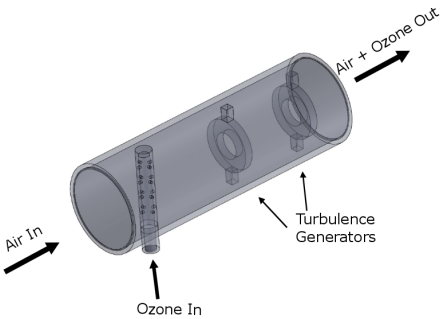

Figure 5: *Iniettore di ozono.*

Per poter studiare anche l'interazione con specie presenti nel condotto di aspirazione a causa dell'attuazione di strategie di ricircolo dei gas di scarico (EGR), è stato messo a punto un sistema di controllo per l'aggiunta di monossido di azoto. Questa è soltanto una delle specie tipicamente presenti nei gas esausti e lo studio dell'interazione con altre, ad esempio monossido di carbonio ed acqua, viene proposto come futuro sviluppo di questa analisi. Nelle figure sottostanti vengono mostrati lo schema ed una foto del setup sperimentale definitivo.

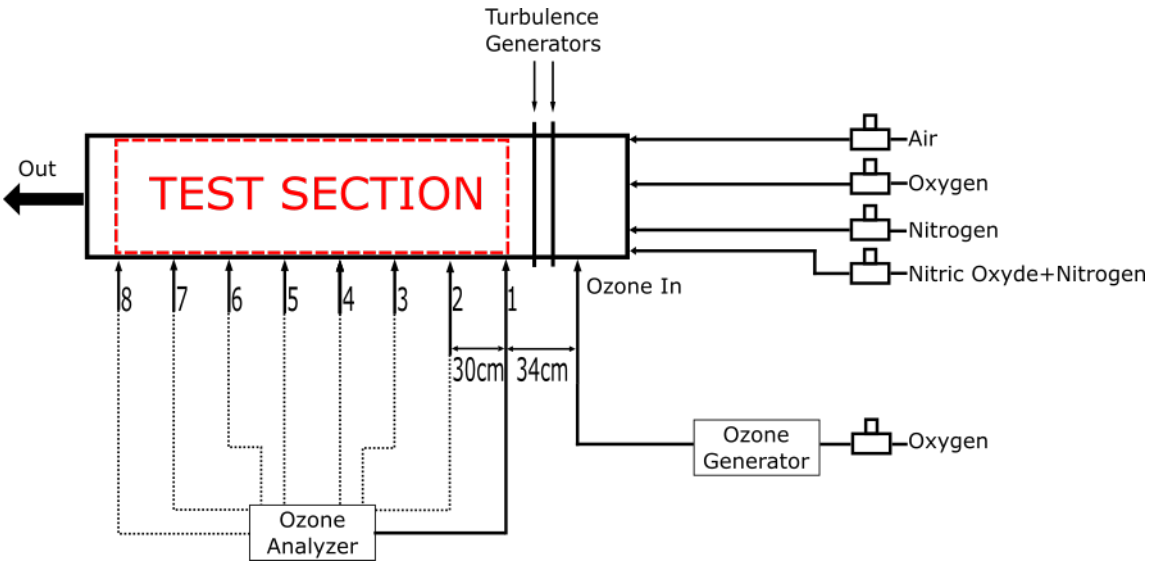

Figure 6: *Schema del setup sperimentale definitivo.*

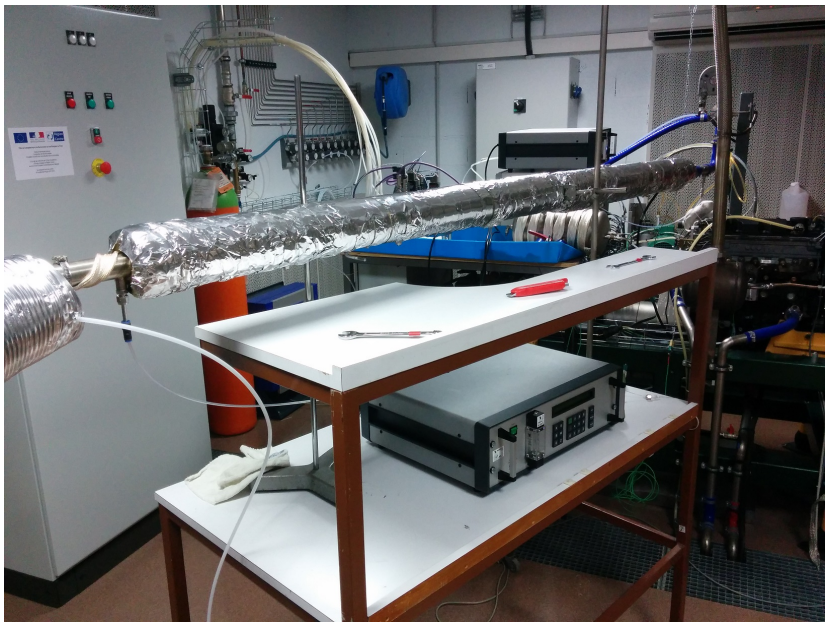

Figure 7: *Setup sperimentale.*

È stata quindi eseguita una campagna sperimentale con diverse temperature e diverse concentrazioni iniziali di NO, mentre la quantità iniziale di ozono è rimasta invariata, è stato definito il rapporto NO/O_3 come discriminante tra le varie prove. Inoltre, al fine di verificare i risultati ottenuti ed ampliare la finestra temporale di osservazione, sono state effettuate una serie di simulazioni con il software Senkin.

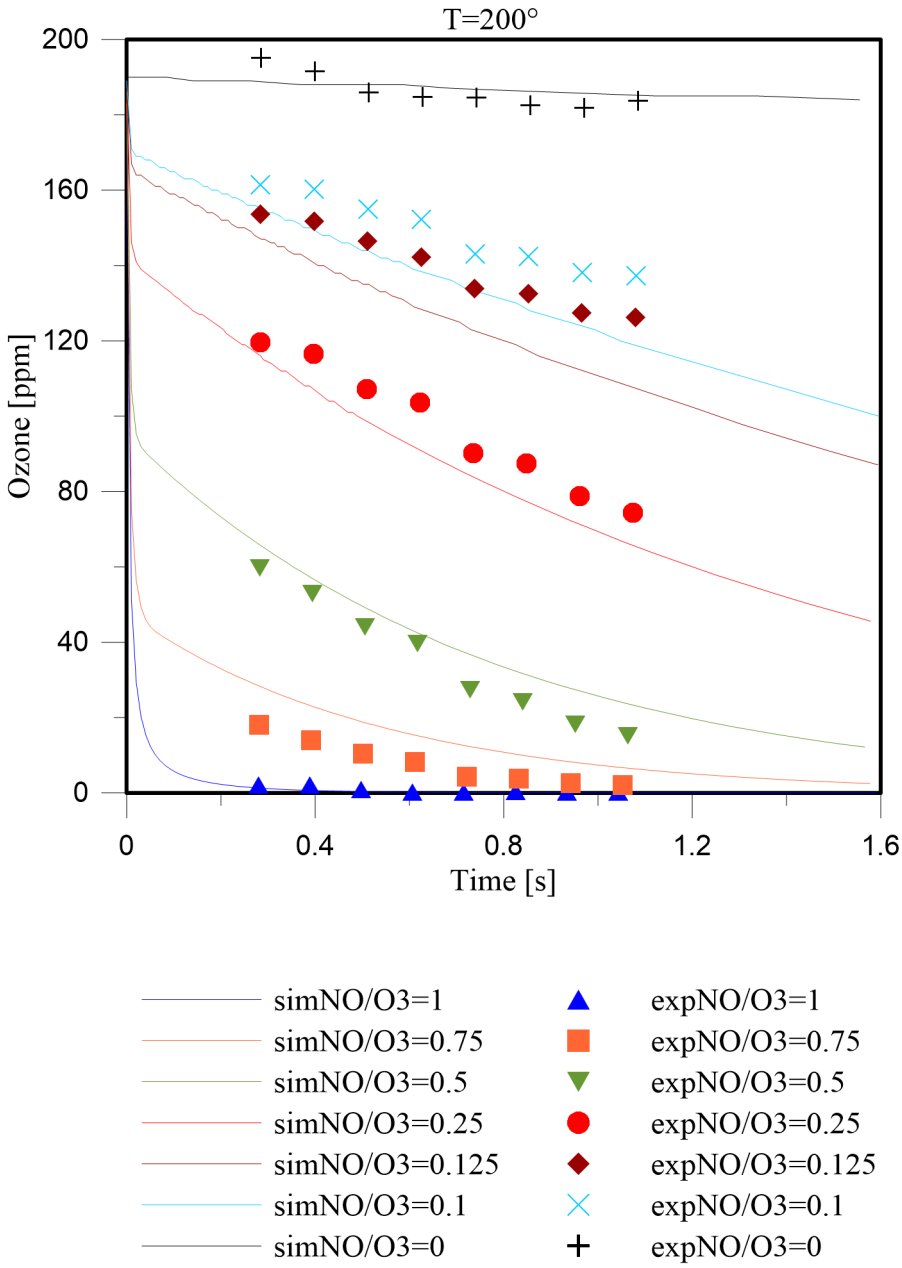

Figure 8: *Confronto tra simulazioni e risultati sperimentali, a* $T = 200\ °C$.

Dalla Fig. 8 si può notare la compatibilità tra i trend dei punti sperimentali e delle curve relative alle simulazioni, tuttavia la sovrapposizione non è perfetta probabilmente a causa di errori di misura o discrepanze tra il modello di cinetica chimica usato nelle simulazioni e la realtà.
Con $T = 200\ °C$ è possibile apprezzare sia la decomposizione dell'ozono (pendenza

della curva in assenza di NO) che l'interazione tra monossido di azoto ed ozono. L'istantanea caduta della concentrazione di ozono nei casi con presenza di NO è imputabile all'interazione tra le due specie ed essendo molto rapida è un fattore da considerare nel caso di applicazione dell'ozono in motori con strategia EGR.

Dopo gli studi separati su motore GCI ed ozono, si è deciso di sovrapporre i due argomenti nell'applicazione di quattro generatori di ozono al condotto di aspirazione del motore GCI. Lo scopo di quest'indagine è stato quello di determinare la quantità di ozono necessaria per ottenere una combustione stabile, prima a bassi carichi variando la temperatura di aspirazione e successivamente, in condizioni di autosostentamento con la minor temperatura usata nel caso precedente.
Infatti, essendo già nota in letteratura la capacità dell'ozono di agire come promotore della combustione, è stata fissata una strategia a doppia iniezione e si è agito in regolazione sulla quantità di ozono necessaria per ottenere una combustione con CA 50 di 6 CAD, a diverse temperature. La strategia sperimentale è stata studiata in modo da evitare il riscaldamento dell'aria in ingresso da parte delle pareti del cilindro e inoltre sono stati ripetuti i punti relativi alla parte superiore della curva al fine di verificare l'attendibilità della strategia scelta. I risultati in Fig.9 mostrano come sia possibile ottenere una combustione stabile con $T = 40\ °C$ e meno di 400 ppm di ozono, l'altro estremo della curva mostra che la minor temperatura alla quale è stato possibile bruciare senza l'aggiunta di ozono è stata $T = 150\ °C$, tuttavia in questo punto si è in presenza di un processo avente un CA 50 di 3 CAD, che risulta quindi anticipato rispetto a quello precedentemente fissato.

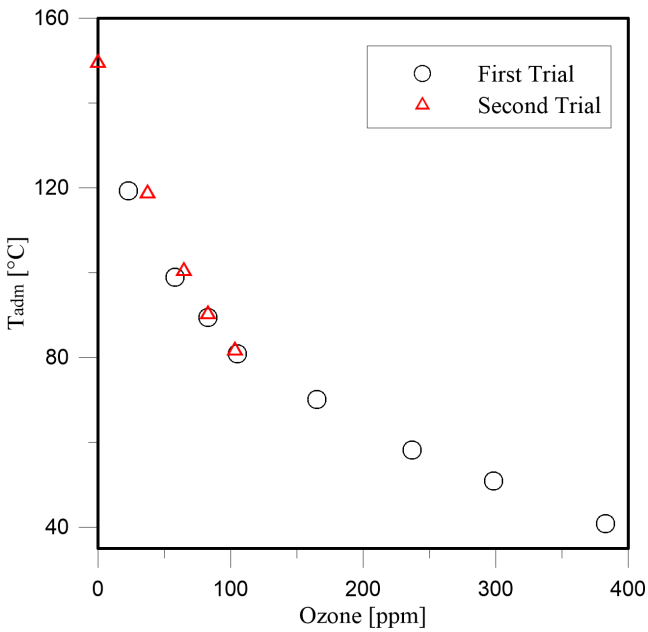

Figure 9: *Grafico ozono-temperatura di aspirazione ai bassi carichi.*

Per quanto riguarda le prove in regime di autosostentamento, è stata fissata la temperatura di aspirazione a $T = 40\ °C$ mentre è stata variata la quantità di ozono. Sono state adottate due strategie a singola iniezione, una a punto morto inferiore e una a punto morto superiore per riprodurre le condizioni di HCCI. Utilizzando la prima

strategia si ha una carica meno omogenea e quini vi è meno tempo a disposizione dell'ozono per interagire con il combustibile, ciò è in accordo con i dati relativi alla concentrazione di ozono, che risulta più alta a parità di CA 50 rispetto al caso di tipo HCCI.

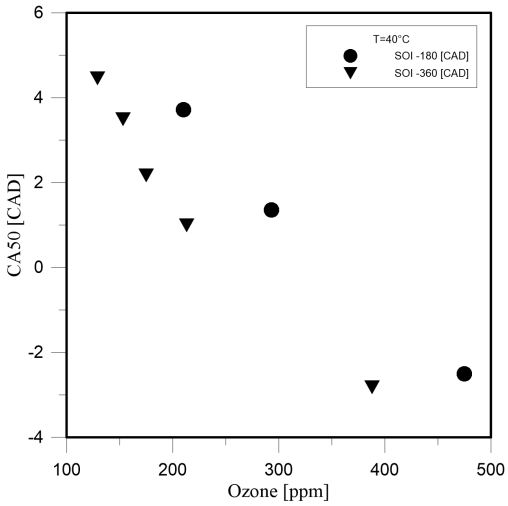

Figure 10: *Influenza dell'ozono sul CA 50, in condizione di autosostentamento.*

Alla luce dei risultati ottenuti nel corso dell'intero lavoro, si riscontra la praticabilità di questa soluzione tecnologica per ridurre il consumo di combustibile nei motori a combustione interna e di conseguenza le emissioni di CO_2. Nonostante ciò, sussistono ancora diversi aspetti tecnici che devono essere affrontati, come l'ingombro dei produttori di ozono, la sua interazione con altre specie presenti nell'EGR, la sua produzione a partire dall'aria e l'ottimizzazione di vari parametri motoristici. Per quanto riguarda la produzione di ozono, una soluzione può essere rappresentata da un prototipo che il *Laboratorio PRISME* sta sviluppando, questa soluzione si propone di risolvere sia i problemi di ingombro sia quelli di produzione a partire dall'aria, ma necessita di alcune ottimizzazioni dal punto di vista dell'affidabilità e della quantità di ozono prodotta.

Figure 11: *Prototipo di generatore di ozono.*

Introduction

The most important aim in matter of environmental sustainability is to reduce global CO_2 production. This is a problem that involves all kind of human activity, as shown in Fig.12, regarding the transportation sector and in particular the automotive industry, it is possible to reach this goal with different approaches such as improving the vehicle aerodynamics, reducing the masses and the wheels rolling resistance and enhance the engine efficiency.

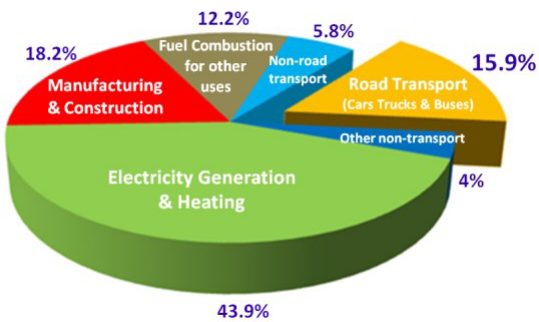

Figure 12: *CO2 production.[OICA]*

Nowadays on the global market coexist two main internal combustion engine solutions that differ for the method used to ignite the fuel: compression ignition (CI) and spark ignition (SI) . The CI engines are more efficient than SI engines but their cost is much higher, moreover diesel and its surrogate are largely less diffused than gasoline fuels as shown in Fig.14.

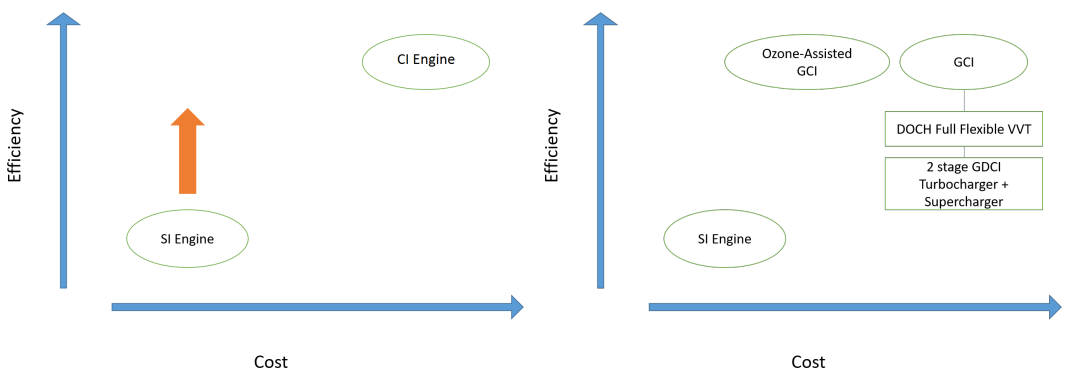

Figure 13: *Comparison between cost and efficiency*

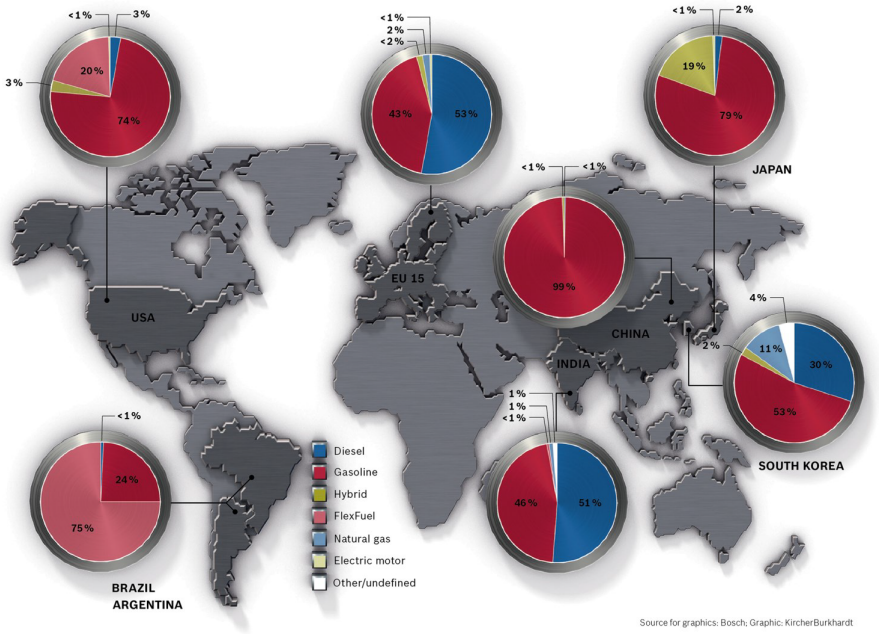

Figure 14: *Distribution of fuels across the world.[Bosch Graphics]*

According to the global rate of diffusion of gasoline, it could be useful develop an engine fuelled with gasoline but with higher efficiency than SI engine, in order to go down this path there are several studies on "gasoline compression ignition" engine (GCI). Briefly GCI engines are CI engines that work with gasoline fuels, a better explanation will be done in the next chapter. Using GCI engine permit to reach an efficiency reasonably comparable with the one of CI engine, one solution is to have GCI engine with DOHC Full flexible VVT and two stage turbocharger + supercharger ([31] [33] [30] [32] [4]) but this configuration increases the cost; an other less expensive strategy (see Fig.13) could consists in Ozone-assisted GCI. With the latter solution it is possible to substitute VVT technology and turbochargers with an ozone producer in order to enhance combustion with ozone seeding. This work starts with the study of a GCI engine without ozone seeding, variable valve train technology and turbocharger in order to understand the limits of GCI operation. After this phase it was decided to move on the study of the ozone behaviour out of the engine and then to come back on engine, but with ozone addition.

Chapter 1

Theoretical Background

1.1 Internal combustion engines

To better evaluate this work it is useful to have a general overview of some engine aspects. There are several way to classify internal combustion engines, two of that are: by $fuel$ and by $method\,of\,ignition$. Starting from the ignition, there are mainly two ways to ignite fuel in an internal combustion engine:

- Spark ignition (SI)
- Compression ignition (CI)

In the SI engine the combustion process consists in the ignition of a fuel-air mixture triggered by an electrical discharge in the combustion chamber at the and of the compression stroke. To ensure the stoichiometric combustion the equivalence ratio must be kept as constant as possible at about 1, this to allow a proper work of the three-way catalyst. The appropriate mixture in the past was provided by a carburetor, nowadays the solutions are fuel injection into the intake manifold or direct injection in the cylinder. A feature of SI engines is to operate with a well-mixed charge before the ignition, then to start the combustion is necessary a trigger actuated from the spark. The combustion is quite slow and progressive and so it's important to determine the right timing of the spark for each operative condition. Since the flame propagates spherically, in this kind of engine the fuel taking part to the combustion is not constant but it increases with the cube of the distance from the trigger point and thus it is necessary to advance the timing of the spark in order to exploit all the expansion stroke. Regarding the regulation in the SI engine, the load variation depends on the amount of mixed charge, so to increase load it is necessary an higher amount of charge in the combustion chamber keeping constant the equivalence ratio through an appropriate control system.
Regarding the pollutants emissions of the SI engines, they generally consist of carbon monoxide (CO), unburned hydrocarbon (HC) and Nitric oxides (NO_x). CO emission is mainly due to the fact that the oxidation from carbon to carbon monoxide is faster than the one from carbon monoxide to carbon dioxide, while HC formation is a consequence of a partial hydrocarbon combustion generally due to wall quenching and inhomogeneity of distribution of the charge that leads to region in which combustion

doesn't occur due to low temperature or wrong equivalence ratio [5].
As concerns NO_x emissions they are not due to the quality of the combustion, but related to the combustion process. A relevant role in the formation of nitric oxides is played by the peak temperature reached during the combustion, in fact in the atmosphere nitrogen an oxygen coexist without reacting. So in SI engines the NO_x formation is related to the hight temperature in the flame propagation zone.
In order to reduce emissions and respect pollutant requirements the equivalence ratio of the fuel is kept close to stoichiometric, thus it is possible to use the three-way catalyst to post-treat the exhaust gases. In Fig.1.1 are shown the emission of the SI engine before the post-treatment system, the ECU actuates an oscillation between slightly lean charge, CO and HC oxidation, and slightly rich charge where NO_x are reduced to N_2 and O_2.

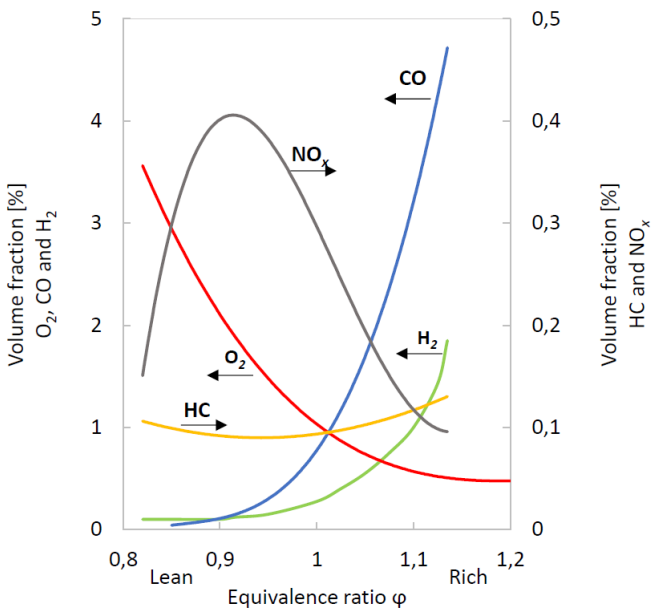

Figure 1.1: *Typical emissions from SI engines as a function of the equivalence ratio.* [21]

In CI engines the ignition of the fuel is due to the high temperature reached by air in the compression stroke, the fuel is injected in the combustion chamber and then it ignites. This kind of combustion is not progressive, as in SI engines, but it is diffusive. Due to the fact that the air fuel mixing occurs after the injection, there won't be an homogeneous distribution of the fuel in the combustion chamber at the start of the combustion process. The combustion starts at first on the edge of the spray and then spreads around the combustion chamber.
In order to enhance autoignition the compression ratio is usually kept around 16 and so CI engines can reach high efficiencies, also thanks to the lean global equivalence ratio (0.7 in average). Regarding the emissions, the principal pollutants emitted by CI engines are generally nitric oxides (NO_x), carbon monoxide (CO), soot and unburned hydrocarbons (HC). As concerns to formation of the pollutants it is the same seen in SI engine and moreover there is soot caused by the competition between pyrolysis

and oxidation reactions during the combustion, in Fig.1.2 it is possible to observe the various zones of formation of the pollutant emissions.
Focusing on the classification of the engines by fuel, until few years ago there were two

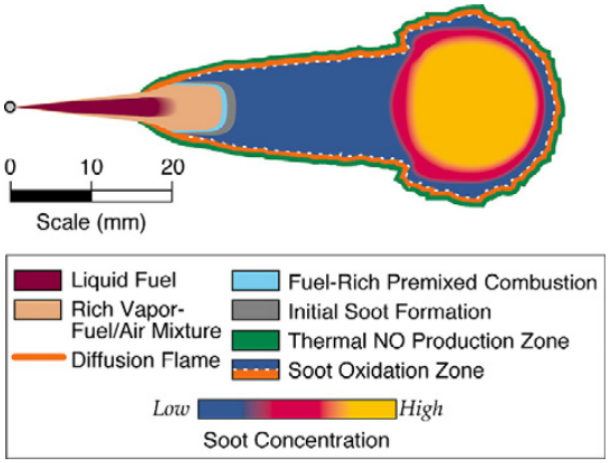

Figure 1.2: *Conceptual schematics of conventional CI conbustion.*[7]

main fuels related to the two main engines classes: gasoline for SI engines and diesel for CI engines. Nowadays there are several alternatives fuel for either of them, but as in this work the only fuel used is gasoline, it was chosen not to perform an overview about fuels.
As previously explained, the internal combustion engines are commonly classified in two main groups depending on combustion methods: CI and SI, but there are also other kind of combustion processes. In the last few years the stricter requirements in term of emissions had led research center to an higher attention on innovative combustion process, such as:

- *Homogeneous Charge Compression Ignition* (HCCI)
- *Reactivity Controlled Compression Ignition* (RCCI)
- *Partially Premixed Compression Ignition* (PPCI)
- ...

The combustion processes listed before are given as example, this isn't an exhaustive list of all the combustion methods applicable to internal combustion engines. Without trying to engage in an in-depth discussion about these processes, the aim of $HCCI$ is to obtain the combustion of an homogeneous charge that auto-ignites at certain condition of temperature and pressure, in this way it is possible to have a fairly homogeneous combustion of all the charge and high efficiency, that lead to low emission in NOx and particulate; however this kind of combustion is violent and can't be controlled easily. It is possible to actuate $HCCI$ combustion both with Gasoline and Diesel. $RCCI$ is a new method of combustion that relies on the different reactivity (i.e. octane number or cetane number) of the fuels injected to control the autoignition; normally a low-reactivity fuel is injected with a port-injection system, while an high-reactivity one

is injected directly in the combustion chamber in order to operate a control on the combustion. As concerns to $PPCI$, in this case only a part of the charge is premixed, in order to control combustion with the injection timing and, as in the other combustion methods, with an accurate EGR strategy if necessary to control pressure rise rate and noise.[21]

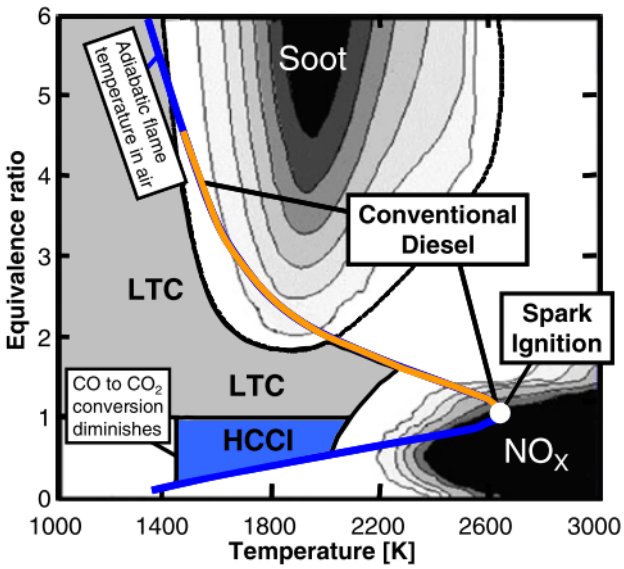

Figure 1.3: *Diagram showing the equivalence ratio-temperature ranges for soot and NO_x formation and the regions for conventional diesel, SI, HCCI, and diesel LTC engines.*[8]

The objectives of all this kind of combustions applied on internal combustion engines are to reduce both fuel consumption (by increasing efficiency) and pollutant emissions. In Fig1.3 [8] it is possible to observe that emissions are related to the local equivalence ratio and the local temperature as previously mentioned.
Regarding the conventional Diesel combustion region of the graph is easily noticeable that it crosses the regions favorable both for soot and NO_x production, in term of temperature an local equivalence ratio respectively. On the other hand $HCCI$ combustion in the diagram doesn't cross the soot production region and marginally crosses the NO_x region, because of low temperatures and no rich zones, soot and NO_x are avoided.
In this work it was chosen to study the *Gasoline Compression Ignition Engine* (GCI), the particularity of this engine is to ignite gasoline by compression, in order to do this it was used a commercial Diesel engine, this method differs from $HCCI$ because of the possibility to actuate a control of the combustion through the injection strategy, as generally are applied multiple injection in order to have a stratified charge.

1.2 Overview of the main engine parameters

In this section are provided the definitions of some of the parameters that will be used later to describe and analyze the experimental results. In particular:

- Heat Release Rate: It is the rate at which the combustion releases the energy of the fuel. It can be calculated from in cylinder pressure data, as the energy needed to create the measured pressure.[11]

- Max in cylinder pressure gradient: It is the maximum rate with which the pressure rises in the combustion chamber, it is an indicator of the solicitations that the engine experiences and from this it is possible to understand if the level of noise produced is acceptable.

- CA50, CA10, CA90: It represent the crank angle (CA) in which the 50% of the Heat release occurs, likewise for 10 and 90 per cent. These indicators are useful to understand the combustion phasing and can also be seen as the crank angle in which the given percentage of the fuel that takes part to the combustion has burned. Usually CA10 defines the start of comustion while CA90 its end.

- Indicated Mean Effective Pressure (IMEP): As the name suggest is the mean pressure that has the indicated diagram and can lead to the value of the power when multiplied by the displacement. Two types of IMEP can be distinguished, $IMEP_g$ (Gross) and $IMEP_n$ (Net), in this study the former is in use, thus only the compression and expansion strokes are considered for its calculation. IMEP is also directly connected with the load of the engine.

- Indicated efficiency: Is the real efficiency of converting fuel energy into mechanical work, it is calculated from the measurements of the indicated diagram.

- Combustion efficiency: Represents the ratio between the amount of fuel injected and the amount of fuel that takes part to the combustion, in this work it was calculated from the measured quantity of HC and CO at the exhaust and the equivalence ratio.

Chapter 2

Study of GCI Engine with UA=120°C Injector

Other experiments carried out in *PRISME Laboratory* [28] show a comparison between two injectors with different Umbrella Angle (UA), 90° and 156°, in order to evaluate the better solution for GCI engine only for what concerns the injector, without any adaptation of the bowl geometry. It was thus decided to study a third injector with a 120° UA, to better evaluate the performance of this solution and the following data were used in [27] to perform a comparison between three injectors with different UA.

2.1 Experimental Set-up

The experimental setup needed to perform this work counted a number of vital components both hardware and software.
On the hardware side the most important element is obviously the engine: a Peugeot DW 10-series Diesel adapted for single cylinder operation; its characteristics are presented in Tab.2.1 and below it is shown a scheme of the experimental setup, Fig.2.2.

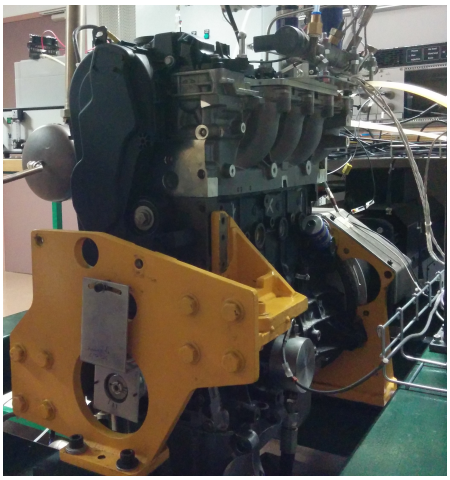

Bore	85 mm
Stroke	88 mm
Rod length	145 mm
Displaced volume	499 cc
Geometric compression	16:1

Figure2.1 & Table2.1: *Peugeot DW 10 and its characteristics.*

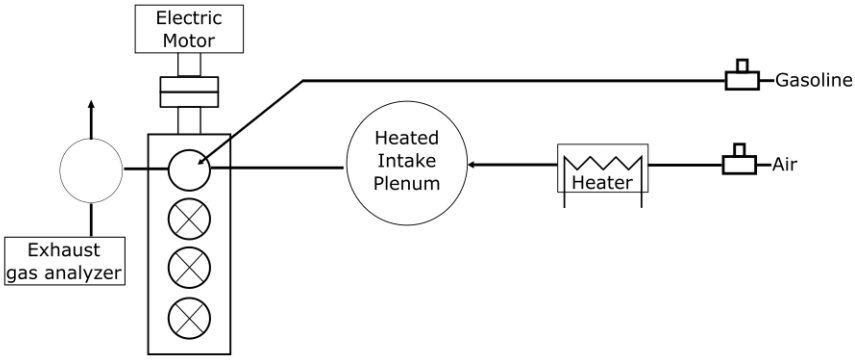

Figure 2.2: *Scheme of the experimental setup.*

The fuel used was commercial 95 RON gasoline and it was provided to the engine at 400 bars via a Diesel common rail system connected to a high pressure pump. All the experiments were executed with a constant rotation speed of 1500 rpm granted by an electric engine. During this work it was tested a *Delphi Diesel Injector* with an Umbrella Angle of 120° and with eight $131\mu m$ diameter holes (Fig.2.3). In order to have a global fuel-air equivalence ratio of 0.3 a constant $7.8mg/cycle$ fuel rate was provided.

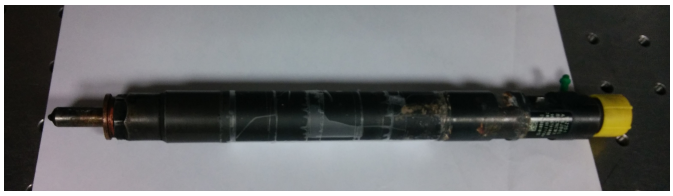

Figure 2.3: *Delphi Diesel Injector.*

The intake pressure was maintained at 1 bar so that it was possible to re-create a situation without turbocharging that corresponds to low load operation. In order to focus the attention on the impact of the injection system it was necessary to avoid the influence of the air management system substituting the VVT systems with electrical heaters so that it was possible to control the thermal content of the intake charge. The intake temperature was kept to 205 $°C$ with electrical heaters for all the experiments. All the fluid flows were controlled by *Brooks* 5800 *series mass flow controllers* which all have an accuracy of ±0.7% on the measure and ±0.2% of the full scale. Dry air was supplied by a compressor and Pollutant emissions at the exhaust were measured by a *Horiba* 7100 *gas analyzer*, Fig.2.4.

Figure 2.4: *Horiba 7100 exhaust gas analyzer.*

On the software side, acquiring the amount of data coming from all the sensors installed on the engine is a very challenging task and thus two computers were necessary, each one with a different LabView configuration; one dealt with the acquisition of signals from the sensors that did not require a fast response (Slow acquisition computer) the other one (Fast acquisition computer) was specifically reserved for the in cylinder pressure sensor since the great quantity of data transmitted in a very short time. In the figures below are reported the LabView interfaces created by the professors and technicians at the PRISME Lab.

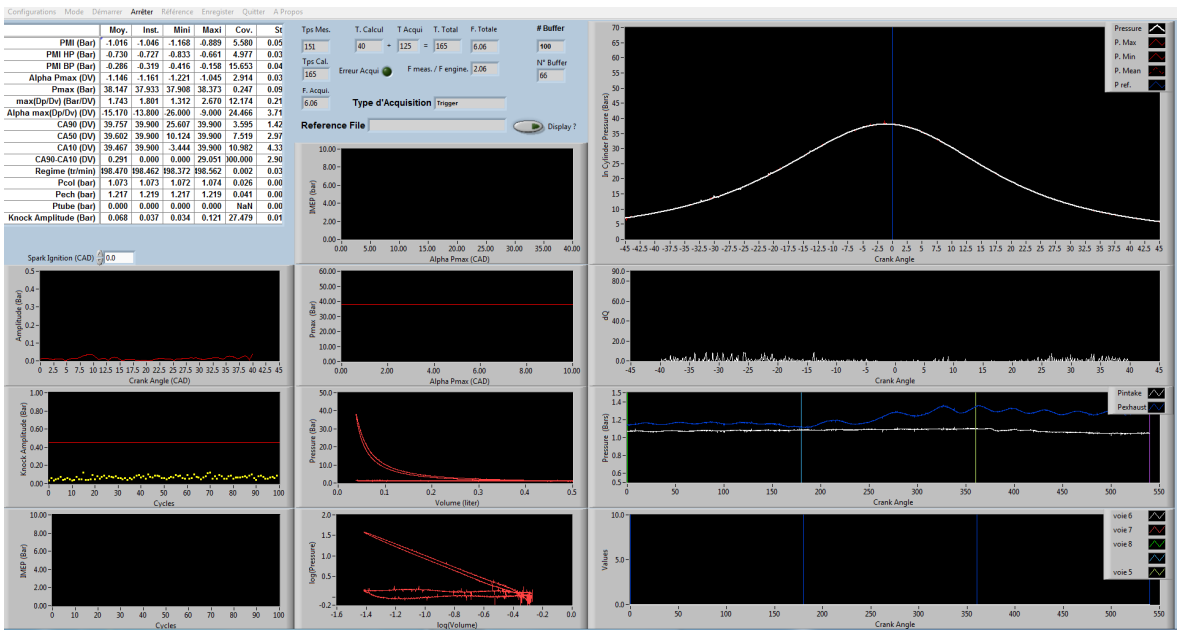

Figure 2.5: *Fast Acquisition interface.*

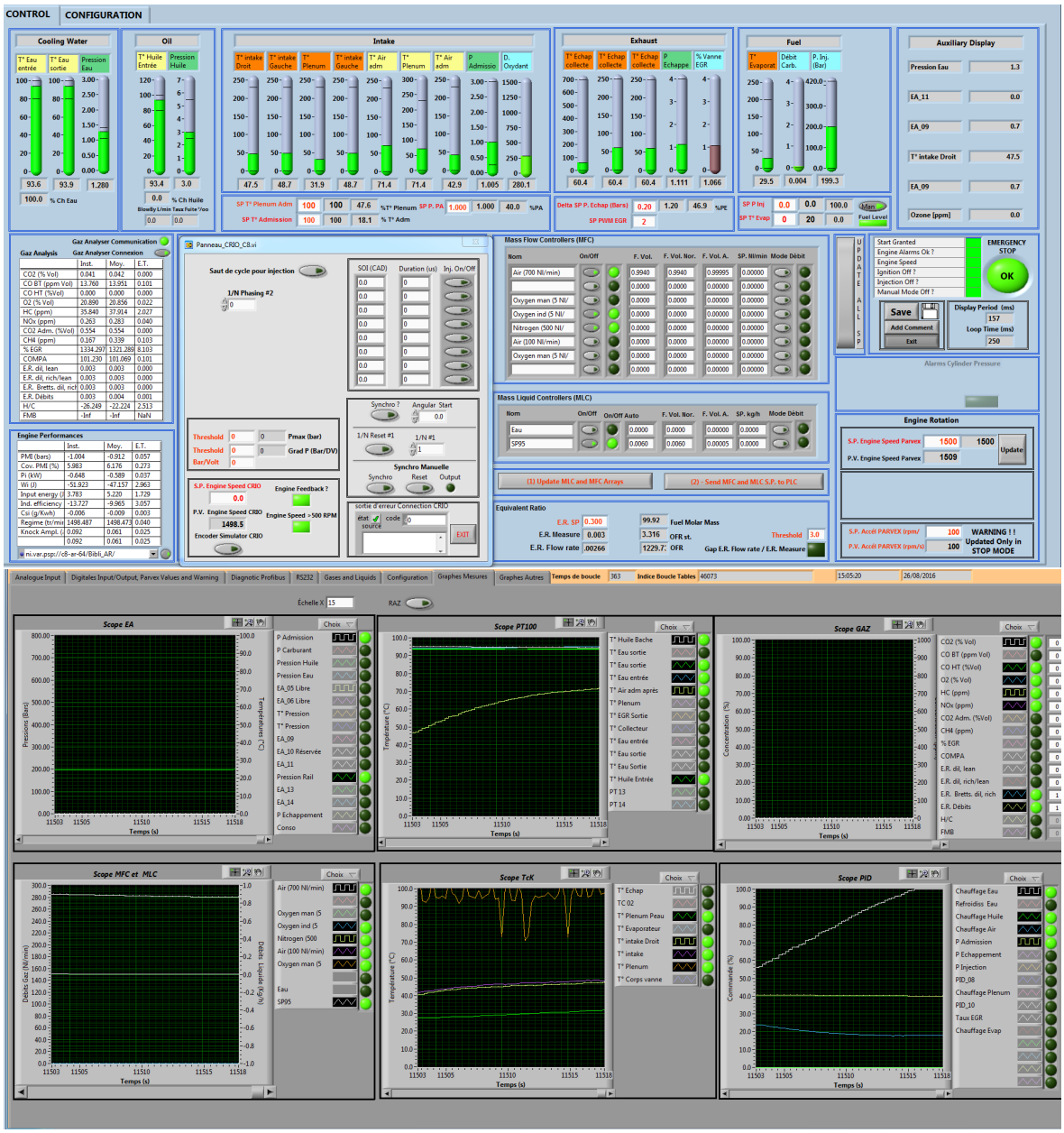

Figure 2.6: *Part of Slow Acquisition interface.*

Another important phase was the development of a standardize engine starting procedure that allowed a safe and easeful warm up for the engine; it consisted of the following steps:

- Turn on ventilation system: essential in order to maintain a healthy environment by expelling the exhaust gases.
- Open bottles of the working gases, if needed.
- Switch on electricity for the working area.
- Open acquisition software on both slow and fast acquisition computers and load configurations.
- Set values for:
  - Rotation speed: 1500 rpm.
  - Intake pressure: 0.7 bar in order to have an easier start for the engine.
  - Exhaust pressure: 1.2 bar in order to overcome the exhaust duct losses.
- Activate circulation pumps and heaters for both lubricant and cooling water; wait until they reach the standard operating temperature before running the engine.
- Turn on Horiba gas analyzer and prepare it for the analysis:
  - Open calibration gas bottles.
  - Set Horiba in Stand-by mode.
  - Follow software procedure: Reset, Purge, Zero, Span, Calibration.
- Switch on electric motor.
- Verify the absence of errors on the acquisition software.
- Start the engine and the fast acquisition to check the in-cylinder pressure.
- Set intake pressure to 1 bar.
- Open fuel line.
- Start the fuel high pressure pump.
- Set rail pressure to 400 bar.
- Set injection parameters: SOI and duration.
- Wait for the engine to warm up.

2.2 Results

In this work were carried out experiments with both single and double injection in order to study the influence of the multiple injection on combustion, mechanical solicitation and noise due to the thermodynamical conditions.

2.2.1 Single injection

As the aim of these experiments is to study the impact of the injection timing on a Gasoline Compression Ignition (GCI) engine, the fuelling rate, intake temperature and pressure were kept constant while the Start of Injection (SOI) was moved from Top Dead Center (TDC) toward earlier injections timings. In Table 2.2 are shown operative conditions.

Table 2.2: *Operative conditions.*

	Mean	Standard deviation	RSD
Speed	1500[rpm]		
P admission	1[bar]		
Fuel mass	0.3403$[kg/h]$	0.0023	0.67
Brettsinger Equivalence ratio	0.291	0.0085	2.92%
T admission	206.12°C	0.3182	0.154%

Moving on to a more detailed analysis of the various parameters observed, it is possible to notice that combustion efficiency, shown in Fig.2.7 as a function of SOI clearly displays a range of admitted SOI for the injector in order to have an high combustion efficiency.

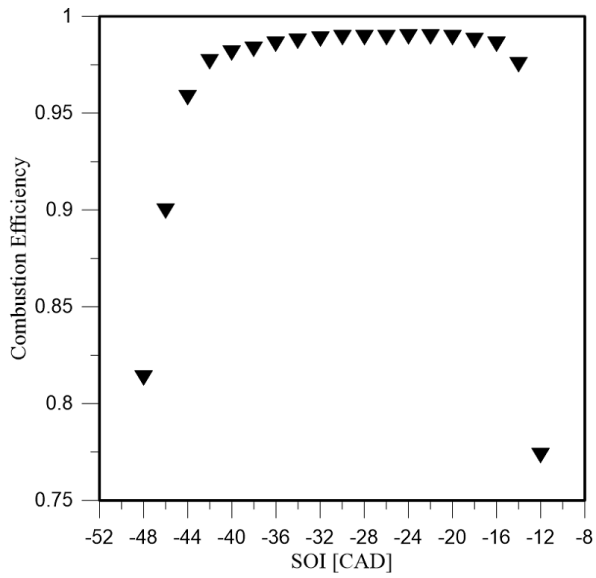

Figure 2.7: *Combustion efficiency with a single injection.*

The early boundary of the SOI range (about -40÷-38 [CAD]) is probably affected by the UA and it is also for this reason that the UA 120° has been chosen for this study (being a fairly wide UA), on the other hand for the later injection, it was noticed that gasoline should be injected at about 20 [CAD] before TDC so that it is possible to avoid misfire and have a stable combustion. This limit is mainly related to the autoignition propensity of the fuel (i.e. octane number) with a fixed compression Ratio (CR).

Focusing on CA50 in Fig.2.8, it has a minimum with SOI -32 [CAD] and this is probably due to the interaction between the fuel spray and the head of the piston, Miles et al. [25] and Aronsson et al.[1] in fact confirm that this phenomenon is very important and that the right targeting of the spray on the piston leads to a lower quantity of fuel in the "squish" region and thus an higher amount of fuel taking part to the combustion, after the end of this effect the CA50 delays.

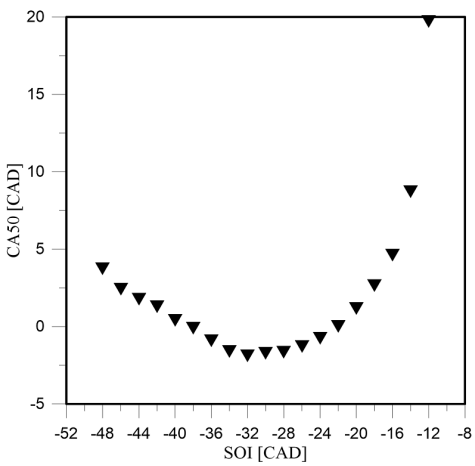

Figure 2.8: *CA50 with a single injection*

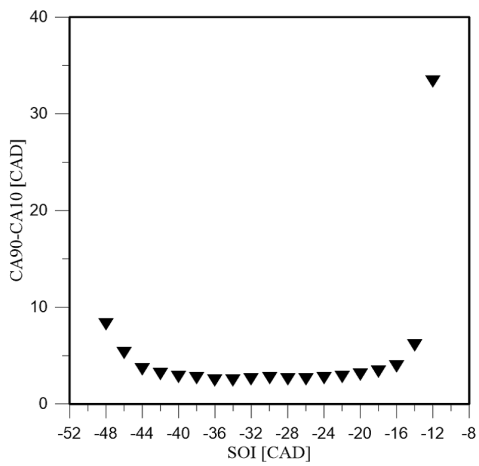

Figure 2.9: *CA90-CA10 with single injection*

As shown in Fig.2.9, the combustion duration, expressed as the CA90 minus the CA10, becomes significantly shorter and stable with SOI -42 [CAD] and above, then it increases as the combustion efficiency drops and there is misfire with SOI -12 [CAD].

Regarding the Indicated Mean Effective Pressure (IMEP) reported in Fig.2.10, it has a minimum for SOI -24 [CAD] due to a more advanced combustion then rises following the CA50 until misfiring; the maximum of IMEP is for SOI -40 [CAD] that corresponds to the point where the CA50 is above zero CAD, this leads to a lower amount of work loss in the attempt of compressing the expanding charge, it is not the only point with these characteristics but probably in the others the interaction between the fuel spray and the head of the piston leads to a lower IMEP. Same goes for the indicated efficiency in Fig.2.11, moreover in other works [27] it was proved that under these conditions the injector with a 120° UA has an high efficiency compared to other injectors with different UA.

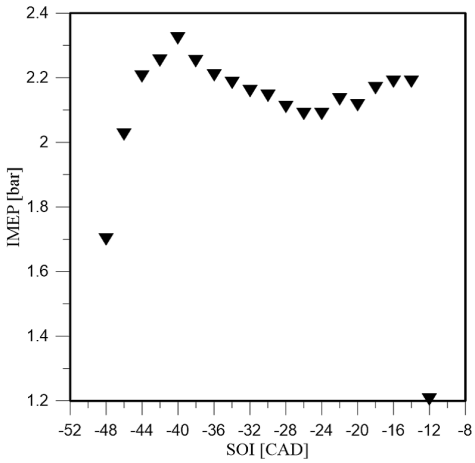

Figure 2.10: *IMEP with a single injection*

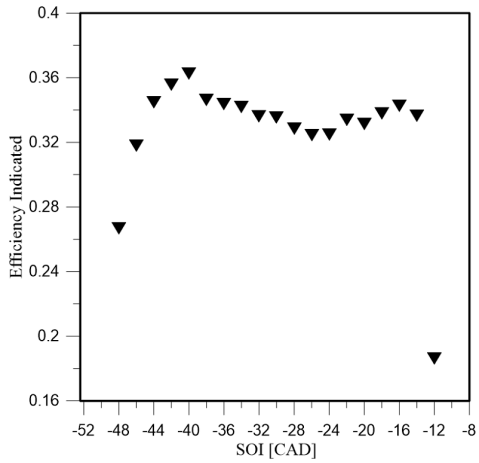

Figure 2.11: *Indicated efficiency with single injection*

The Max In Cylinder Pressure Gradient (Fig.2.12) reaches values of about 10$[bar/dV]$, although this certainly does not create a problem in terms of structural integrity, where the limit is set in about 30$[bar/dV]$, it is not ideal in terms of comfort inside the vehicle as there could be undesired vibrations and noises; this is one of the reasons why it was decided to study a double-injection strategy where the charge is more stratified and the combustion is less isochoric.

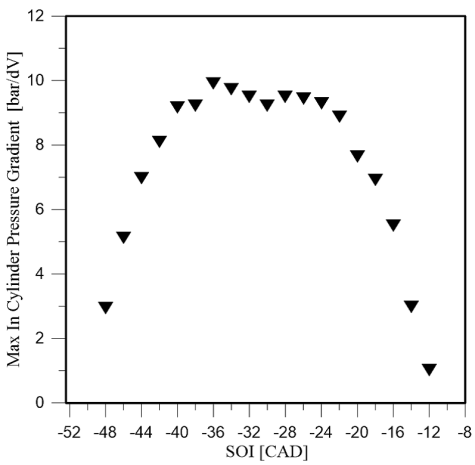

Figure 2.12: *Max in Cylinder pressure rate with a single injection.*

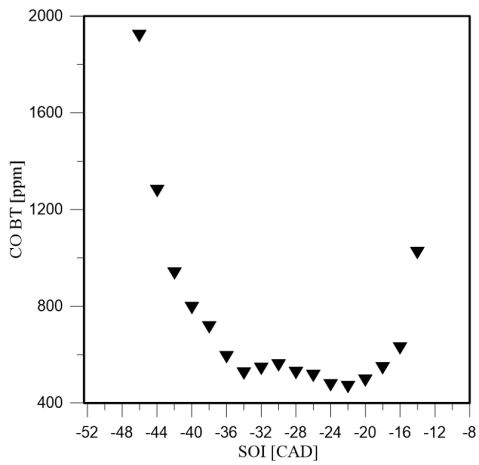

Figure 2.13: *CO emissions with a single injection.*

As seen in chapter 1, the mechanisms of formation of the pollutant are related to the temperature; the emissions found are in line with the trend of the mean in cylinder temperature and show the maximum NO_x (1600 ppm) at SOI -32 [CAD] that is in accordance with the CO and HC concentrations (Figg.2.14,2.15 and 2.13).

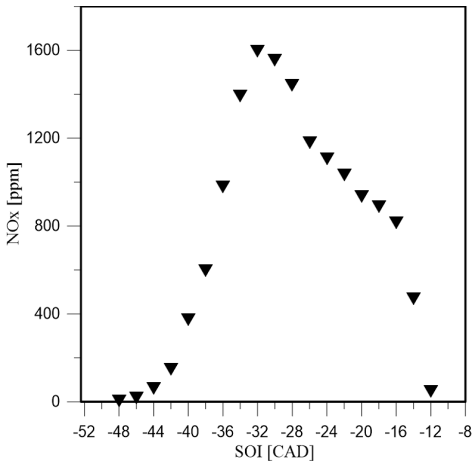

Figure 2.14: *NOx emissions with a single injection.*

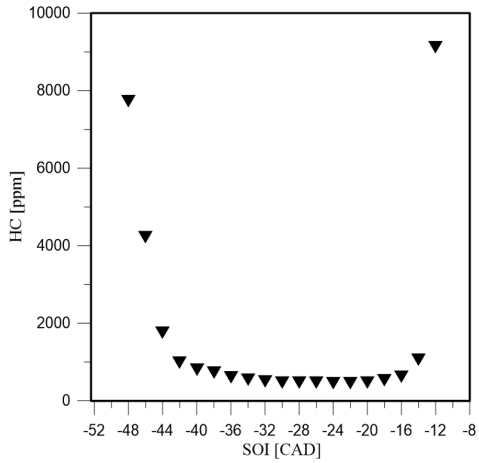

Figure 2.15: *HC emissions with a single injection.*

In order to better evaluate these results some comparison at iso-CA50 were carried out. Comparing SOI -40 [CAD], at which IMEP reaches its maximum, and SOI -22 [CAD], that is approximately iso CA50 but with lower IMEP, it is possible to notice:

- Different emissions (i.e HC and NO_x).
- Same Combustion Duration and same Max Pressure Gradient.
- Combustion Efficiency slightly higher with SOI -22 [CAD].

The differences in HC and CO emissions could be explained with a better "spray-piston" interaction, as previously reported Miles et al. [25] confirm that this can affect the emissions because the amount of fuel actually injected in the cylinder bowl varies. Moreover with SOI -22 [CAD] NO_x emission could be higher as this point presents an higher combustion efficiency. Comparing other two iso-CA50 points such as SOI -36 [CAD] and SOI -24 [CAD], it is possible to appreciate similar tendencies but with smaller gaps, probably due to:

- the fact that the SOIs are less apart in terms of CAD.
- a different influence of the "spray-piston" interaction.

2.2.2 Double injection

As in the single injection case, also in the double injection experiments the intake temperature and pressure were kept constant while the injections varied over a wide range of SOI as shown in Tab. 2.4. The fuelling rate was kept constant maintaining an equal repartition between the two injections. In Tab.2.3 are shown the operative conditions.

Table 2.3: *Double injection operative conditions.*

	Mean	Standard deviation	RSD
Speed	1500[rpm]		
P admission	1[bar]		
Fuel mass (50%SOI1 - 50%SOI2)	0.344[kg/h]	0.001629	0.47%
Brettsinger Equivalence ratio	0.2996	0.002918	0.97%
T admission	204.6°C	0.2545	0.12%

Table 2.4: *Injection strategy.*

SOI1 [CAD] \ SOI2 [CAD]	-35	-30	-25	-20	-15	-10	-5	0
-45	•	•	•	•	•	•	•	•
-40	•	•	•	•	•	•	•	•
-35		•	•	•	•	•	•	•
-30			•	•	•	•	•	•
-25				•	•	•	•	•
-20					•	•	•	•

One solution in order to control the combustion phasing could be acting on the injection timing of the second injection as shown by Sellnau et al [31]; in fact, as it is possible to see in Fig.2.16 where CA 50 is a function of SOI2 at different fixed SOI1 from -45 to -20 [CAD], there is a range in which this correlation is almost linear. In particular there are two different trends: CA 50 is fairly constant for SOI2 $<$ 15 [CAD], instead, after SOI2 -15 [CAD] there is an almost linear correlation between SOI2 and CA 50 with different sensibility depending on SOI1. This is true apart from SOI1 -45 [CAD] that has an acceleration between -25 and -15 [CAD] probably due to an improvement of the "spray-piston" interaction, this fact is confirmed by the increment in Combustion Efficiency, and for the same reason the Combustion Duration (Fig.2.17) with this SOI1 has a different trend compared to the others.

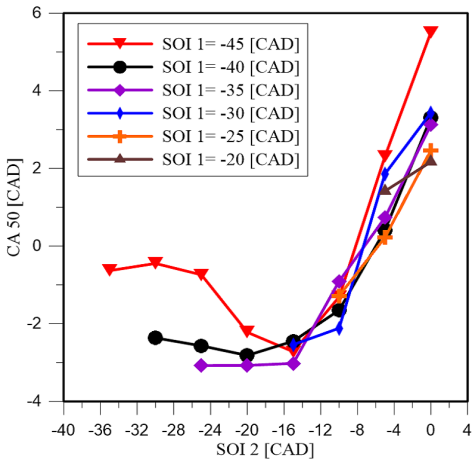

Figure 2.16: *CA50 with double injection.*

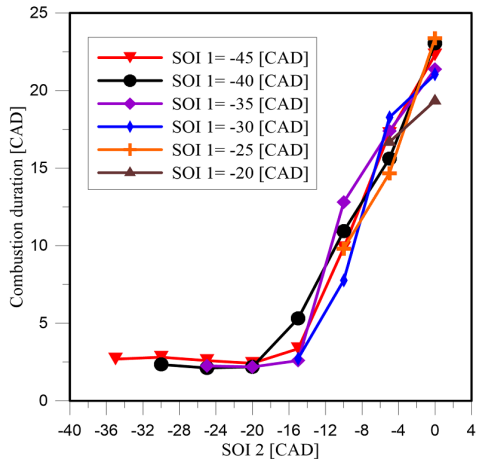

Figure 2.17: *Combustion duration with double injection.*

This hypothesis is supported by the fact that data of the Max in Cylinder Pressure Gradient, shown in Fig.2.18, have a decreasing trend from SOI2 -20 [CAD] to SOI2 -5 [CAD] and it is probably due to the charge stratification given by the late injection that leads to a more progressive combustion which implies less noise and mechanical stress on the engine.

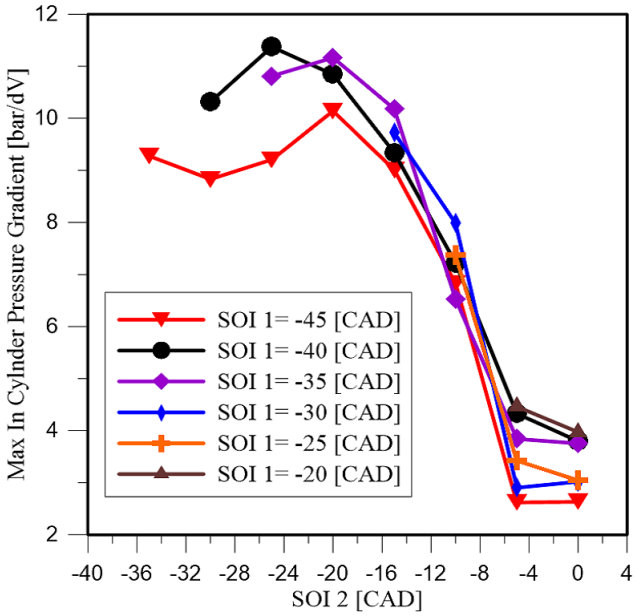

Figure 2.18: *Max In Cylinder Pressure.*

As concerns to Indicated Mean Effective Pressure (IMEP) in Fig.2.19 it presents only slight variations but it can be distinguished a peak for SOI2 -5 [CAD]. Efficiency Indecated has consequently the same trend of IMEP, Fig.2.20.

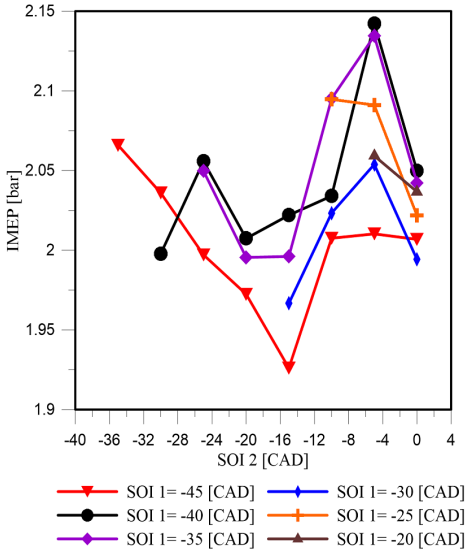

Figure 2.19: *IMEP with double injection.*

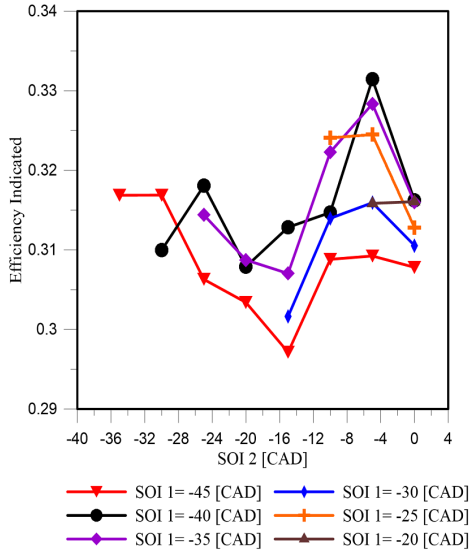

Figure 2.20: *Indicated Efficiency with double injection.*

The Combustion Efficiency in Fig.2.21 has a fairly constant trend depending on SOI1 a part from SOI1 -45 [CAD] and this could be again explained by the "spray-piston" interaction. Generally efficiency rises when retarding the first injection that is probably due to variations in the local equivalence ratio, however this is very difficult to observe without proper studies in engines with optical access combined with a simulative approach.

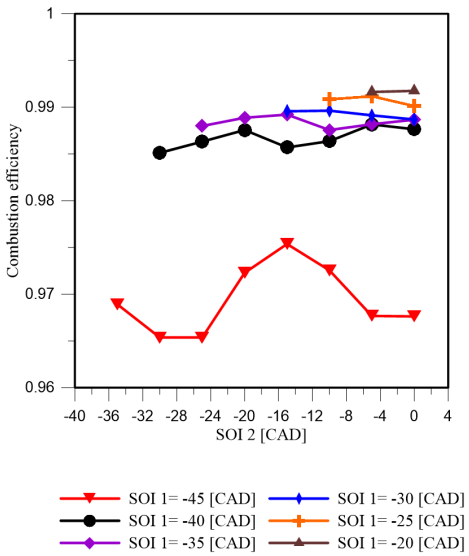

Figure 2.21: *Combustion Efficiency.*

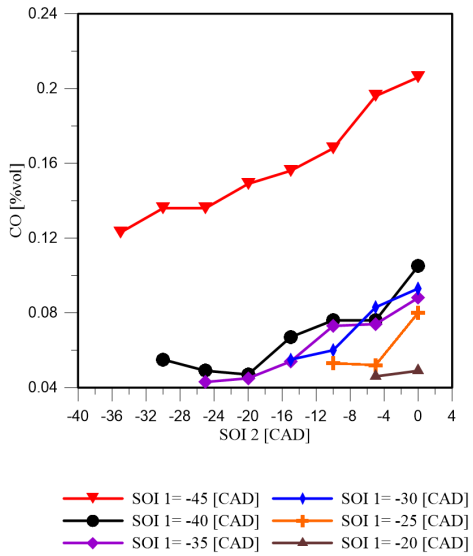

Figure 2.22: *CO emissions with double injection.*

Regarding the pollutant emissions, an high level of stratification leads to lower local temperatures that are unfavourable to the formation of NO_x, thus it can be observed in Fig.2.23 that the NO_x decreases when delaying the second injection and it is possible

to control emissions with the injection strategy. As concerns the HC emissions it could be observed that delaying the first injection may help with reducing the HC emissions, probably due to the fact that less fuel is injected out of the cylinder bowl and in the squish region; moreover for each SOI 1 delaying the second injection timing leads to a further reduction of these emissions, Fig.2.24.
CO emissions in Fig.2.22 may be reduced delaying the first injection, but late second injection cause an increment of CO that could be explained with lower temperatures and differences in local equivalence ratio that contrast its oxydation in CO_2.

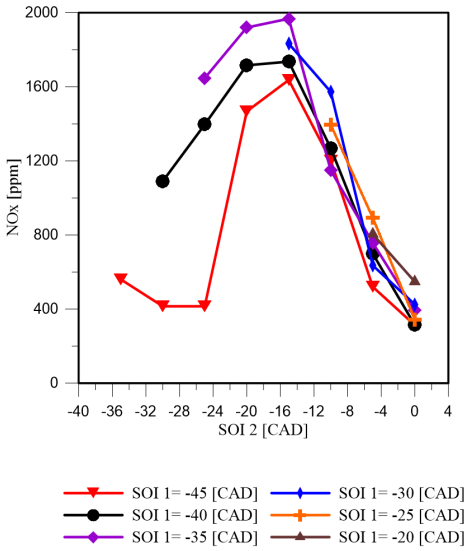

Figure 2.23: *NOx emissions with double injection.*

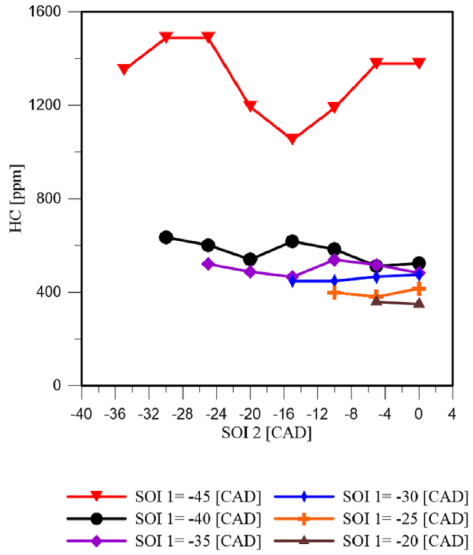

Figure 2.24: *HC emissions with double injection.*

2.2.3 Comparison between single injection and double injection

The main reason that makes the single injection strategy not applicable is the fact that it leads to an almost homogeneous combustion with levels of noise that are not acceptable in commercial engines. A double injection strategy instead could be used to shape the heat release rate and consequently the in cylinder pressure gradient by improving the capacity of the injection system to control fuel stratification, extending the region in which it occurs. Below is shown a table with a resume of all the SOI combinations studied in this work.

Table 2.5: *SOI combinations.*

	SOI 1 -46÷-18 [CAD]	SOI 2 -35÷0 [CAD]
Single injection	100% Fuel Mass	
Double Injection	50% Fuel Mass	50% Fuel Mass

Comparing the two injection strategies it is possible to notice that only with high distance in CAD between the two injections there is a reduction in NO_x emissions, Fig.2.25. Generally HC emissions with a double injections strategy appear to be lower than with single injection. This trend could be explained with a more gradual combustion that leads to the oxidation of more hydrocarbons, moreover a delayed second injections reduce the amount of fuel injected out of the piston bowl, Fig.2.27. It has to be remarked that what told before about HC emissions is true apart from double injection with SOI1 -45 [CAD] probably this is due to a bad "spray-piston interaction". Regarding CO emissions in Fig.2.26, widening the gap between the two injections results in higher emissions probably due to the lower temperatures reached that lead to less CO oxidation. Also in this case double injection with SOI1 -45 is not a good solution probably because part of the fuel is injected out of the bowl in the piston head leading to differences in the local equivalence ratio.
As concerns the indicated efficiency in Fig.2.29, the single injection strategy results in an overall higher efficiency and this is consistent with the other results that show a less punctual combustion process leading to a smaller fraction of energy converted into work.

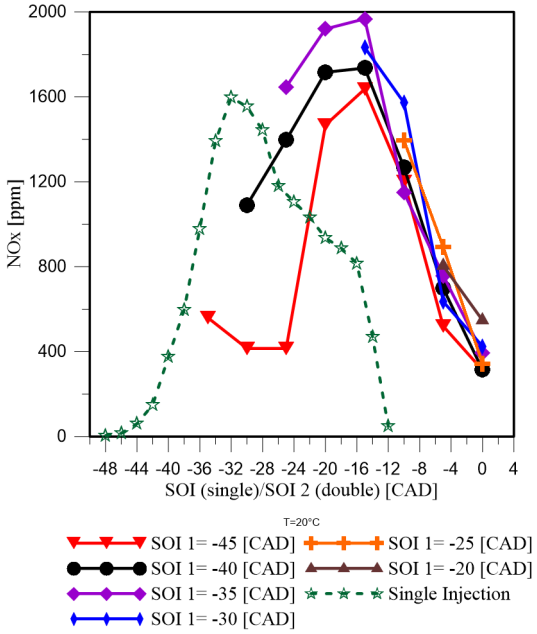

Figure 2.25: *NOx comparison.*

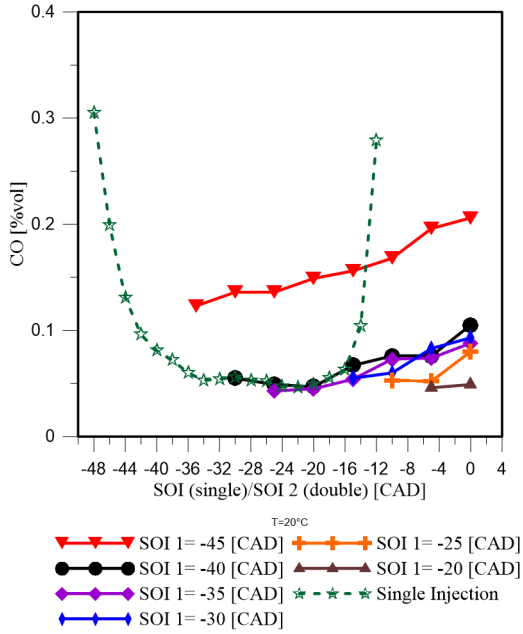

Figure 2.26: *CO comparison.*

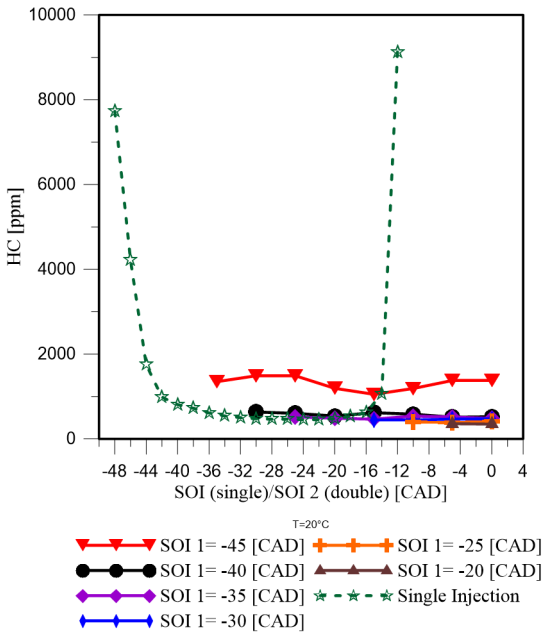

Figure 2.27: *HC comparison.*

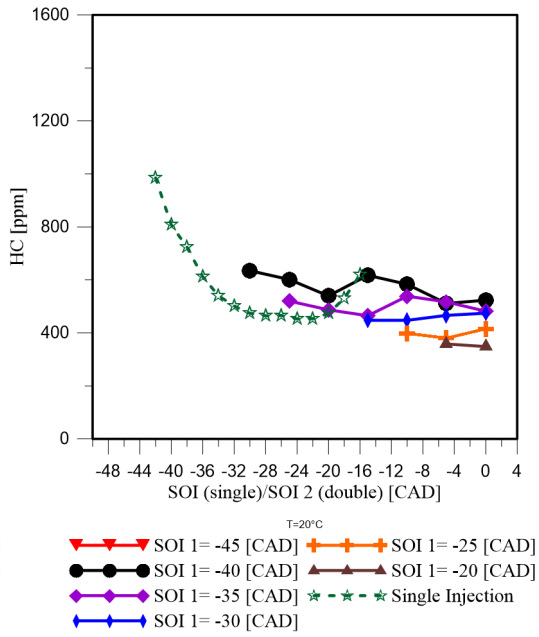

Figure 2.28: *HC zoom.*

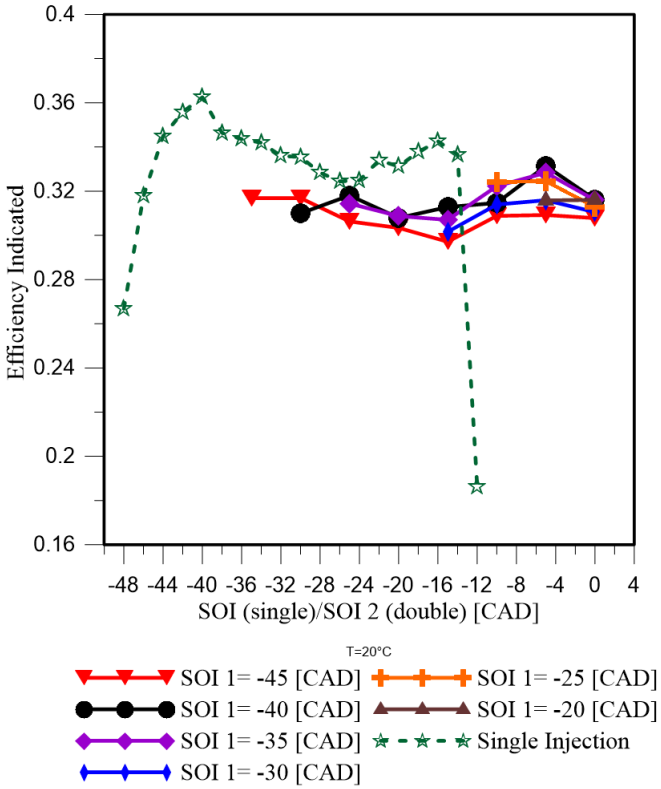

Figure 2.29: *Indicated Efficiency Comparison.*

For the analysis of the results of the mean heat release rate (MHRR), it was decided to narrow down the view and focus on the different SOI1 but with a fixed SOI2, as shown in Tab.2.6.

Table 2.6: *SOI combinations*

	SOI 1 (-46÷-18 [CAD])	SOI 2 (-5 [CAD])
Single injection	100% Fuel Mass	
Double Injection	50% Fuel Mass	50% Fuel Mass

With a Single Injection strategy (Fig.2.30) the curves of the MHRR have only one peak, their values are mostly between 100 and 120 $[J/CAD]$ and they have a minimum of 40 $[J/CAD]$ for SOI1 -48 [CAD]. With a double injection strategy (Fig.2.31) instead, the curves present a double peak shape until the distance in CAD between the two injections is below 15 CAD. Regarding the values of the MHRR for the double injection, the lower peak height occurs for SOI1 -45[CAD] and SOI1 -30 [CAD] with about 30 $[J/CAD]$ and with the same SOI1 in the single injection strategy the values were higher. The maximum Mean Heat Release Rate results for SOI1 -20 [CAD] and is about 55 $[J/CAD]$ which is half the maximum value found in the single injection strategy. This data could mean that the combustion with a double injection strategy is less punctual and more gradual.

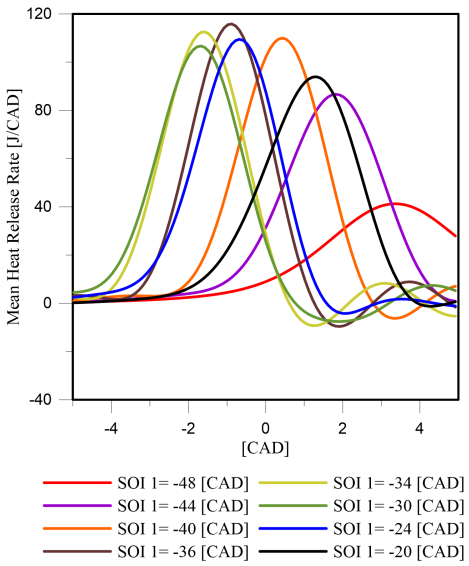

Figure 2.30: *Single injection mean heat release rate with various SOI.*

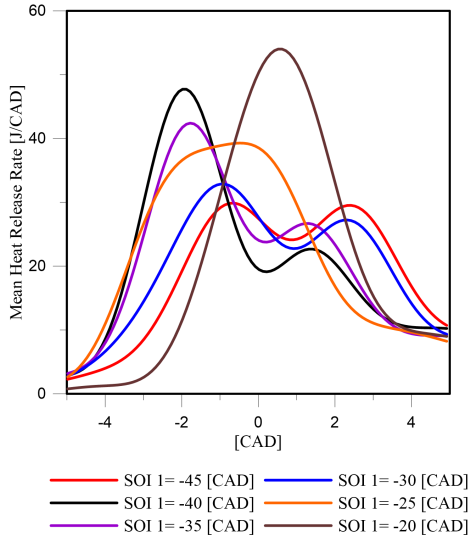

Figure 2.31: *Double injection mean heat release rate with SOI2=5[CAD].*

The double injection strategy leads to a significantly lower Max in Cylinder Pressure Gradient (Fig.2.32), confirming the previous analysis of a less stressful and less noisy operation using this method. The single injection approach on the other hand leads to higher indicated efficiency, in Fig.2.33, most of all with SOI1 -40 [CAD]; this could be explained with a more gradual combustion in the double injection strategy leading to a lower amount of energy converted into work and this is consistent with the previous results.

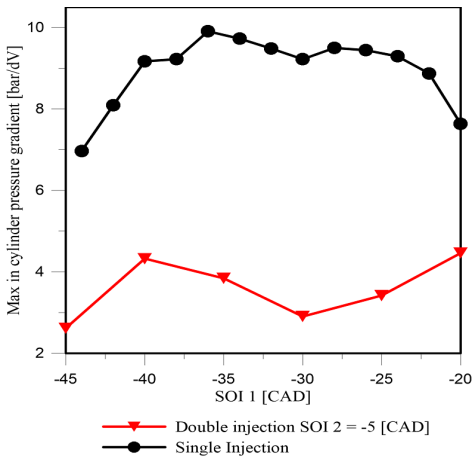

Figure 2.32: *Max in cylinder pressure comparison.*

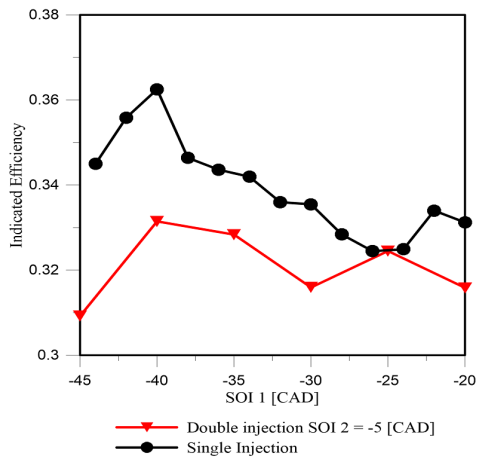

Figure 2.33: *Indicated efficiency comparison.*

Using two injections results also in a lower amount of NO_x emissions, apart from very advanced SOI1 (-45,-40 [CAD]) for whom these emissions are considerably higher.

This fact could be justified with a lower quantity of the fuel injected in the squish volume and out of the piston bowl. The general trend of lower NO_x emissions with the double injection may be explained with lower temperature peaks that contrasts the Nitrogen oxidation, Fig.2.34. Unburned hydrocarbons emissions are in general lower with the double injection strategy, and this could mean that the combustion is generally more complete and gradual than in case of single injection, Fig.2.35.
CO emissions (Fig.2.36) are generally higher using the double injection, this could be due to lower temperatures in the combustion chamber and thus less CO oxidation, this confirms the analysis made for NO_x emissions.

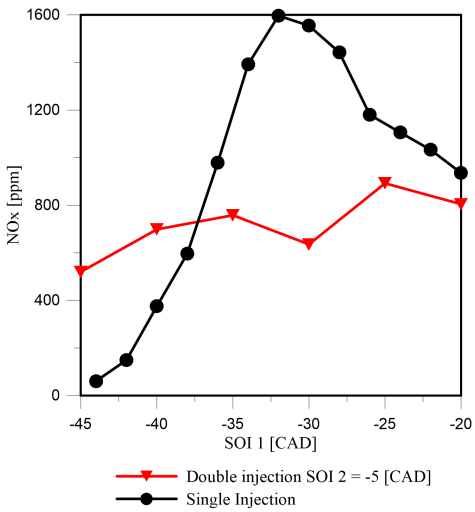

Figure 2.34: *NOx comparison.*

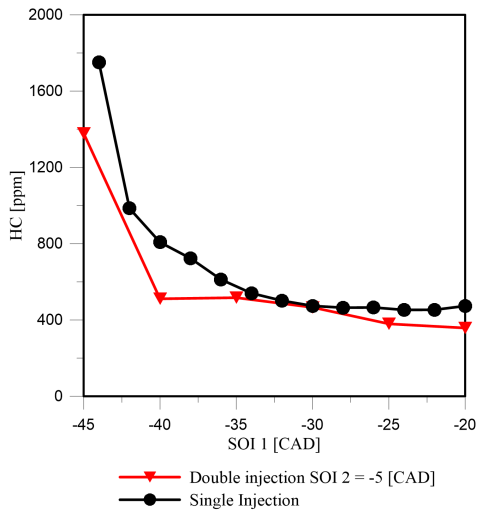

Figure 2.35: *HC comparison.*

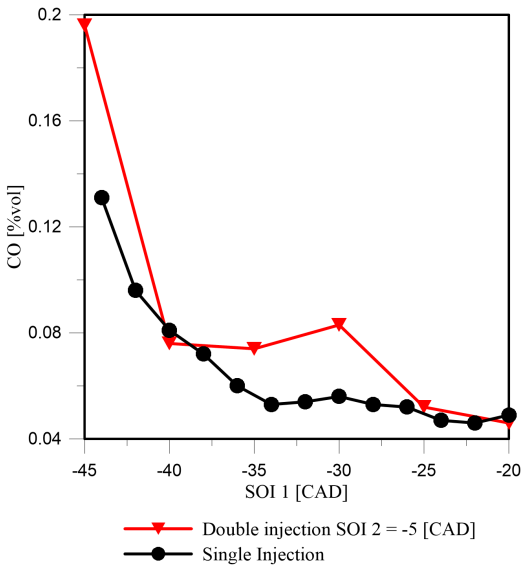

Figure 2.36: *CO emissions.*

2.3 GCI engines challenges

In literature it is possible to find works related with the GCI engine at high load, such as Manente et al. [17] and Kalghatgi et al. [13], where this kind of engine delivers high efficiency and performances when operating at high loads. The main challenge that engineers have to face when developing this technology is the low-load operations, in fact under these condition there are limits caused by a number of factor, such as low propensity of the fuel to auto-ignition and difficulties in the control of the combustion phasing.
The first issue is observable in this work as the intake temperature had to be brought to about 200°C in order to obtain a stable combustion and the results reported; the second limit occurs because in this kind of engine there isn't a tool, such as the spark plug in the SI engine, that allows the control of the combustion phasing but it is all left to the chemical kinetics, and thus the condition of temperature and pressure inside the combustion chamber are the ones that control the time of the ignition.
The efforts with the aim of addressing these problems, as reported in the introduction to this work, rely mainly on VVT or turbochargers with variable geometry capable of boosting the intake pressure already at low loads. Another promising method consists in seeding the intake air with an oxidizing species, in order to enhance the processes inside the combustion chamber and overcome the limits displayed above; previous works, by Foucher et al. [9] and Masurier et al. [19] [20] [22] [23], showed how this technique could be very effective with HCCI engines fuelled with various type of gasoline, alcohol and natural gas, as it possible to see in Fig.2.37 where is shown the in-cylinder pressure and the heat release rate in an engine seeded with various oxidant [23]. In particular ozone turned out to be very effective and it is for this reason that it was decided to carry on the experimental work that will be discussed in Chapter 3 and afterwards investigate its effect on a GCI engine, in Chapter 4.

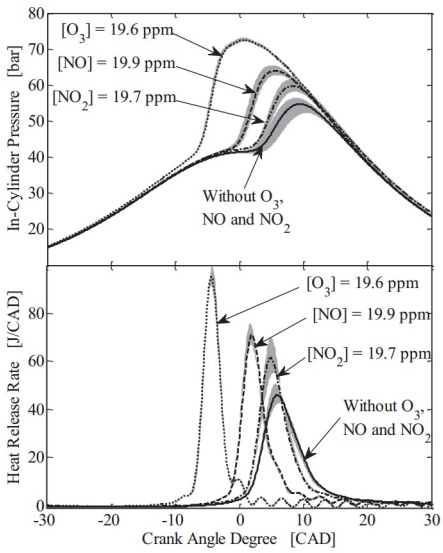

Figure 2.37: *In-cylinder pressures and heat release rates as a function of the nitric oxide and ozone concentrations when simultaneously seeding the intake of the engine.[23]*

Chapter 3

Study of ozone decomposition

3.1 Ozone Theoretical Background

3.1.1 Definition and applications

Ozone (O3) is an allotropic form of the oxygen molecule, at room temperature it is a pale blue toxic gas with a strong instability and a pungent smell. It is naturally formed in the upper level of the atmosphere with the action of ultraviolet light or electric discharges on oxygen molecules. The effects of ozone in the upper atmosphere (specifically, the stratosphere, 15-55 km above the Earth's surface) are essential to the survival of life on Earth, here it filters harmful ultraviolet radiation from sunlight. This ultraviolet radiation is highly energetic and would damage both plants and animals exposed to it. Diatomic oxygen absorbs the highest-energy ultraviolet radiation from the sun, namely, all radiation with wavelengths shorter than 240 nm. However, there is a great deal of ultraviolet radiation between 240 nm and 290 nm that is not absorbed by O2 molecules. This radiation is absorbed by ozone[36] [37].
The use of this compound is generally related to water treatment and disinfection, for example it is used to:

- Disinfect laundry.
- Disinfect water in place of chlorine.
- Deodorize air and objects.
- Kill bacteria on food or on contact surfaces.
- Kill yeast, mold, bacteria and insects.
- Sanitize swimming pools.

In particular ozone can be used to remove iron and manganese from water, forming a precipitate which can be filtered:

$$2Fe_2 + +O_3 + 5H_2O \rightarrow 2Fe(OH)_3(s) + O_2 + 4H^+$$

$$2Mn2 + +2O_3 + 4H_2O \rightarrow 2MnO(OH)_2(s) + 2O_2 + 4H^+$$

Ozone will also reduce dissolved hydrogen sulfide in water to sulfurous acid:

$$3O_3 + H_2S \rightarrow 3H_2SO_3 + 3O_2$$

These three reactions are central in the use of ozone based well water treatment.

3.1.2 Ozone Production

Due to the fact that ozone has a relatively short half life and that it is very difficult to store, as in liquid form it is explosive, ozone is almost always produced on-site with an ozone generator. The main methods used to produce ozone are the following:

- Corona Discharge.
- Ultraviolet Radiation.
- Electrolysis.
- Radiochemical.

The first is probably the one that is employed the most commercially. It can occur also in old electric motors, faulty light switches and photocopiers because essentially it is an high voltage, low current electrical discharge passing through an air gap, this can break down the bi-atomic molecule of oxygen and lead to the formation of a tri-atomic molecule, ozone. In detail, it is a three-body reaction involving O, O_2 and M, this one is a collision partner that could be O or O_2 if the supplied gas is oxygen, but also N_2 if it is used air.

$$O + O_2 + M \rightarrow O_3^* + M \rightarrow O_3 + M$$

Where O_3^* is a transient excited state in which ozone passes before stabilizing. There are also side reactions that limit the production of ozone as they compete with the reaction above; some of them involve only O and O_2 and thus are present both with the oxygen and the air supply, others are based on N and so they occur with the air supply, this and other factors contribute to an higher formation time estimated in about $100\mu s$, ten times more than the case with oxygen supply[14].
In nature this process occurs during thunderstorms when lightning supply the energy required to slpit the molecular oxygen, while industrially usually it all takes place in a cell, that can be planar or cylindrical, in which two electrodes are separated by an air gap and a layer of dielectric material, as in Fig.3.1 [40].

This layer helps spreading the electrical discharge in a wider area to maximise efficiency and the production can be regulated via controlling the voltage or the frequency (or both) of the current supplied. As it can be seen in Kogelschatz's work [14], over the last few years ozone generators have implemented important innovations in the power supply units and thus are becoming more and more compact and efficient. In general these kind of producers have the advantage of being reliable, require low maintenance and produce an high quantity of ozone, on the other hand require a conspicuous initial investment, need to be supplied with a very clean gas (dry air or pure oxygen) and produce also a great deal of heat that needs to be removed with a proper system. The generator used in this work, an Anseros COM-AD-01 uses this technology.

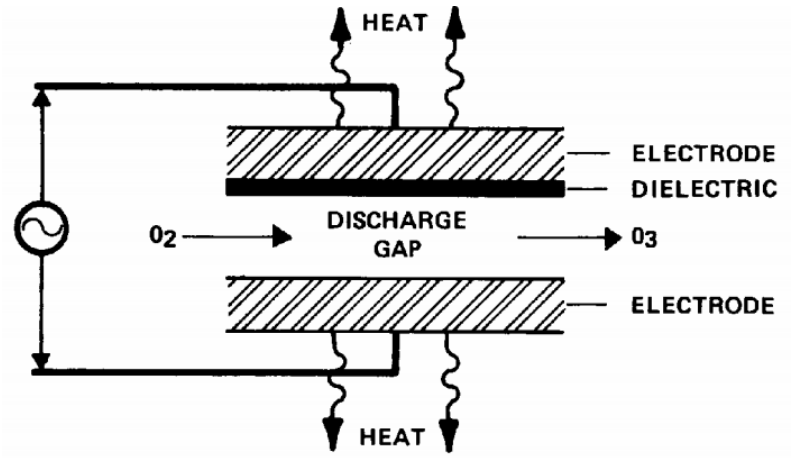

Figure 3.1: *Corona discharge cell. [40]*

Ultraviolet radiation generators instead use the physics phenomena that naturally occurs in the upper layer of Earth's atmosphere, with the employment of an UV lamp with a specific peak wavelength (185 nm) it is possible to produce ozone from the oxygen contained in the air. The main asset of this kind of generators is the simplicity (Fig.3.2) in fact the only two things needed are the UV lamp and a fan, while the greatest drawback is the output since usually they can produce only a very little amount of ozone.

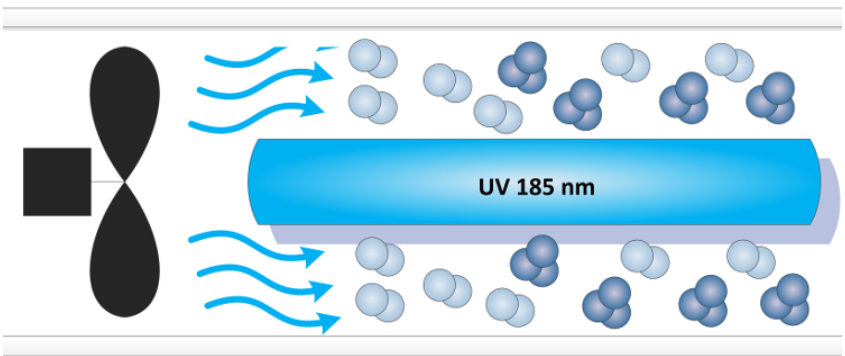

Figure 3.2: *UV ozone generator scheme.[38]*

Regarding the production of ozone through an electrolytic process, it consists in the passage of an electric current through a liquid, supplying energy and therefore allowing for chemical reactions to occur. Usually water is used as electrolyte, but there has been studies with H_2SO_4; others works were focused on the electrodes but the main goal for every one of them was the improvement of the efficiency and increase the lifespan of the components employed. Mainly these producers are in use due to their compact form factor and the fact that ozone is produced directly in water so it cannot come in contact with materials or other compounds that may contaminate the gas.

Another potential method to produce ozone consist in bombarding air or pure oxygen with radiation coming from radioactive material, despite the results were promising this process presents a lot of complications, such as the filtration of harmful isotopes, and thus this technique is not considered viable as a commercial application.

3.2 Objectives

Subsequently to the work on the engine it was decided to move the focus on a more basic study about ozone and its behaviour, in literature are present some interesting works about this topic [6] [9] [10] [19] [24] but all of them show the effect of ozone seeding in various engines and with different fuels, while the aim of this work is to study the phenomena that take place. In particular in the article by Foucher et al. [9] there is a graph (Fig.3.3) showing a simulation of the behaviour of ozone inside the engine; it is clear how this compound, from -45 crank angle degrees (CAD) experiences these reactions:

$$O_3 + N_2 \Leftrightarrow O_2 + O + N_2$$

$$O_3 + O2 \Leftrightarrow O_2 + O + O_2$$

$$O_3 + M \Leftrightarrow O_2 + O + M$$

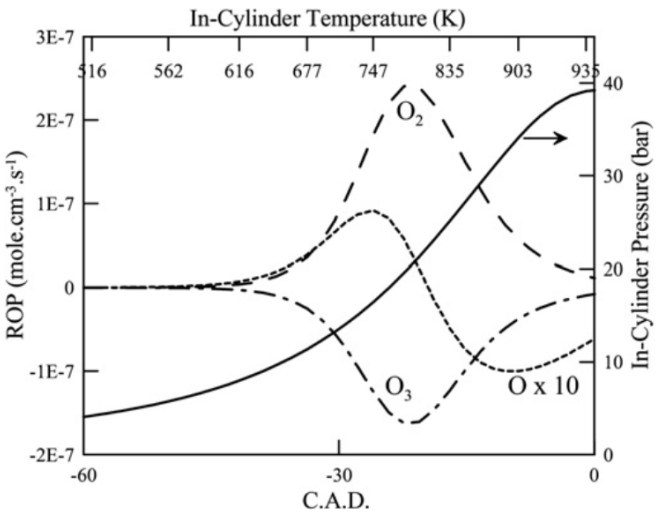

Figure 3.3: *Rate of product of O_3, O and O_2 species (left axis) and in-cylinder pressure (right axis) as function of CAD. In-cylinder gas temperature is represented at the top axis for 10 ppm of ozone concentration.*[9]

Observing these reactions inside the actual engine is nearly impossible due to the large amount of parameters and related phenomena that develop during the operation of the engine. In order to simplify the system and thus be able to examine the behaviour of ozone in conditions similar to the ones found in the intake pipe, an experimental set-up was developed, as described in the next section.

Another goal of this part of the work is the analysis of the interaction of ozone with Nitric Oxide (NO), this is interesting because NO can be found in the intake if an exhaust gas recirculation (EGR) strategy is actuated, moreover during the O_3 generation process a small amount of this compound may be generated as a side product and lastly NO has been proven to be a promoter of the combustion with a smaller effect compared with ozone [24] and thus the study of the interaction of these two species is very important during GCI operations.

3.3 Experimental set-up

In order to study the ozone decomposition it was necessary to develop an appropriate experimental set-up; its parts are listed below:

- A steel tube with eight predispositions to place the sampler; the segment between the first and the last sampler was called Test Section (TS).

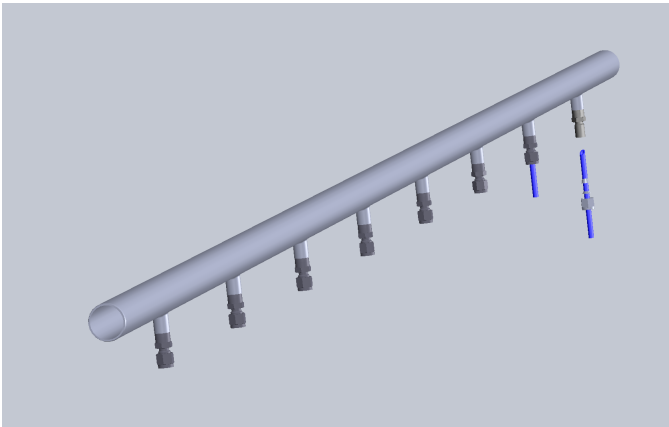

Figure 3.4: *Steel tube CAD.*

- An ozone injector, that will be presented in section 3.3.1.

Figure 3.5: *Ozone injector.*

- Brooks 5800 series mass flow controllers (MFC) to manage the flow of the working gases. They all have an accuracy of ±0.7% on the measure and ±0.2% of the full scale.

Figure 3.6: *Mass Flow Controller.*

- A primary heater to regulate the temperature of air at the entrance of the measuring pipe, equipped with a K-thermocouple with an accuracy of $\pm 2\ K$.

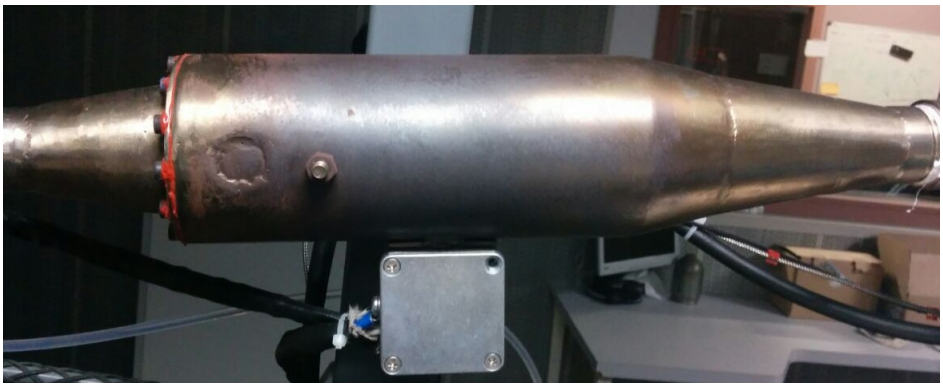

Figure 3.7: *Primary heater.*

- A secondary heater on the surface of the tube to maintain the temperature constant, also equipped with a K-thermocouple.

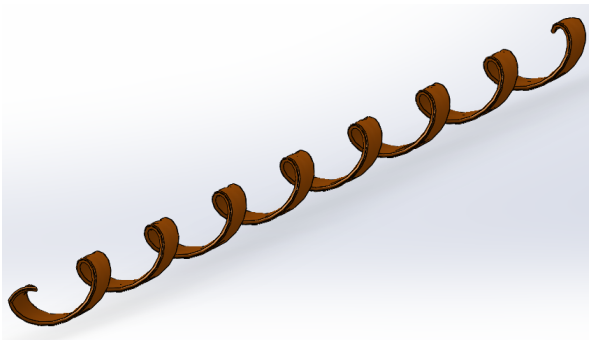

Figure 3.8: *CAD drawing of secondary heater to be placed around the tube.*

- A compressor which supplied dry air.
- An ozone generator, the Anseros COM-AD-01, to produce the gas via dielectric barrier discharge; it was supplied with a constant 3 Nl/min flow of pure Oxygen and the production was controlled adjusting the discharge frequency; it was then necessary to add to the flow of air a flow of pure Nitrogen to restore an N/O ratio similar to the one of air.

Figure 3.9: *Anseros COM-AD-01 ozone generator.*

- An ozone analyzer, Anseros MP6060, that measured the UV absorption of a sample of the gas flowing in the pipe in order to determine the ozone concentration, with an accuracy of ± 0.1 ppm.

Figure 3.10: *Anseros MP6060 ozone analyzer.*

The whole set-up is presented in Fig.3.11.

Figure 3.11: *Experimental set-up*

3.3.1 O3-Injector Configuration

One of the most relevant part of the set-up design was the ozone injector, several experiments with different geometry were carried out. In Fig.3.12 and Fig.3.13 are shown the pipe scheme and the first three configurations of the injector, for each of them a series of experiments were executed with different air temperature and different air flow rate.

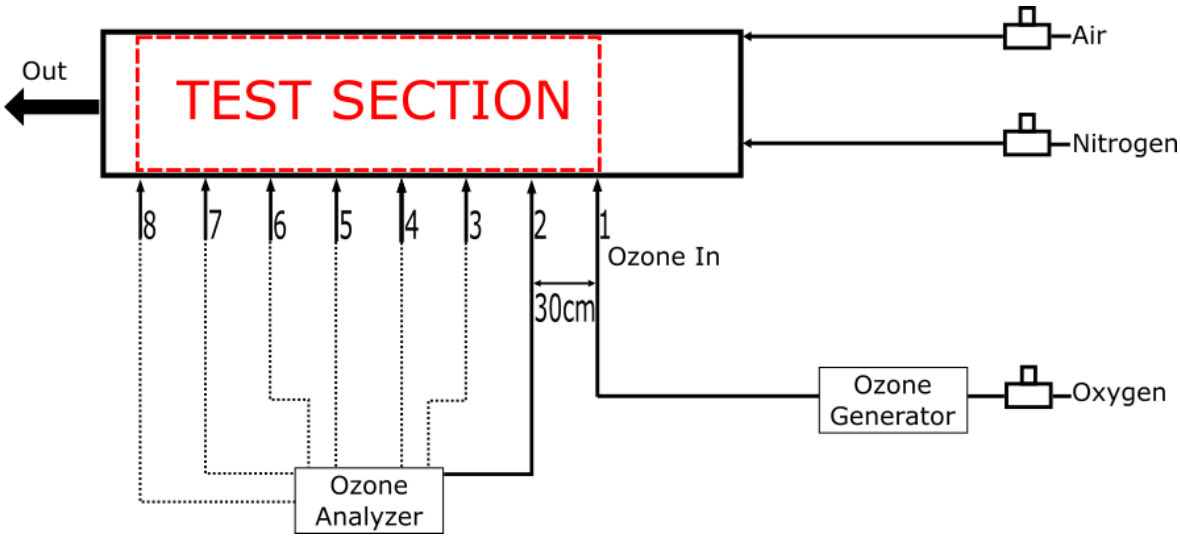

Figure 3.12: *Pipe scheme.*

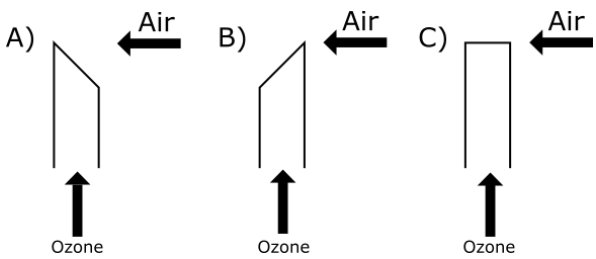

Figure 3.13: *Injectors.*

Since every flow rate in this work was measured in Normal litres per minute, a variation of either temperature or flow rate meant a variation in speed along the tube and therefore a different portion of time detectable with our set-up.

For example, at $T = 20\ °C$, Tab.3.1 shows the section of time detectable with various air flow rates and Fig.3.14 the variations in terms of speed varying the temperature.

Table 3.1: *Detectable Time Portion with* $T = 20\ °C$.

Air Flow [Nl/min]	Detectable Time Portion [s]
100	0.627
125	0.513
250	0.27
400	0.173

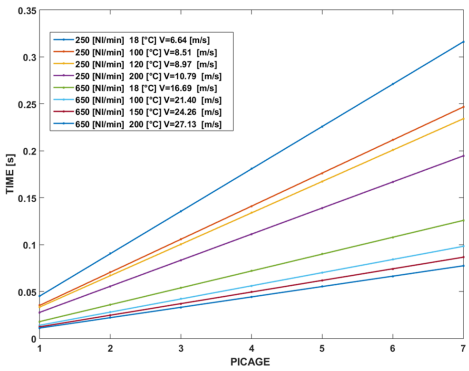

Figure 3.14: *Comparison between different air flow rates and temperatures,a variation in either leads to a different flow speed.*

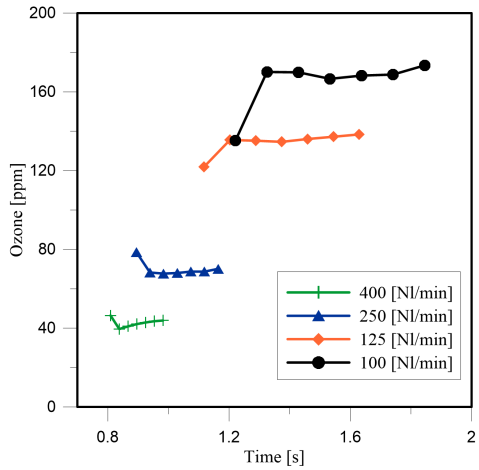

Figure 3.15: *O_3-in oriented towards flow inlet.*

The first ozone injector configuration employed was "O_3-in oriented towards flow inlet", with this configuration it has been noticed an increase of the O_3 concentration between first sampler and second sampler for every mass flow rate, at room temperature and atmospheric pressure (Fig.3.15).

Switching to the "O_3-in oriented towards flow outlet" configuration lead a similar trend for the lower flow rate but an opposite one for the higher flow rate, an akin tendency is visible also for the third configuration, "O_3-in flat" (Fig.3.16 and 3.17).

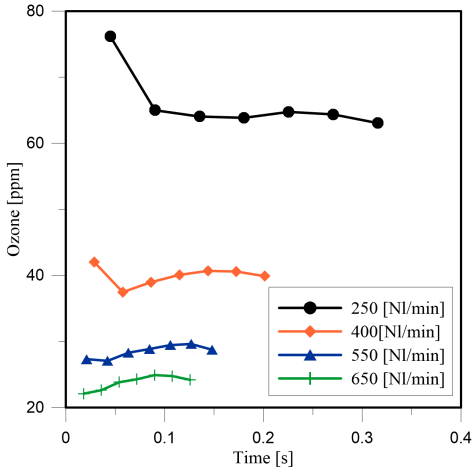

Figure 3.16: *Ozone concentration O_3-in towards flow outlet at room temperature and atmospheric pressure for various flow rates.*

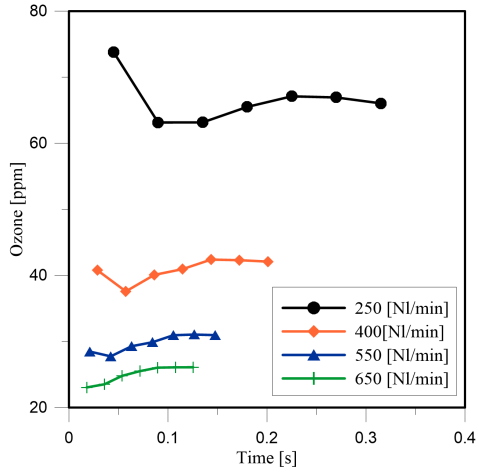

Figure 3.17: *Ozone concentration O_3-in flat at room temperature and atmospheric pressure for various flow rates.*

There is no pattern or trend detectable between the ozone concentration and the three ozone injectors apart from the one discussed above, thus the main differences were between the first configuration and the others; among them the differences were not relevant but the most reliable was proved to be the flat one.

After the analysis at room temperature, the study moved on to higher temperature with different air flow rates.

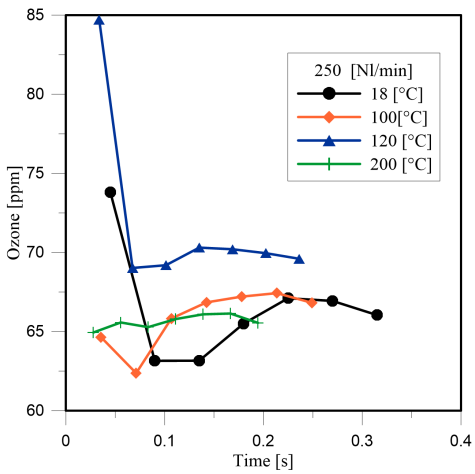

Figure 3.18: *Ozone concentration O_3-in flat at different temperatures with a 250 Nl/min flow.*

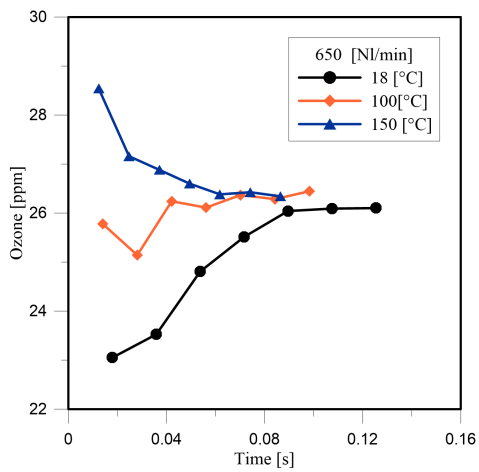

Figure 3.19: *Ozone concentration O_3-in flat at different temperatures with a 650 Nl/min flow.*

Fig.3.18 and 3.19 present higher values of ozone concentration for higher temperatures, this is at least counterintuitive since the decomposition of ozone is enhanced by the temperature, moreover the discrepancies between the curves are wider at the first sampler and smaller along the tube, converging to a single value at the end; this made it clear that a problem with the ozone injector was in place, most likely with the

mixing between the air and the ozone before getting to sampler, thus a redesign of the system was necessary in order to eliminate this issue and to have better set-up for the successive experiments.
With the goal of injecting the ozone evenly along the section of the pipe and obtaining a well-mixed flow, various simulations with Dassault Systmes SolidWorks have been carried out with different injection methods and for each solution the simulation was configured to reproduce as accurately as possible the conditions found in the actual pipe, i.e.: atmospheric pressure, imposed flow speed and constant temperature. The choice of this particular software was not casual, in fact its suite comprehend both a 3D modelling tool and a flow simulation tool, essential for this study. The first step was the validation of the procedure, for this purpose the Reynolds number inside the tube was manually calculated and then a simulation of the original tube was launched, the results were equivalent and thus the simulation could be considered valid.
Afterwards the creation of a 3D model had to be done and it was designed as shown in Fig.3.20, where the ozone is injected via a small steel tube (d=6 mm) with 16 holes (d=1 mm); other solutions, such as a coaxial tube or a different number and diameter of the holes, were analyzed and discarded due to a negative effect on the ozone molecules, in fact these are highly unstable and tend to break down easily, e.g. when passing through narrow gaps.

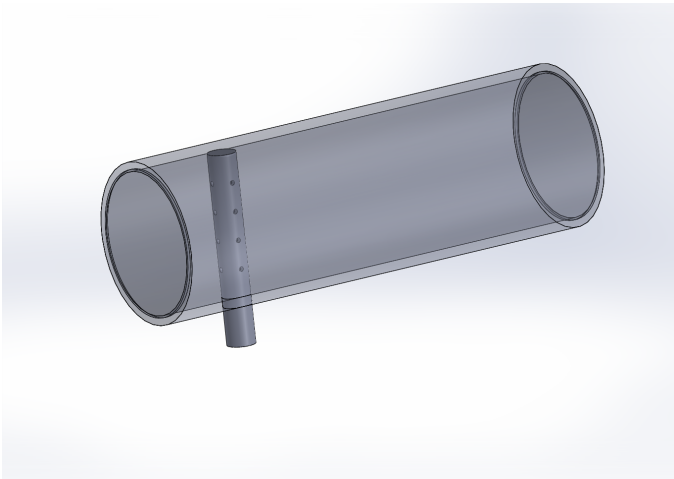

Figure 3.20: *Solidworks 3D model of ozone injector pipe.*

Regarding the creation of turbulent vortices, several solutions were studied but here are shown the most promising three:

- A perforated plate: Fig 3.21 (a).
- A grid: Fig. 3.21 (b).
- A washer: Fig. 3.21 (c).

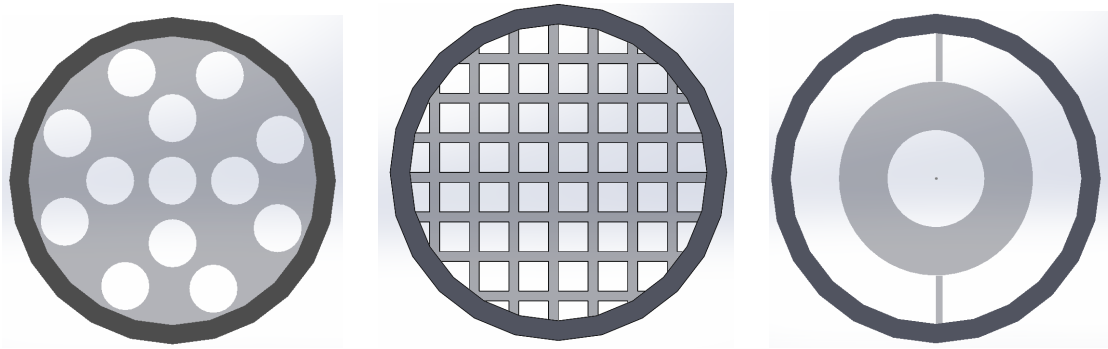

(a) *Perfored plate.* (b) *Grid.* (c) *Washer.*

Figure 3.21: *Turbulence generators.*

The design that gave better results in terms of turbulence intensity was the washer, moreover it was the one that could be built and firmly attached to the tube without complicated solutions, such as welding.
It was then performed a series of tests with the final configuration of the part with both the injector tube and the turbulence generator. In Fig.3.22 is shown a cut plot on the longitudinal plane of the simulations results in terms of turbulence intensity.

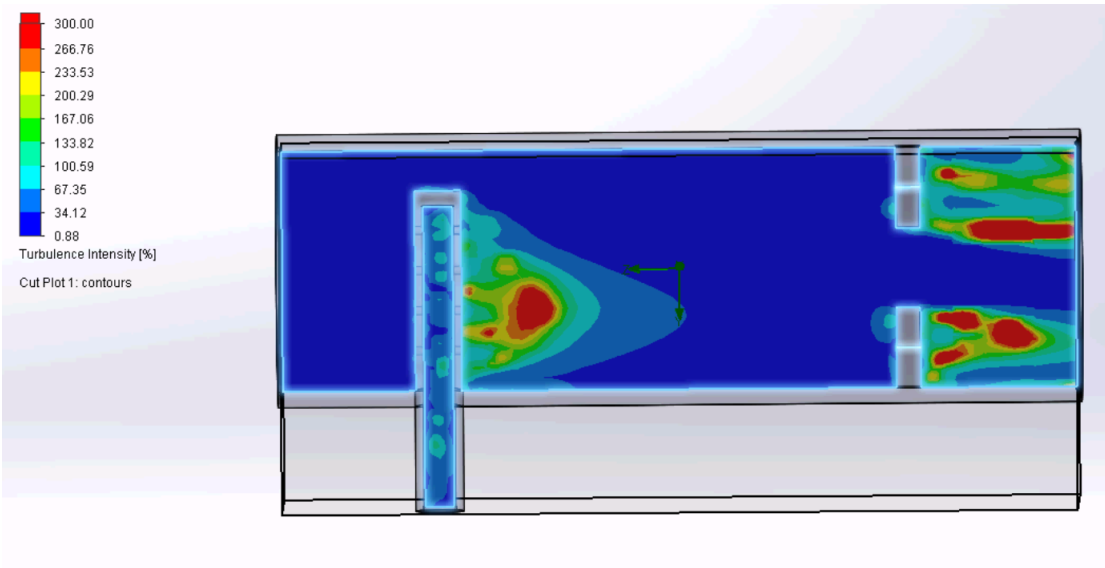

Figure 3.22: *Turbulence intensity of the flow with a washer as turbulence generator.*

During the construction of the model, in order to increase the turbulence generated it was decided to add another washer after the first one and the resulting injector is presented below.

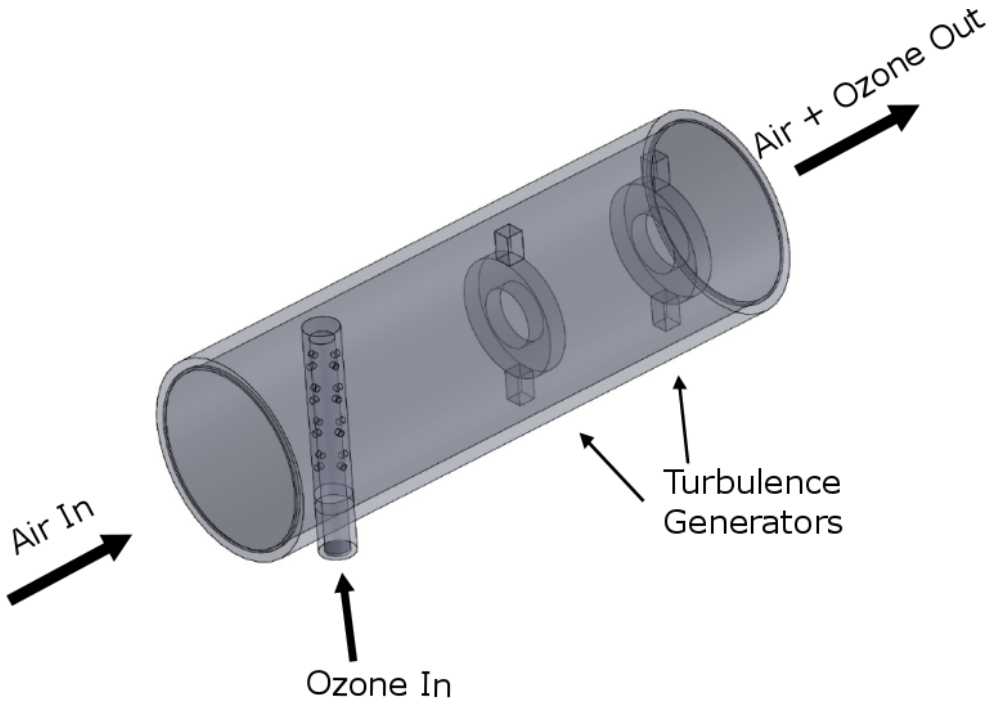

Figure 3.23: *Definitive configuration of the ozone injector.*

3.3.2 Test section insulation

Another major improvement made to the set-up was the introduction of an insulating layer over the test section, this was proved to be necessary in order to reach and maintain higher temperatures, especially with low air flow rates. This layer of mineral wool was placed around the pipe leaving out only the predisposition for the sampler with the goal of containing the heat loss and thus enable the system to reach the temperature of 200 $°C$ even with 50 Nl/min of air flow rate. This configuration led to a slower thermal response of the system and consequently the time needed to reach a certain temperature and to stabilize onto it became considerably higher, but once the set temperature was attained the system turned out to be very stable and not easily perturbable by external changes, such as the displacement of the sampler.

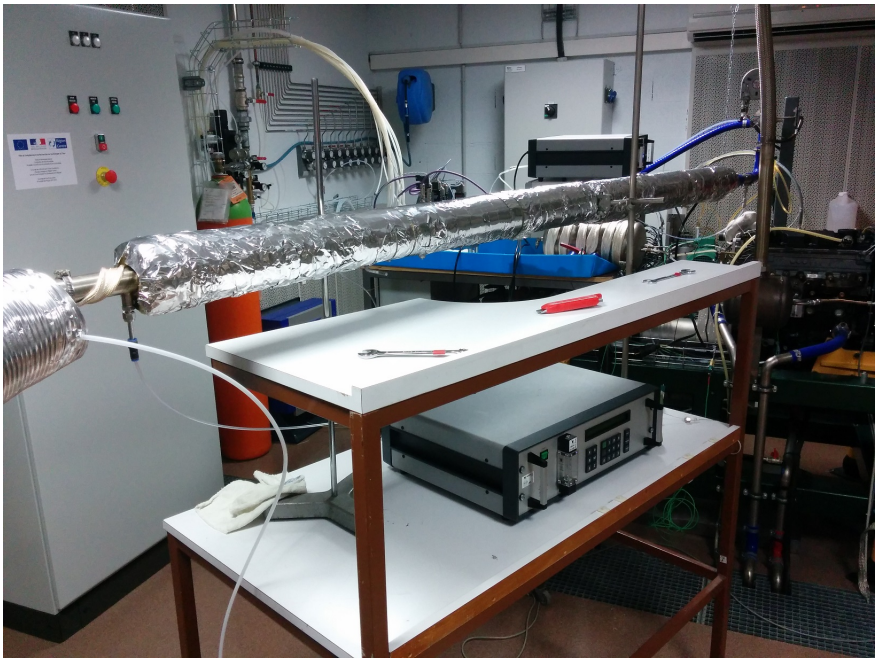

Figure 3.24: *Tube insulation.*

3.3.3 Nitric oxide addition

The last improvement to the set-up was the configuration of the piping and control systems to add nitric oxide to the air-ozone flow. There are several reasons for which it was decided to add this compound to the flow, the main two being its presence in the intake pipe when an EGR strategy is in place and the fact that NO is also a promoter of the combustion. Their interaction has an impact on ozone levels and consequently on engine behaviour.

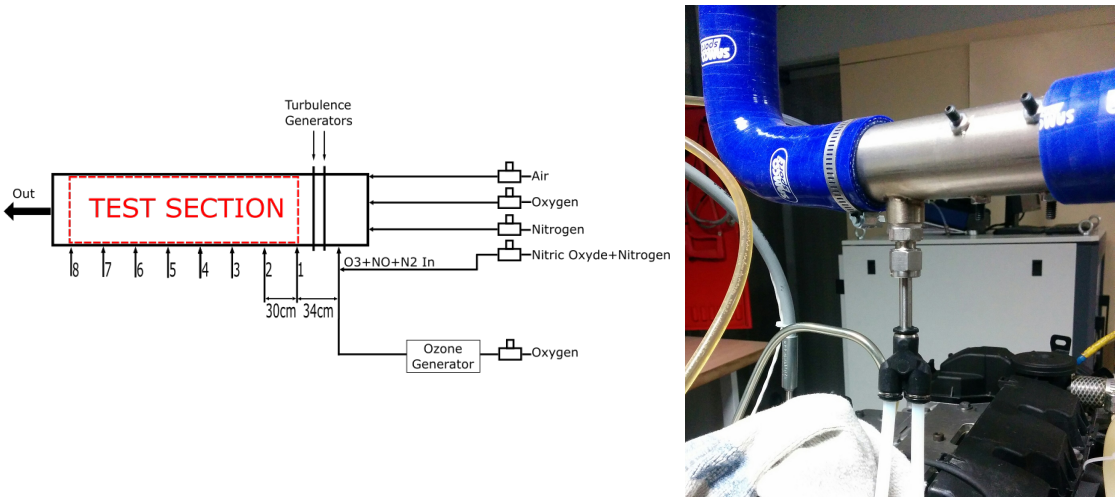

Figure 3.25: *Intermediate configuration with nitric oxide addition.*

The nitric oxide employed during the experiments was supplied by a bottle containing 99.5%N_2 and 0.5%NO, so it was necessary to add an MFC to control the flow coming from this bottle and another one to control a flow of oxygen needed to restore an N/O ratio equivalent to the one of the air.This configuration required two steps: the first, shown in Fig.3.25, consisted in injecting NO and O_3 together using the injector shown in section 3.3.1. However the fact that there was no ozone left in the test section meant that the reaction was very fast and it was impossible to observe it with this configuration, so the second step was to inject ozone through the injector and mix the nitric oxide with the air flow in order to give less time before the test section for the reaction to occur. The definitive configuration for the experimental set-up is shown in Fig.3.26.

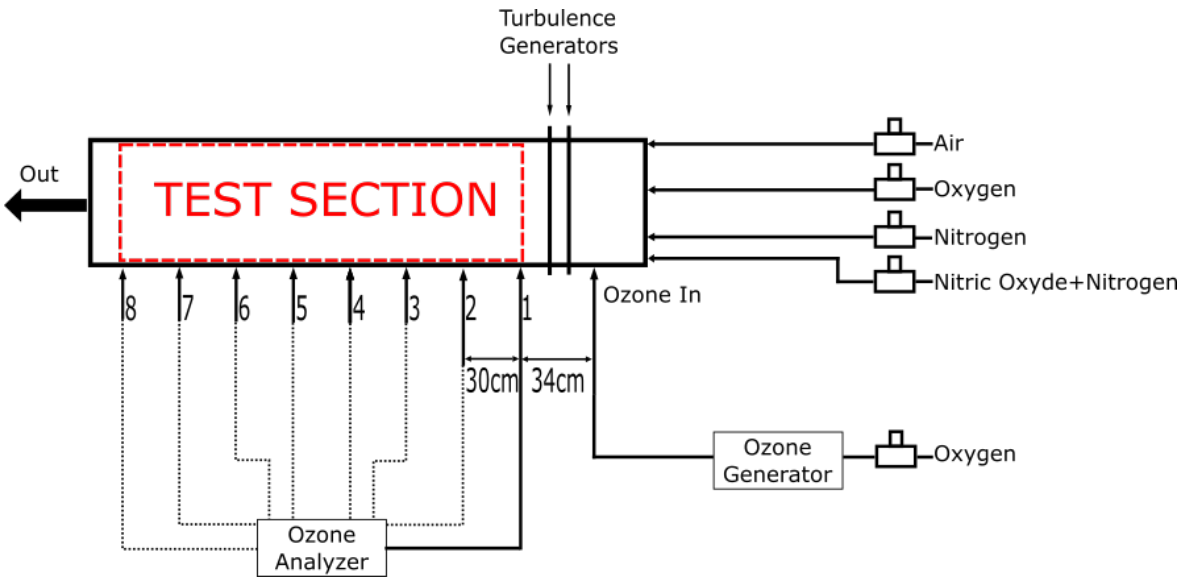

Figure 3.26: *Definitive configuration.*

3.4 Results and discussion

3.4.1 Experimental Results

As explained in the previous section, in order to properly configure the experimental set-up, many trials were carried out and their results were very useful, however not all of them are reported here for the sake of brevity. The conditions of the test section in which the experiments were performed were chosen with the aim of emulating the ones found in the intake conduit of a GCI engine; regarding the temperature, it ranges from $T = 20\ °C$ up to $T = 200\ °C$, this upper limit was adopted due both to the thermal range of usability of certain components of the set-up and the fact that previous work have shown that with this temperature is possible to perform GCI operations without ozone seeding [19]. The pressure was held constant at $p = 1\ bar$ since the case without a turbocharger represents the low load conditions that is the most difficult for GCI engine to work at. The air flow rate was 50 Nl/min, and every flow rate of the gases in use was constant. The ozone generator was supplied with a constant 3 Nl/min flow of pure oxygen and the tube transferring the ozone to the test section was a $\phi = 2\ mm$ and $L = 1.5\ m$ not heated teflon pipe where the gases stayed for about 0.2 s. Also the sampling pipe had the same characteristics but here the residence time was about 0.15 s as the analyzer had a constant 115 l/h flow passing through. Concerning the nitric oxide (NO) addition, the first essay was the injection of the same quantity, in moles, of ozone and NO with the intermediate configuration previously presented. As the analyzer in use could only detect O_3, the process of calculating the flow rate coming from the NO bottle which had to be employed consisted in a few steps:

1. Heating the tube up to the desired temperature, in this first case 200 $°C$;
2. Settling on to a concentration of ozone, 190 ppm;
3. Calculating the molar flow rate (mol/min) of ozone;
4. Imposing the same molar flow rate of NO, which means a certain flow rate from the bottle and consequently an oxigen flow rate to even the nitrogen and restore the N/O ratio of air in the test section.

The fact that in the TS after this process there was no ozone left brought up the idea that the reaction between O_3 and NO was too fast to be observed with this configuration and these conditions; a further investigation with lower temperature ($T = 20\ °C$) with the aim of slowing down the reaction resulted again in the total absence of ozone in the TS. The solution found for this issue is dual, on one hand the configuration changed to the definitive one seen in the previous section, on the other, the addition of NO was set in different quantities relative to the one of O_3, defining a NO/O_3 ratio as in Tab.3.2.

Table 3.2: *Amount of NO injected depending on the NO/O_3 ratio.*

O_3 $*10^{-4}[mol/min]$	NO $*10^{-4}[mol/min]$	NO/O_3 ratio
5.4	5.4	1
5.4	4.05	0.75
5.4	2.7	0.5
5.4	1.35	0.25
5.4	0.68	0.125
5.4	0.54	0.1

Afterwards the experiments were carried out again with the same temperature settings and changing the amount of NO injected; in Fig.3.27 are presented the results for $T = 20\ °C$, it is possible to notice that the concentration of ozone remains constant along the Test Section, indicating that every reaction took place before reaching the first sampler.

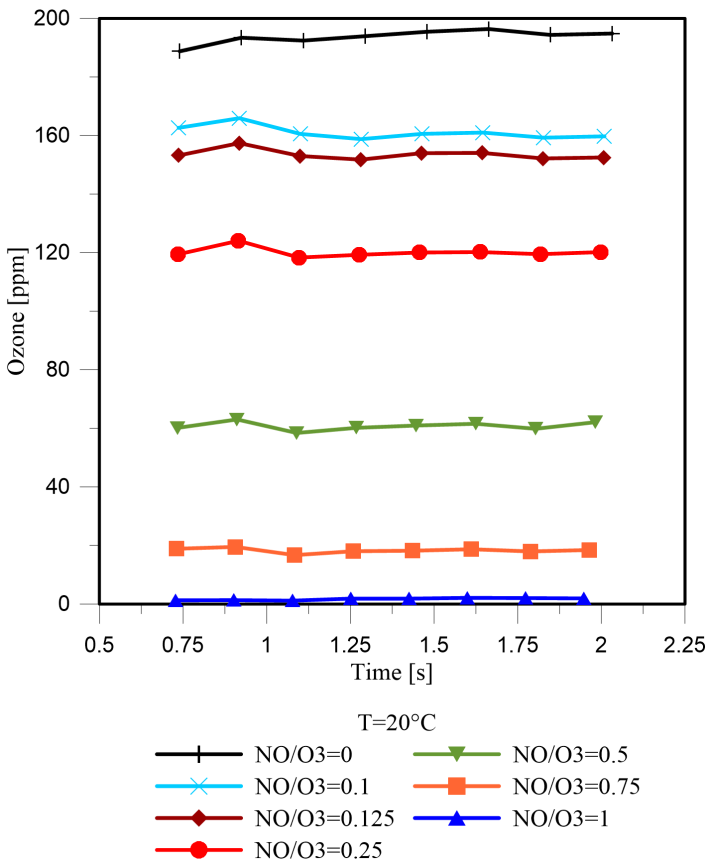

Figure 3.27: *Ozone concentration with $T = 20\ °C$ and every NO/O_3 ratio tested.*

With $T = 200\ °C$ instead, the concentration tends to decrease with time for every amount of NO injected, meaning that reactions could be still in place, Fig.3.28.

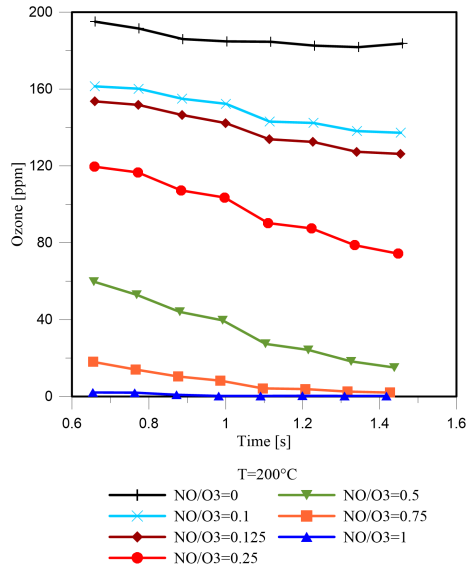

Figure 3.28: *Ozone concentration with $T = 200\ °C$ and every NO/O_3 ratio tested.*

In order to better analyze the behaviour of the species in Fig.3.29 is shown a comparison between the results of both temperatures.

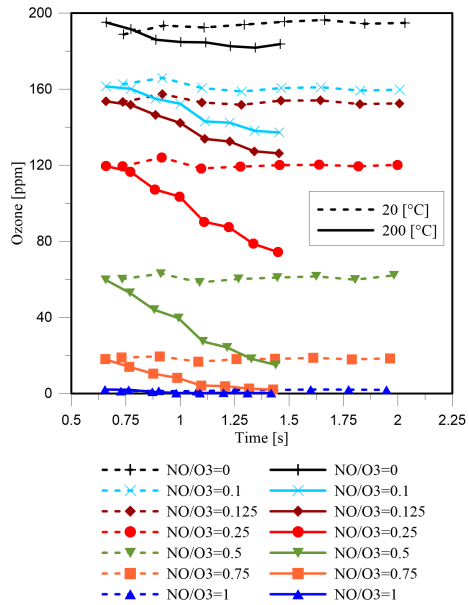

Figure 3.29: *Comparison between ozone concentration with $T = 20\ °C$ and $T = 200\ °C$.*

From this figure it is possible to see that, despite a different amount of time spent in the tube due to a change in speed, for every NO/O_3 ratio the concentration at both temperatures is similar at the first sampler, then one remains quite constant while the other drops monotonically in the following samplers. This could mean that the higher temperature may trigger some reactions that were not present or had little relevance at room temperature. Subsequently were performed test with $T = 100\ °C$ and $T = 150\ °C$ for every NO/O_3 ratio, results show that the former gave a constant trend similar to the one with $T = 20\ °C$, while the latter had a decreasing trend but the resulting ozone concentration is higher than the case with $T = 200\ °C$. In Fig.3.30 are shown results regarding only two NO/O_3 ratios, 0.5 and 0.25, for the sake of clarity.

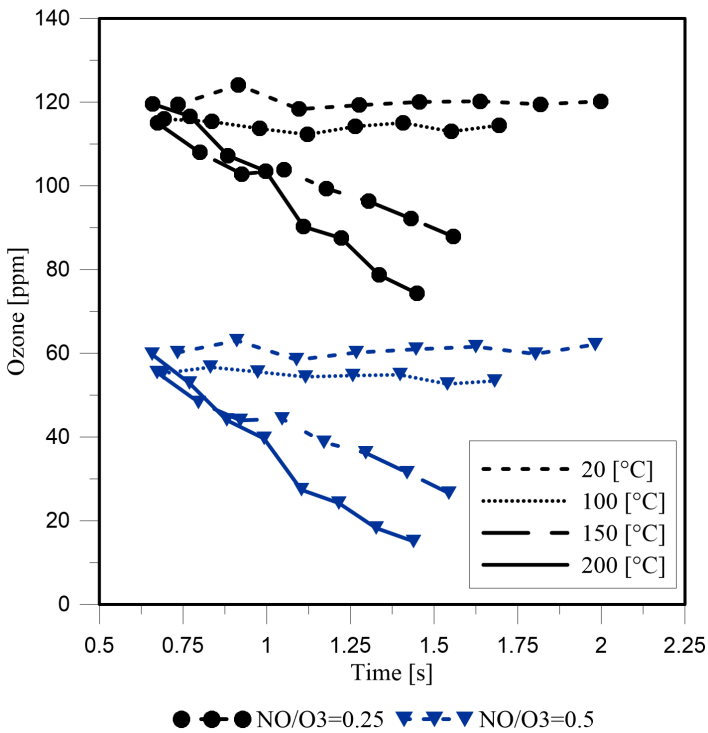

Figure 3.30: *Comparison between ozone concentration with different air temperature and NO/O_3 ratio of 0.5 and 0.25*

3.4.2 Simulation Results

In order to better explain the experimental results obtained, simulations were run using the Senkin [16] executable of the Chemkin II suite. The kinetic scheme used was proposed by Halter et al., perfectioned by Foucher et al.[9] and employed by Masurier et al.[19], it comprehends the ozone submechanism reported in Tab.3.3.

Table 3.3: *Ozone reactions submechanism.*[10]

Reaction	A	n	E	Reference
$O_3 + N_2 \rightarrow O_2 + O + N_2$	$4.00 \cdot 10^{14}$	0.0	22667	[26]
$O_2 + O + N_2 \rightarrow O_3 + N_2$	$1.60 \cdot 10^{14}$	-0.4	-1319	[26]
$O_3 + O_2 \rightarrow O_2 + O + O_2$	$1.54 \cdot 10^{14}$	0.0	23064	[26]
$O_2 + O + O_2 \rightarrow O_3 + O_2$	$3.26 \cdot 10^{19}$	-2.1	0	[26]
$O_3 + O_3 \rightarrow O_2 + O + O_3$	$4.40 \cdot 10^{14}$	0.0	23064	[26]
$O_2 + O + O_3 \rightarrow O_3 + O_3$	$1.67 \cdot 10^{15}$	-0.5	-1391	[26]
$O_3 + H \leftrightarrow O_2 + OH$	$8.43 \cdot 10^{13}$	0.0	934	[29]
$O_3 + O \leftrightarrow O_2 + O_2$	$4.82 \cdot 10^{12}$	0.0	4094	[2]
$O_3 + OH \leftrightarrow O_2 + HO_2$	$1.85 \cdot 10^{11}$	0.0	831	[18]
$O_3 + HO_2 \leftrightarrow O_2 + OH + O_2$	$6.02 \cdot 10^{9}$	0.0	938	[26]
$O_3 + H_2O \leftrightarrow O_2 + H_2O_2$	$6.62 \cdot 10^{1}$	0.0	0	[15]
$O_3 + CH_3 \leftrightarrow O_2 + CH_3O$	$3.07 \cdot 10^{12}$	0.0	417	[3]
$O_3 + NO \leftrightarrow O_2 + NO_2$	$8.43 \cdot 10^{11}$	0.0	2603	[2]
$O_3 + N \leftrightarrow O_2 + NO$	$6.03 \cdot 10^{7}$	0.0	0	[3]
$O_3 + H \leftrightarrow O + HO_2$	$4.52 \cdot 10^{11}$	0.0	0	[12]
$O_3 + H_2 \leftrightarrow OH + HO_2$	$6.00 \cdot 10^{10}$	0.0	19840	[34]
$O_3 + CH_4 \leftrightarrow CH_3O + HO_2$	$8.13 \cdot 10^{10}$	0.0	15280	[34]

Arrhenius equation $k = AT^n exp[-E/(1.9872T)]$. Units in mol, cm^3, s, K, and cal.

The validation of this entire kinetic scheme had already been carried out in previous works [19]. In order to reproduce the conditions occurring in the test section, Senkin was configured to run simulations with a constant 1 *bar* pressure and fixed both temperature and reactants concentrations in molar fraction. Considering that the experimental work was conducted with the aim of injecting the same quantity in moles of ozone and nitric oxide, the fact that in the simulations is required a concentration in molar fraction could cause discrepancies; in fact, mainly for high NO/O_3 ratio, the injection of nitric oxide causes a dilution of the original concentration of ozone and a 5% error with $NO/O_3 = 1$ (Fig.3.31). Thus it was necessary to calculate the right concentration of ozone to give to the simulation program in order to avoid this issue, reported in Tab.3.4.

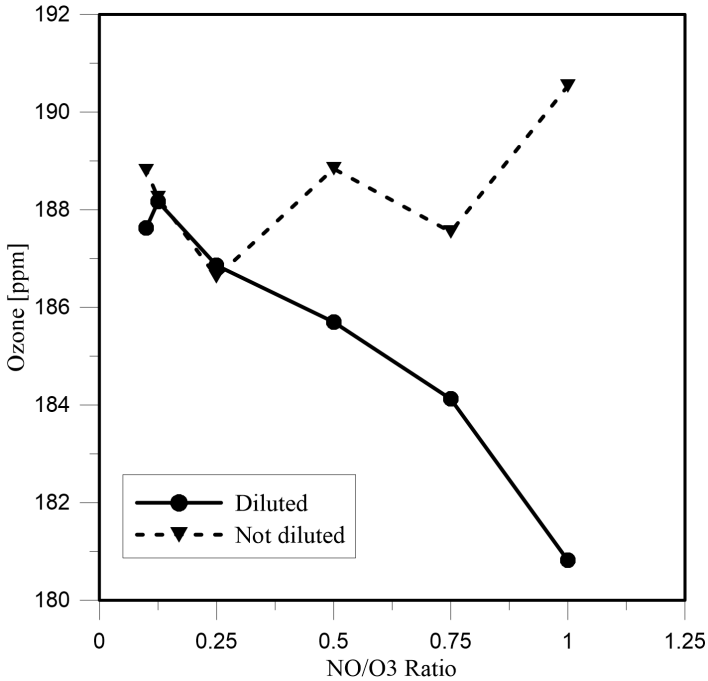

Figure 3.31: *Different concentration of ozone when injecting NO.*

Table 3.4: *Concentration of ozone and nitric oxide given to the simulation software.*

NO/O_3 ratio	O_3 [ppm]	NO [ppm]	O2·10^5 [ppm]	N2·10^5 [ppm]
0	190	0	2.0996	7.8985
0.1	189	19	2.0996	7.8984
0.125	188	23	2.0996	7.8983
0.25	187	46	2.0995	7.8981
0.5	185	92	2.09944	7.8978
0.75	183	137	2.0993	7.8975
1	181	181	2.0992	7.8971

Regarding the temperature, simulations were carried out for a wide range of values, even if the experimental limit is $T = 200\ °C$ due to the thermal resistance of certain parts of the set-up.
To begin the analysis, is shown in Fig.3.32 the variation in ozone concentration as a function of time, at different temperatures.
It is clear that from $T = 20\ °C$ to $T = 150\ °C$ the amount of ozone remains constant and it is possible to conclude that there is no ozone decomposition with these levels of temperature. For $T = 200\ °C$ and $T = 300\ °C$ instead, ozone levels tend to decrease rapidly and for this reason it is likely that the ozone decomposition reactions are occurring.

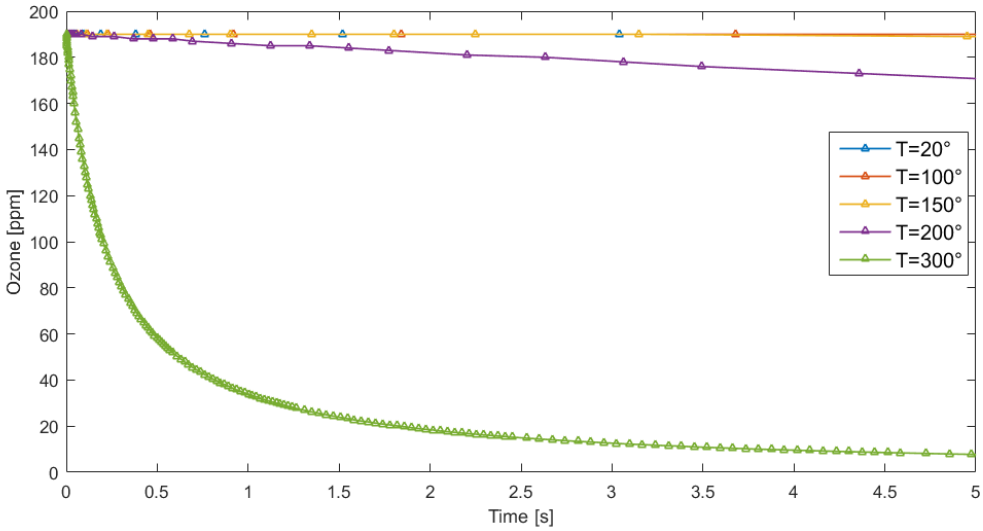

Figure 3.32: *Simulated ozone concentration without nitric oxide adduction, variable temperature.*

Moving our focus on the interaction between ozone and nitric oxide, below are presented the results of the simulations carried out with several quantities of NO (differences in NO/O_3 ratio) for various levels of temperature.
From these results it is clear that the reaction between ozone and nitric oxide is almost instantaneous and then settles on a different concentration depending on the NO/O_3 ratio; when the NO is not injected the ozone concentration remains almost constant, adding just a little amount reduces rapidly the concentration of ozone and so on with all the quantities. Regarding the effect of temperature, it enhance the reaction leading to an higher speed and a lower final concentration.

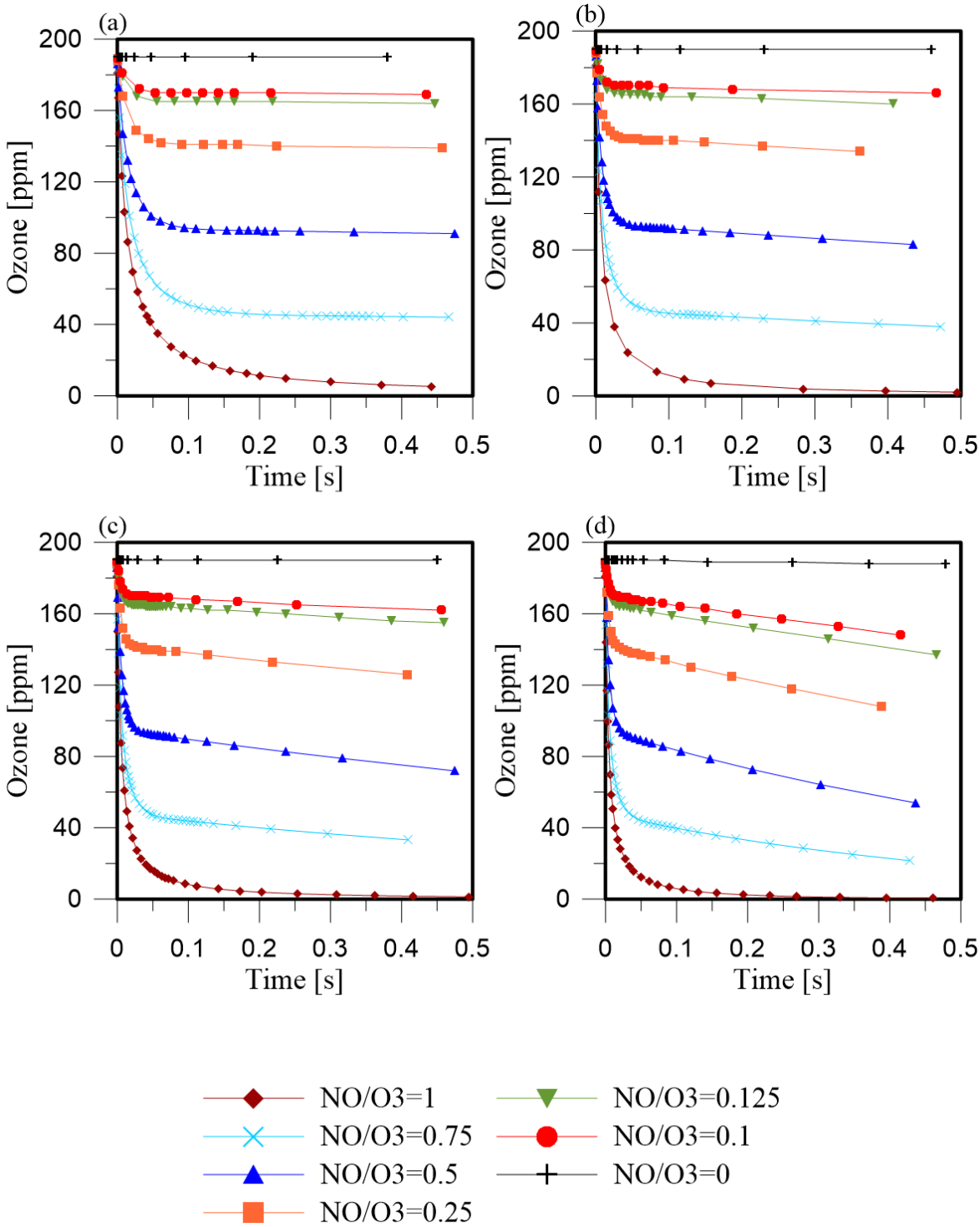

Figure 3.33: *Comparison between simulations at different temperatures: (a)* $T = 20\ °C$*, (b)* $T = 100\ °C$*, (c)* $T = 150\ °C$*, (d)* $T = 200\ °C$*.*

3.4.3 Simulation vs. Experimental

In this section will be shown a comparison between the results presented in the previous sections, however, before that it is necessary to discuss an issue regarding the time scale that will be used. First of all the time of the experimental part could be divided in three portions (Fig.3.34):

- $T_a \simeq 0.37\ s$, ozone adduction time, needed for the ozone to pass from the generator to the injector.
- T^*, variable with temperature, is the time that intervene between the injection and the first sampler. It is approximable with the time between two consecutive samplers (Step Time).
- T_{TS}, also variable, see Tab.3.5, is the time needed to pass through the Test Section.
- $T_m \simeq 0.15\ s$, ozone out time, needed for the ozone to pass from the test section to the analyzer.

Table 3.5: *Time portion variability with temperature.*

Temperature $[°C]$	Mass Flow $[Nl/min]$	Step Time $[s]$	Test Section Time $T_{TS}[s]$
20	50	0.1743	1.3941
100	50	0.1383	1.1068
150	50	0.1220	0.9759
200	50	0.1091	0.8730

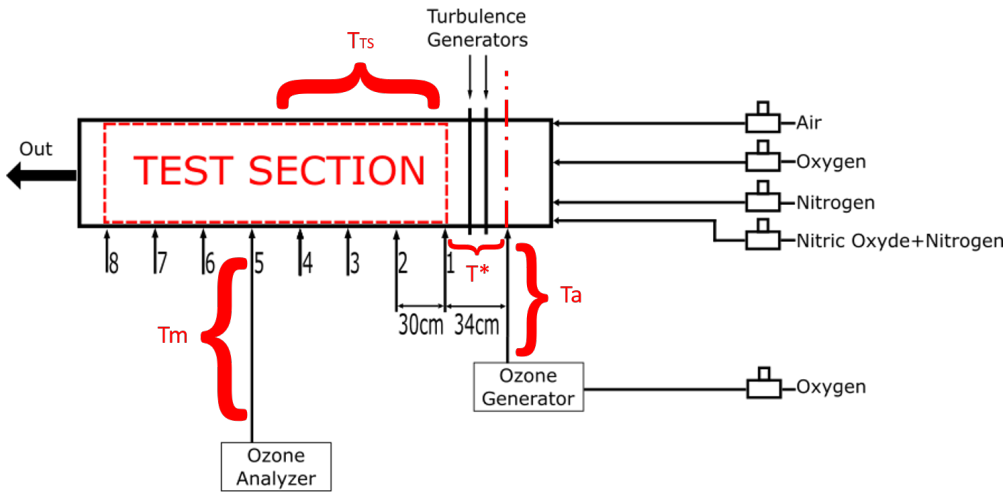

Figure 3.34: *Pipe scheme with indication of the time portions.*

Since at the beginning of the simulations the species are in contact at the set concentrations, it is not possible to compare the experimental and simulative results unless T_a is left out. Although, in order not to make any mistakes by not considering T_a and the reactions that may occur during that segment of time, a simulation of the adduction pipe with high concentrations of the species and $T = 20\ °C$ was carried out. Results show that in this time portion no reaction is in place (Fig.3.35) and thus it is safe to change the time scale of the experimental data so that it concurs with the simulative one.

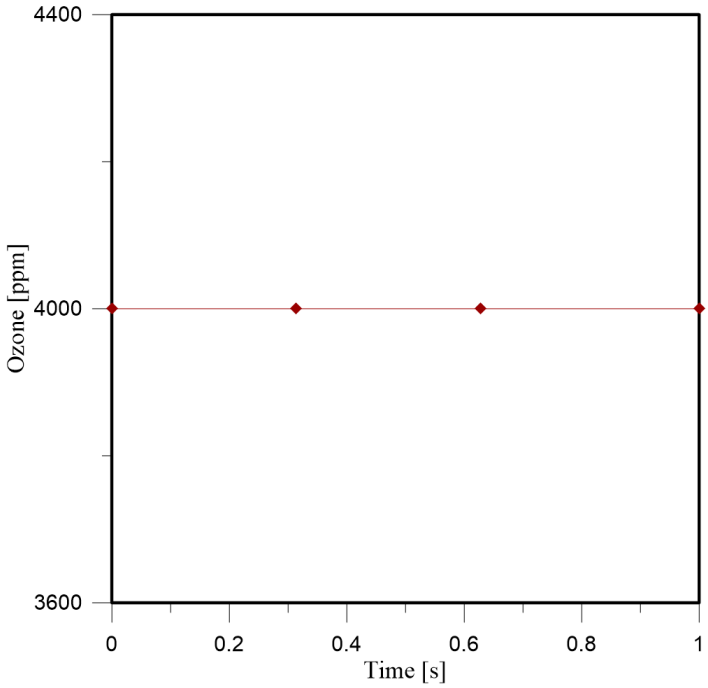

Figure 3.35: *Adduction pipe simulation.*

It is now possible to compare the experiments with the simulations. In Fig.3.36 it is possible to see that the results coming from the simulations and from the experiments have the same trends which means that it was possible to reproduce the actual phenomena that occur in the test section. However, it also noticeable that the dots, representing the experimental points, are not exactly on the line representing that simulated situation. These discrepancies could be caused by measuring errors (i.e. lack of precision of the instruments), differences between the model and the reality or other factors, but the overall results are satisfying.
Furthermore it is observable that the experimental data cover only a small part of the simulated time and that the first instants in which occur most of the reactions (T^*) cannot be studied experimentally with this set-up, a measurement much closer to the ozone injection could probably solve this issue. At this temperature, after T^* and T_{TS}, the simulation reveals that the concentration ozone reaches 0 *ppm* due to the joint reaction with NO and O_3 decomposition, although this could not be observed with the experimental set-up in use.

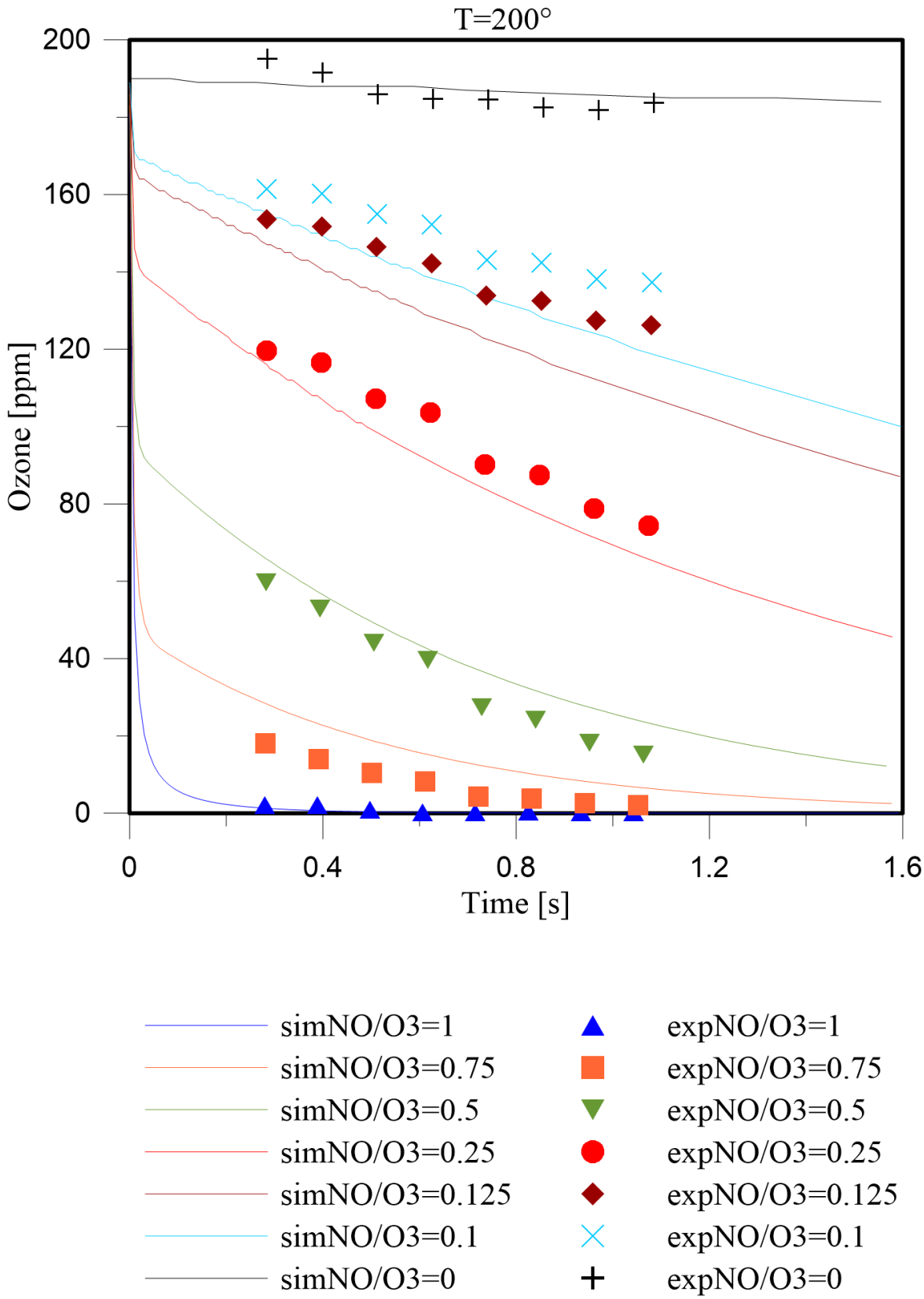

Figure 3.36: *Comparison between simulation and experimental data, with* $T = 200\ °C$.

Chapter 4

Ozone seeding in a GCI engine

After the study of the injector with a 120° UA in Chapter 2 and the work carried out on the Ozone decomposition in Chapter 3, the work focused on the application of ozone generators to the intake manifold of a GCI engine. This solution could be helpful in overcoming the low load limits of GCI engines without the implementation of expensive systems, such as VVT or variable geometry turbines, and instead apply an ozone generator, since their technology is developing very compact and cheap solutions. In order to study the GCI combustion assisted by ozone it was decided to begin with the evaluation of the amount of ozone needed to attain a stable combustion, first at low load varying the intake temperature, then at idle speed.

4.1 Experimenal set-up

The configuration used in this part of experimental work is approximately the same seen in Chapter 2, with a few additions; in fact the engine and its controls remain the same, as the injector and the exhaust gas analyzer, while there was the inclusion of four ozone generators, the MFCs essential to regulate the flow of oxygen through every ozone generator and an ozone analyzer. In particular, the main ozone generator was the Anseros COM-AD-01 (see section 3.3) and it could be controlled remotely through the LabView interface shown in Fig.4.1; in addition to it were used the Anseros COM-AD-02, COM-AD-01-IP and COM-SD-500 in order to supply the amount of ozone required, for these three a remote controlling system was not available and they had to be switched on and adjusted manually.

Table 4.1: *Characteristics of the ozone generators employed.*

Ozone Producer	Max Capacity $[gO_3/h]$	Carrier Gas	Adjustable
Anseros COM-AD-01	5	Oxygen	Yes
Anseros COM-AD-02	10	Oxygen	Yes
Anseros COM-AD-01-IP	3.5	Oxygen	Yes
Anseros COM-SD-500	0.5	Oxygen	No

Regarding the ozone analyzer, since the high quantity supplied, the Anseros MP-6060 previously presented was not suitable and it was replaced with the Anseros MP-6020 which also applies the principle of UV absorption in order to measure the concentration of ozone but has a wider operative range.

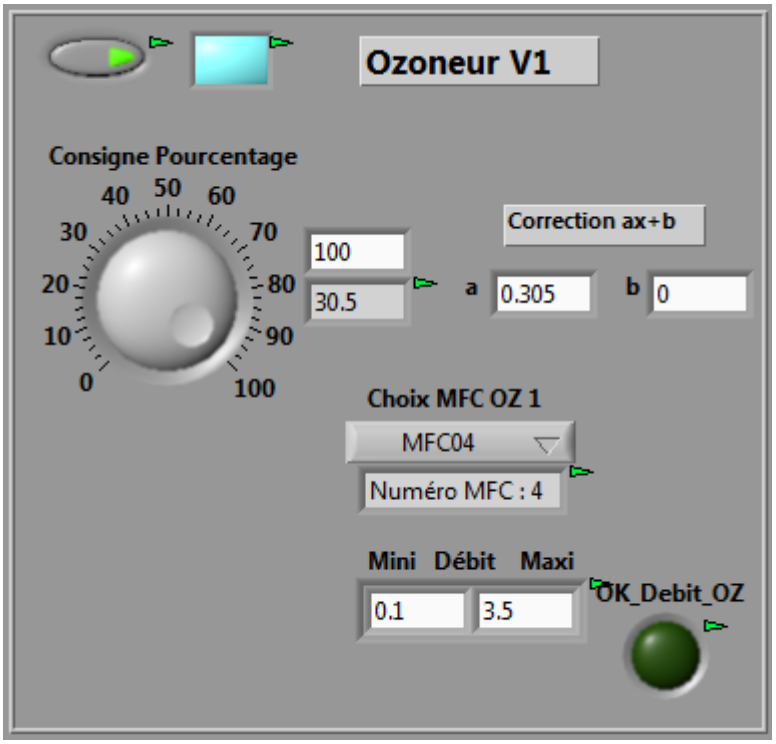

Figure 4.1: *Labview interface to control ozone production.*

As it is possible to see in Fig.4.2 the ozone producers work in parallel, with a constant oxygen supply of 3 Nl/min and the ozone generated is inserted in the intake manifold along with the air and the nitrogen needed to restore the N/O ratio of air. All these species come in contact in a plenum that helped creating an homogeneous mixture. Subsequently, a few centimeters above the intake valves, it is possible to find the sampling tube that carried a small quantity of the mixture to the analyzer in order to determine the concentration of ozone at the intake of the engine.

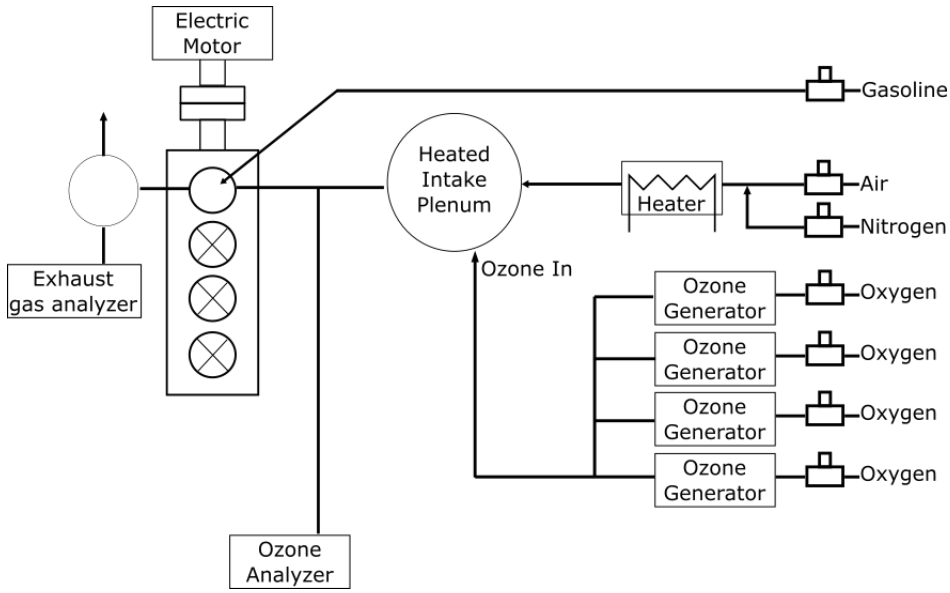

Figure 4.2: *Scheme of the experimental setup.*

4.2 Low Load Operation

As seen in previous works by Foucher et al. [9] and Masurier et al. [19] ozone acts as a promoter of the combustion enhancing the processes of oxidation. In this section, instead of quantifying the effect of ozone by observing the advanced combustion with a fixed intake temperature, it was possible to set the phasing and to observe that the addition of ozone can allow for lower intake temperatures. The injection strategy was kept constant with a first injection at bottom dead center and a second one five CAD before top dead center; the fuel mass, the IMEP, the intake pressure and the CA50 were also constant, as reported in Tab.4.2.

Table 4.2: *ozone seeded engine operative conditions*

	Mean	Standard deviation	RSD
Speed	1500[rpm]		
P admission	1[bar]		
Fuel mass (50%SOI 1 - 50%SOI 2)	0.5254[kg/h]	0.008535	1.6%
Brettsinger Equivalence ratio	0.3538	0.02493	7.04%
CA50	6.146[CAD]	0.2235[CAD]	3.6%
IMEP	3.029[bar]	0.05092[bar]	1.68%

In order to avoid the effect of the cylinder walls heating up the intake air, it was decided to start with T_{adm} = 40°C and then increasing it. In every step the ozone concentration started from 0 ppm and then was gradually increased in order to reach a fixed CA50 of about 6 [CAD]. Unfortunately when it was reached a level of temperature (150°C) in which the combustion occurred without ozone seeding, it was not possible to obtain the desired CA50 but the combustion was stable with a CA50 of about

3 CAD; although in order to reach the chosen phasing various strategies can be actuated, such as EGR or a delayed second injection, these solutions are not discussed in this work.

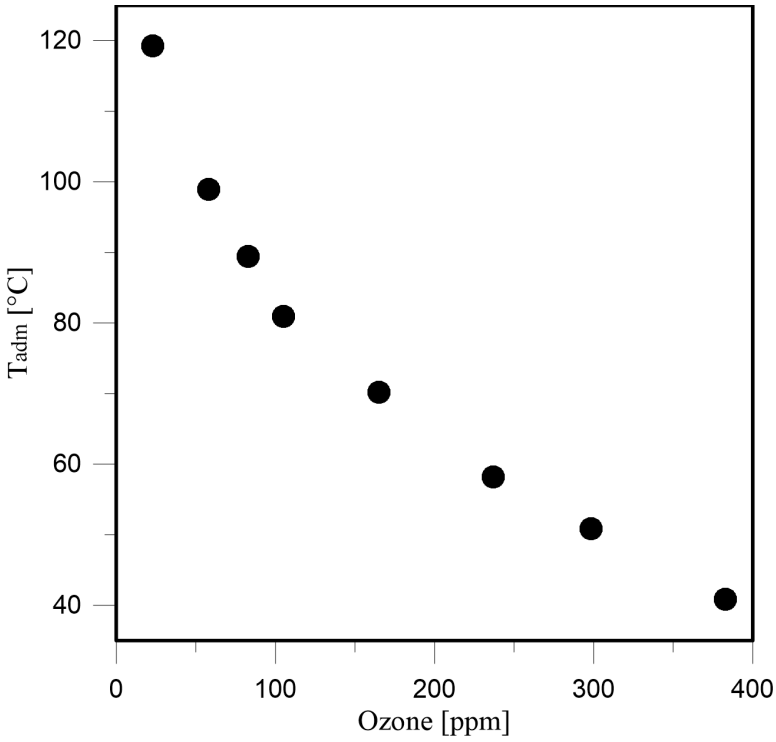

Figure 4.3: *Tadm vs ozone.*

Regarding Fig.4.3 it is possible to notice the influence of the ozone on the admission air temperature, as T_{adm} rose less and less ozone is needed to reach the desired CA50. With less than 400 [*ppm*] of ozone the chosen combustion occurs at 40°C and, probably due to the positive effect of the cylinder wall temperature, at 120°C it burns almost without ozone.
Combustion efficiency in Fig.4.4 has a maximum at 120°C with an ozone concentration of 23 [*ppm*], then it drops and remain almost constant until the minimum temperature reached with a concentration of 383 [*ppm*], this trend could be explained with the fact that, as mentioned at the beginning of Chapter 2, this efficiency represents the amount of fuel that takes part to the combustion in relation to the fuel injected and with this operative strategy there probably is a lot of stratification in the combustion chamber, due to the second injection near TDC, and this leads to a more progressive combustion with less fuel taking part to it.

The Max in Cylinder pressure gradient (Fig.4.5) decreases in accordance with a lower intake temperature as the amount of ozone was increased.

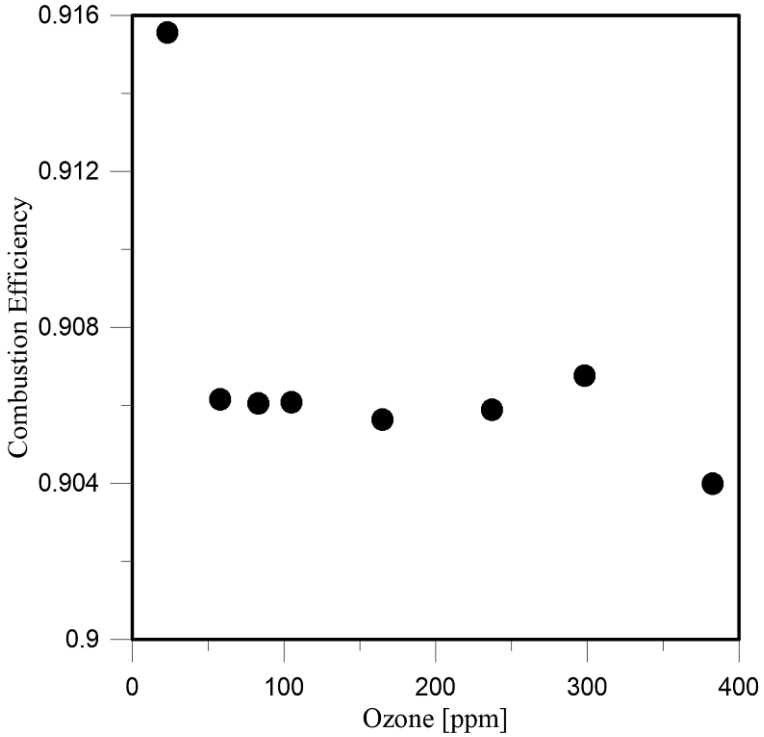

Figure 4.4: *Combustion Efficiency vs ozone.*

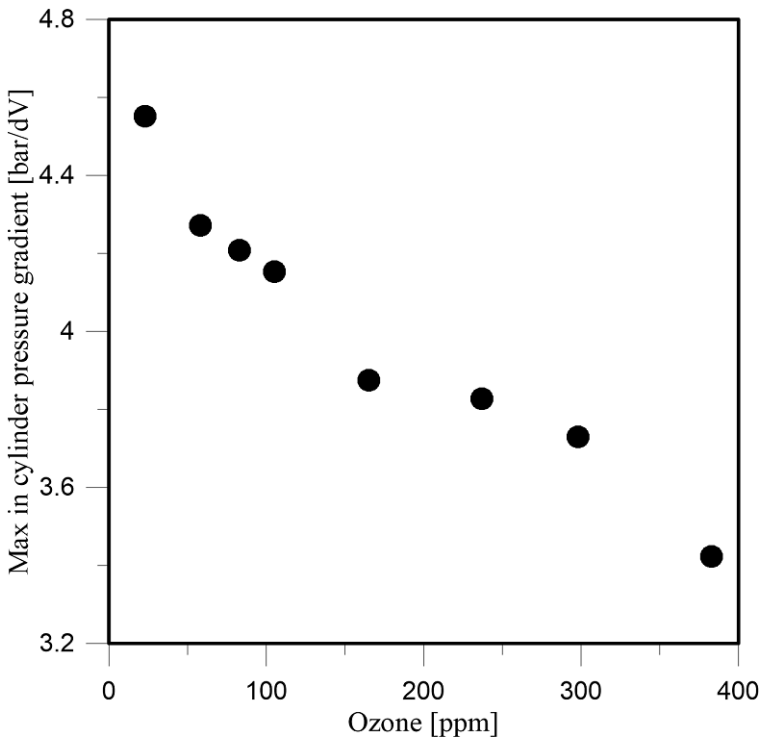

Figure 4.5: *Max in Cylinder pressure gradient.*

This hypothesis could be also supported by Fig.4.6 in which is visible a correlation between the intake temperature and the maximum mean temperature reached in the cylinder; a greater amount of ozone thus leads to lower T_{adm} and consequently lower pressure gradients in the cylinder, which means less noise and less mechanical stress on the engine.

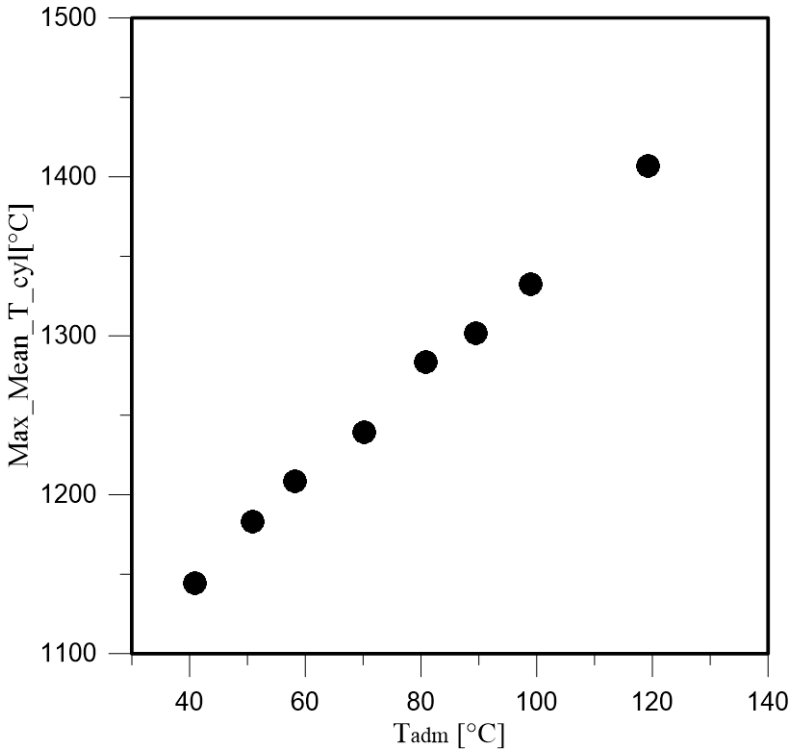

Figure 4.6: *Tadm vs Max Mean T cylinder.*

In order to verify and calibrate the effect of the cylinder walls heating up the intake air, it was repeated this experiment with a different approach: instead of slowly rising the intake temperature, it was set on the minimum value at which the combustion could start and be stable without ozone and then it was brought down following the curve in Fig.4.3. As mentioned before the points present a fixed CA50 of 6 CAD and a fixed fuel mass flow, the only point that differs is the one with no ozone where, with this injection strategy, it was obtained a slightly advanced combustion phasing, with a CA50 of 3 CAD.

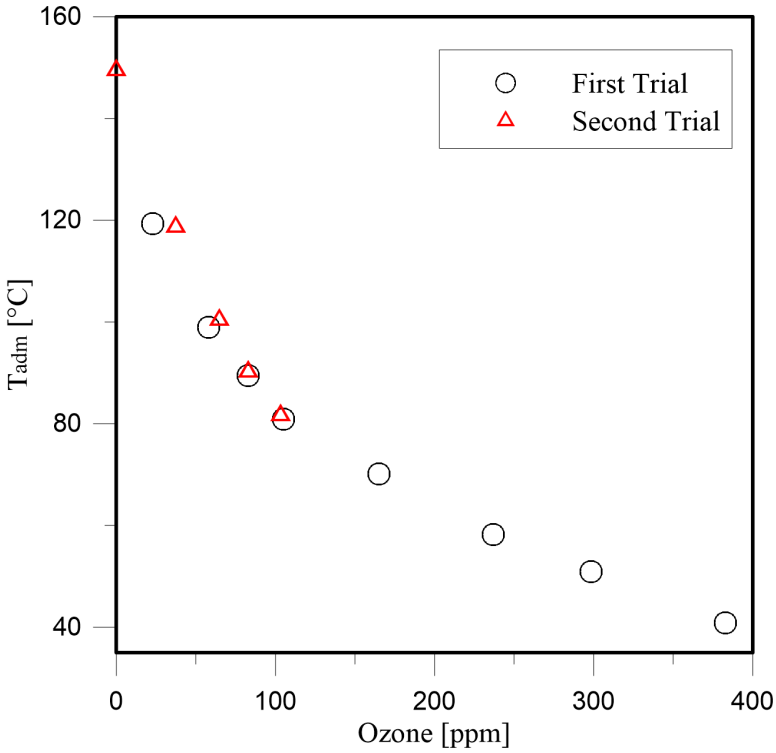

Figure 4.7: *Comparison between different approaches at the same experiment.*

In Fig.4.7 "First Trial" is referred to the one described above, while "Second Trial" stands for the different approach used later. It is clear how the points are less apart as ozone concentration rises and in general the two lines don't differ much.
There are some aspects in which it is possible to notice some differences though, the emissions in fact present similar trends but unalike values, as visible in Fig.4.8 and Fig.4.9.

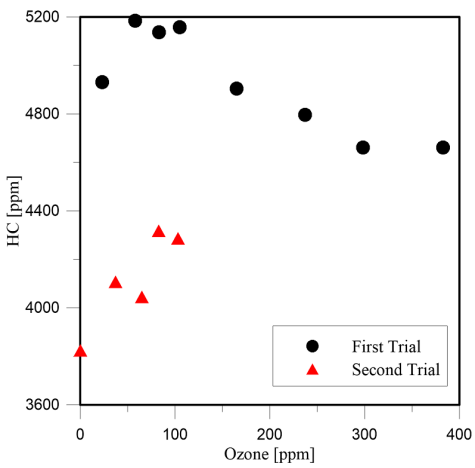

Figure 4.8: *HC emissions with ozone seeded intake.*

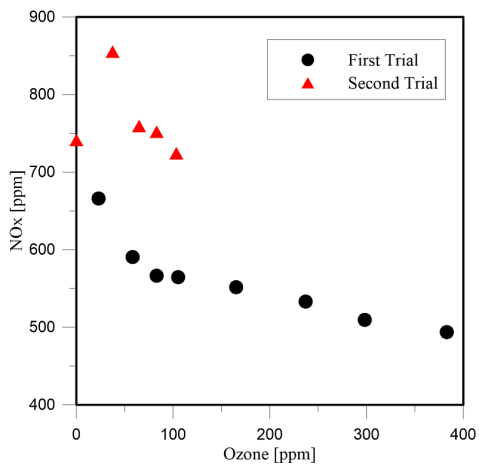

Figure 4.9: *NO_x emissions with ozone seeded intake.*

These differences could be explained with the behaviour of the maximum temperature inside the combustion chamber, in Fig.4.10, as it resulted higher for every point taken in the second trial, leading to an higher concentration of NO_x and a lower amount of HC.

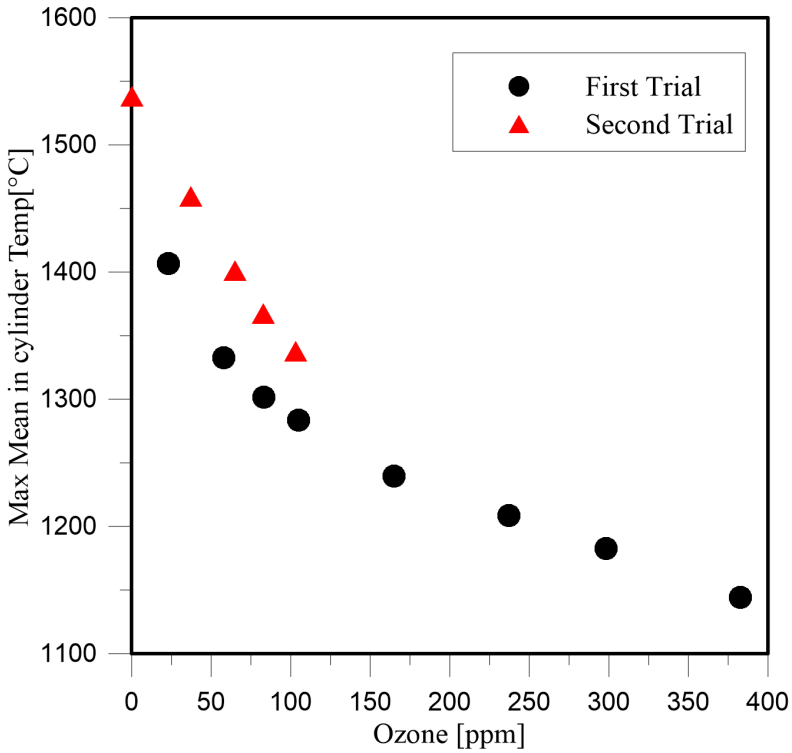

Figure 4.10: *Max temperature with ozone seeded intake.*

The fact that the temperatures reached in the second trial were higher than the ones of the first trial may be due to the fact that the cylinder walls heating up the air leading to the differences in emissions showed above.

4.3 Idle condition

In order to better evaluate the technical feasibility of the GCI combustion at low temperature ($T_{adm} = 40°$) some experiments were carried out at idle condition. The fuel mass flow was kept constant with a single injection varying the ozone concentration. This strategy was carried out for two SOIs: one at top dead center reproducing HCCI conditions and one at bottom dead center. In Tab.4.3 it is possible to see the operative conditions adopted.

Table 4.3: *Operative conditions of engine at idle speed.*

	Mean	Standard deviation	RSD
Speed	800[rpm]		
P admission	1[bar]		
T_{adm}	40,197°C	0,8599	2.1%
Fuel mass	0,1789[kg/h]	0,001126	0.63%

By comparing the results for the two SOIs adopted it is possible to compare the HCCI operative conditions and the partially premixed charge; this because with SOI placed at top dead center the fuel has a sufficient amount of time to create an homogeneous mixture that ignites uniformly, while placing the SOI at bottom dead center gives less time for the fuel to mix and should result in a more stratified charge.

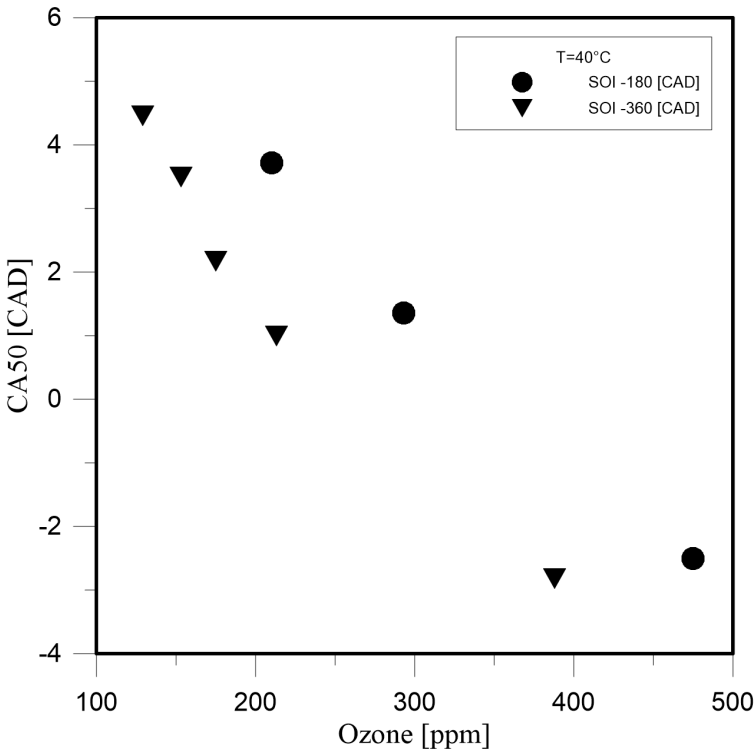

Figure 4.11: *Influence of ozone on CA50.*

As it is possible to notice in Fig.4.11, ozone has a remarkable influence on combustion phasing and the result is an advancing CA50 as the amount of ozone increases.

This result is common between the two injection strategies, but it is also clear that there are differences, in fact if the aim is obtaining the same CA50 the quantity of ozone that needs to be seeded is much lower in the case with an early injection strategy. This phenomenon could be due to the fact that, with an early injection, fuel and ozone come in contact during the intake stroke and thus have more time to react, while with a delayed injection this time is limited and the effect of ozone is less marked.

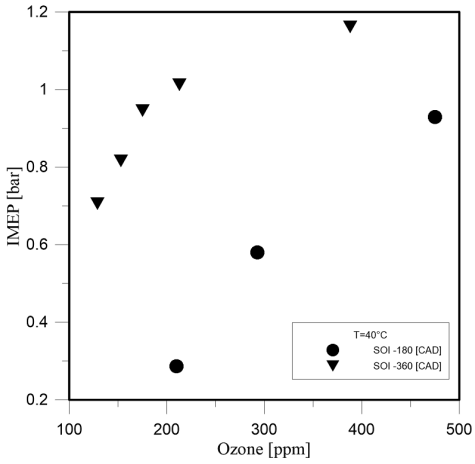

Figure 4.12: *Influence of ozone on IMEP.*

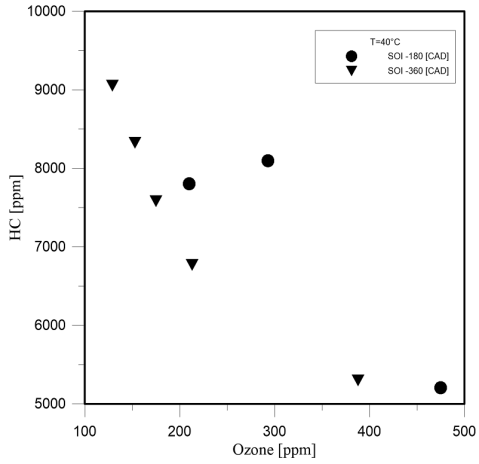

Figure 4.13: *Influence of ozone on HC emissions.*

These differences can also be seen in Fig.4.12, where the promoting effect of ozone on the combustion generally leads to an higher IMEP with higher quantities of ozone but, focusing in the differences between the two strategies, it is clear that with a fixed quantity of ozone seeded at the intake, the highest values of IMEP are the ones using an early injection strategy.
Regarding the HC emissions, it is possible to notice in Fig.4.13 a decreasing trend when an early injection is in place, while for the late injection strategy the trend is visible but not extremely clear and this could be associated with the hypothesis of a lower effect of ozone when this strategy is adopted and consequently an higher amount of this oxidizing species is needed.
Focusing on other pollutant emissions, NO_x where also measured and it was found that in this operative condition there were almost no NO_x at the exhaust, with values lower than 2 ppm for every point taken. Particulate matter was also tested and, as for NO_x, the amount of this pollutant is very low as it always remains under 0.125 FSN.

Chapter 5

Conclusions

This work focused on an innovative approach that aimed to reduce fuel consumption in internal combustion engines and thus respect the more and more strict CO_2 emissions requests.
This goal was pursued with ozone seeding in the intake of a gasoline compression ignition engine. GCI engines were chosen because they could deliver efficiencies comparable with CI engines using a more globally diffused fuel, such as gasoline. In literature there are examples of this technology [31] [33] [30] [32] [4] in which a DOHC VVT and a two stage turbocharger coupled with a supercharger were applied to the engine leading to a very expensive solution; a more cost-effective stategy could consist in ozone assisted GCI.
The first part of this work are presented the experiments on a GCI engine equipped with a 120° UA injector, in order to evaluate the performances of this engine and find out its limits when operating without ozone or any other system previously mentioned. With the operative conditions reported in Tab.2.2, it was studied the impact of injection timing, moving down the SOI from TDC, with a single injection.
Results from these experiment pointed out that there is a range of admitted SOI in order to obtain a stable combustion and an high combustion efficiency, moreover with this injection strategy there is an issue with the maximum pressure gradient inside the cylinder as there are points where this parameter reaches levels that are not acceptable in terms of comfort and noise inside the vehicle. For this reason the focus moved on a double injection strategy that could provide a less punctual combustion and thus less noise and mechanical stress.
Furthermore using a double injection strategy is a mean to control the combustion phasing, as it depends on thermodynamical conditions inside the combustion chamber and a separation between first and second injection can provide an appropriate fuel stratification.
Despite the promising results, there are still challenges that engineering have to face in order to develop this technology. The most important is the low load operation, in fact under these conditions there are limits caused by many factors, such as low fuel propensity to autoignition and difficulties in the control of the combustion phasing. One method to address this problem could be the use of ozone, in literature are present several works related to this topic [6] [9] [10] [19] [24] although they all show the effect of this specie inside the engine; the aim of this investigation was to detect

the reactions that take place in the intake manifold but since this kind of study is nearly impossible to do while the engine is running, it was decided to develop a proper experimental setup.
The setup was created with the intention of reproducing the conditions present in the intake manifold of the engine, where it is also interesting to analyze the interaction between ozone and other species, such as nitric oxide, that can be found at the intake when an EGR strategy is in place.
Results show that ozone does not decompose at room temperature, only if it is set above 150 °C the decomposition is detectable with the experimental setup created. Regarding the interaction with NO, the reaction is very fast and occurs also at 20 °C but increasing the temperature leads to a lower amount of ozone detectable, probably as the decomposition reaction begins.
In order to support the results obtained, simulations were run using the Senkin [16] executable of the Chemkin II suite. These data present the same trend observable in the experimental trials, which means that it was possible to reproduce the actual phenomena that occur in the test section; despite the presence of some discrepancies that may be due to measuring errors, differences between the model and the reality or other factors, the overall results are satisfying. The experimental results cover only a small portion of the simulated time and it could be very interesting, as a future development, the investigation of this phenomena on a lager time scale, especially sampling closer to the injection of ozone, where most of these fast reactions take place. Another promising topic for future works is the analysis of the interaction of ozone with other EGR species and their mixtures, such as carbon oxides, water, etc.
Subsequently to the work about GCI engine and ozone decomposition, it was decided to join the topics through the application of ozone generators to the intake manifold of a GCI engine. In order to study ozone assisted GCI combustion four ozone generators were applied and the goal was to determine the amount of ozone necessary to reach a stable combustion, first at low load varying the intake temperature, then at idle speed. Previous works show that ozone can act as a promoter of the combustion, here it was decided to fix the combustion phasing (CA50=6 CAD) and observe its effect as the intake temperature could be lowered. The experimental strategy for the low load operation aimed to reduce the effect of the hot cylinder walls heating up the intake air and the results show that it is possible to reach the desired combustion with less than 400 ppm of ozone and a 40 °C intake temperature. Moreover, the temperature was increased until 150 °C where no ozone was necessary.
The experiments performed at idle speed had a constant 40 °C intake temperature, while the amount of ozone varied. Two single injection strategies were adopted, one with a BDC injection and the other with a TDC injection to reproduce HCCI conditions. The former allows for a less homogeneous charge and less time for the ozone to react with the fuel, this is confirmed by the fact that in order to obtain the same CA50 the amount of ozone needed is higher than the case reproducing HCCI.

Seen the results obtained throughout this entire work, it is safe to say that this technology could be a practicable solution to reduce the fuel consumption of traditional internal combustion engines and thus reducing the CO_2 production. However, there still are some technical aspects that need to be addressed, such as the compactness of ozone generators, the interaction of other EGR species with ozone, the production of this oxidizing specie from air and the optimization of various engine parameters.
As concern the ozone production, one solution could be represented by a prototype of ozone generator (Fig.5.1) that the PRISME Laboratory is currently developing; this solution should solve both the problems of dimensions and production from air but it needs to be optimized in order to be reliable and to produce the amount of ozone necessary.

Figure 5.1: *Ozone generator prototype.*

Bibliography

[1] Ulf Aronsson, Öivind Andersson, Rolf Egnell, Paul C. Miles, and Isaac W. Ekoto. Influence of Spray-Target and Squish Height on Sources of CO and UHC in a HSDI Diesel Engine During PPCI Low-Temperature Combustion. 4970, 2009.

[2] R Atkinson, D L Baulch, R A Cox, J N Crowley, R F Hampson, R G Hynes, M E Jenkin, M J Rossi, and J Troe. Evaluated kinetic and photochemical data for atmospheric chemistry: Volume I - gas phase reactions of Ox, HOx, NOx and SOx species. *Atmospheric Chemistry and Physics*, 4(6):1461–1738, 2004.

[3] R. Atkinson, D. L. Baulch, R. A. Cox, R. F. Hampson, J. A. Kerr (Chairman), and J. Troe. Evaluated Kinetic and Photochemical Data for Atmospheric Chemistry: Supplement III. IUPAC Subcommittee on Gas Kinetic Data Evaluation for Atmospheric Chemistry. *Journal of Physical and Chemical Reference Data*, 18(2):881, 1989.

[4] Patrick Borgqvist, Per Tunestl, and Bengt Johansson. Comparison of Negative Valve Overlap (NVO) and Rebreathing Valve Strategies on a Gasoline PPC Engine at Low Load and Idle Operating Conditions, 2013.

[5] Massimo Capobianco. Motori a combustione interna - Notes from the course of Internal Combustion Engines. *University of Genoa*, 2014.

[6] Francesco Contino, Jean Baptiste Masurier, Fabrice Foucher, Tommaso Lucchini, Gianluca D'Errico, and Philippe Dagaut. CFD simulations using the TDAC method to model iso-octane combustion for a large range of ozone seeding and temperature conditions in a single cylinder HCCI engine. *Fuel*, 137:179–184, 2014.

[7] John E Dec. A Conceptual Model of DI Diesel Combustion Based on Laser-Sheet Imaging*. In *SAE Technical Paper*. SAE International, 1997.

[8] John E. Dec. Advanced compression-ignition engines - Understanding the in-cylinder processes. *Proceedings of the Combustion Institute*, 32 II(2):2727–2742, 2009.

[9] F. Foucher, P. Higelin, C. Mounam-Rousselle, and P. Dagaut. Influence of ozone on the combustion of n-heptane in a HCCI engine. *Proceedings of the Combustion Institute*, 34(2):3005–3012, jan 2013.

[10] F Halter, P Higelin, and P Dagaut. Experimental and Detailed Kinetic Modeling Study of the Effect of Ozone on the Combustion of Methane. *Energy & Fuels*, 25(7):2909–2916, 2011.

[11] J B Heywood. *Internal Combustion Engine Fundamentals*. Automotive technology series. McGraw-Hill, 1988.

[12] Carleton J. Howard and Barbara J. Finlayson-Pitts. Yields of HO2 in the reaction of hydrogen atoms with ozone. *The Journal of Chemical Physics*, 72(6):3842, 1980.

[13] Gautam T Kalghatgi, Per Risberg, and Hans-erik Ångström. Partially Pre-Mixed Auto-Ignition of Gasoline to Attain Low Smoke and Low NOx at High Load in a Compression Ignition Engine and Comparison with a Diesel Fuel Partially premixed auto-ignition of gasoline to attain low smoke and low NOx at high load in a c. (September 2016), 2007.

[14] Ulrich Kogelschatz. Dielectric-Barrier Discharges: Their History, Discharge Physics, and Industrial Applications. *Plasma Chemistry and Plasma Processing*, 2003.

[15] Ming-Taun Leu, Shiro Hatakeyama, and Kuang-Jung Hsu. Rate constants for reactions between atmospheric reservoir species. I - HCl. (type 11):5784–5789, 1989.

[16] A E Lutz, R J Kee, J A Miller, and Sandia National Laboratories. *SENKIN: A FORTRAN Program for Predicting Homogeneous Gas Phase Chemical Kinetics Wdith Sensitivity Analysis*. SAND (Series) (Albuquerque, N.M.). Sandia National Laboratories, 1988.

[17] P. Manente, V., Johansson, B., and Tunestal. Partially Premixed Combustion at High Load using Gasoline and Ethanol, a Comparison with Diesel. 2009.

[18] Alex Mansergas and Josep M Anglada. The gas-phase reaction between O3 and HO radical: a theoretical study. *Chemphyschem : a European journal of chemical physics and physical chemistry*, 8(10):1534–9, jul 2007.

[19] J Masurier, F Foucher, G Dayma, and P Dagaut. Homogeneous Charge Compression Ignition Combustion of Primary Reference Fuels In fl uenced by Ozone Addition. 2013.

[20] J.-B. Masurier, F Foucher, G Dayma, and P Dagaut. Ozone applied to the homogeneous charge compression ignition engine to control alcohol fuels combustion. *Applied Energy*, 160(C):566–580, 2015.

[21] Jean-baptiste Masurier. Etude expérimentale de la combustion HCCI par l ' ajout d ' espèces chimiques oxydantes minoritaires. 2016.

[22] Jean-Baptiste Masurier, Fabrice Foucher, Guillaume Dayma, and Philippe Dagaut. Effect of Additives on Combustion Characteristics of a Natural Gas Fueled HCCI Engine. In *SAE Technical Paper*, Birmingham, United Kingdom, 2014.

[23] Jean-Baptiste Masurier, Fabrice Foucher, Guillaume Dayma, and Philippe Dagaut. Investigation of iso-octane combustion in a homogeneous charge compression ignition engine seeded by ozone, nitric oxide and nitrogen dioxide. *Proceedings of the Combustion Institute*, 35(3):3125–3132, 2015.

[24] Jean Baptiste Masurier, Fabrice Foucher, Guillaume Dayma, and Philippe Dagaut. Investigation of iso-octane combustion in a homogeneous charge compression ignition engine seeded by ozone, nitric oxide and nitrogen dioxide. *Proceedings of the Combustion Institute*, 35(3):3125–3132, 2015.

[25] P. C. Miles and O. Andersson. A review of design considerations for light-duty diesel combustion systems. *International Journal of Engine Research*, 17(1):6–15, 2016.

[26] Timothy Ombrello, Sang Hee Won, Yiguang Ju, and Skip Williams. Flame propagation enhancement by plasma excitation of oxygen. Part II: Effects of O2(a1Δg). *Combustion and Flame*, 157(10):1916–1928, 2010.

[27] Pietro Matteo Pinazzi, Tony Tahtouh, Oliver Guézet, and Foucher Fabrice. Influence of Umbrella Angle and Injection Strategy on the Low Load Operation of a Gasoline Compression Ignition (GCI) Engine. 2016.

[28] P.M. Pinazzi and F. Foucher. Influence of injection parameters, ozone seeding and residual NO on a Gasoline Compression Ignition (GCI) engine at low load. *Proceedings of the Combustion Institute*, 2016.

[29] S P Sander, R R Friedl, D M Golden, M J Kurylo, G K Moortgat, P H Wine, A R Ravishankara, C E Kolb, M J Molina, San Diego, La Jolla, R E Huie, and V L Orkin. Chemical Kinetics and Photochemical Data for Use in Atmospheric Studies. (15), 2006.

[30] Mark Sellnau, Matthew Foster, Kevin Hoyer, Wayne Moore, James Sinnamon, and Harry Husted. Development of a Gasoline Direct Injection Compression Ignition (GDCI) Engine. *SAE 2014-01-1300*, apr 2014.

[31] Mark Sellnau, Wayne Moore, James Sinnamon, Kevin Hoyer, Matthew Foster, and Harry Husted. GDCI Multi-Cylinder Engine for High Fuel Efficiency and Low Emissions. *SAE International Journal of Engines*, 8(2):775–790, 2015.

[32] Mark Sellnau, James Sinnamon, Kevin Hoyer, and Harry Husted. Gasoline Direct Injection Compression Ignition (GDCI) - Diesel-like Efficiency with Low CO2 Emissions. *SAE 2011-01-1386*, 2011.

[33] Mark C Sellnau, James Sinnamon, Kevin Hoyer, and Harry Husted. Full-Time Gasoline Direct-Injection Compression Ignition (GDCI) for High Efficiency and Low NOx and PM. *SAE International Journal of Engines*, 5(2):2012–01–0384, apr 2012.

[34] A.M. Starik, V.E. Kozlov, and N.S. Titova. On the influence of singlet oxygen molecules on the speed of flame propagation in methaneair mixture. *Combustion and Flame*, 157(2):313–327, 2010.

[35] R Stone. *Introduction to Internal Combustion Engines*. Palgrave Macmillan, 2012.

[36] Unknown. Ozone - Scifun, chemical of the week.

[37] Unknown. Ozone - Wikipedia.

[38] Unknown. Ozone Production - Oxidation Technologies LLC.

[39] R Van Basshuysen and F Schäfer. *Internal Combustion Engine Handbook: Basics, Components, Systems, and Perspectives*. R: Society of Automotive Engineers. SAE International, 2004.

[40] Wayne Smith. Principles of ozone generation.

Glossary

CAD	Crank Angle Degrees, 12
CI	Compression Ignition, 1
CR	Compression Ratio, 12
DOHC	Double OverHead Camshaft, 2
ECU	Engine Control Unit, 3
EGR	Exhaust Gas Recirculation, 32
FSN	Filter Smoke Number, 62
GCI	Gasoline Compression Ignition, 2
HCCI	Homogeneous Charge Compression Ignition, 5
IMEP	Indicated Mean Effective Pressure, 13
MFC	Mass Flow Controller, 34
MHRR	Mean Heat Release Rate, 26
NO/O_3 ratio	Ratio between the quantities of NO and O_3, 44
PPCI	Partially Premixed Compression Ignition, 5
RCCI	Reactivity Controlled Compression Ignition, 5
RON	Research Octane Number, 8
SI	Spark Ignition, 1
SOI	Start of Injection, 11
TDC	Top Dead Center, 12
UA	Umbrella angle., 8
VVT	Variable Valve Train, 2

List of Tables

1 *Condizioni operative con singola iniezione.* ix
2 *Condizioni operative con doppia iniezione.* xi
3 *Mappa della strategia di iniezione.* xi

2.1 *Engine Characteristics* 8
2.2 *Operative conditions.* 13
2.3 *Double injection operative conditions.* 17
2.4 *Injection strategy.* 17
2.5 *SOI combinations.* 21
2.6 *SOI combinations* 23

3.1 *Detectable Time Portion with* $T = 20\ °C$. 36
3.2 *Amount of NO injected depending on the* NO/O_3 *ratio.* 44
3.3 *Ozone reactions submechanism.* 47
3.4 *Concentration of ozone and nitric oxide given to the simulation software.* 48
3.5 *Time portion variability with temperature.* 51

4.1 *Characteristics of the ozone generators employed.* 54
4.2 *ozone seeded engine operative conditions* 56
4.3 *Operative conditions of engine at idle speed.* 62

List of Figures

12 *CO2 production.[OICA]* 1
13 *Comparison between cost and efficiency* 1
14 *Distribution of fuels across the world.[Bosch Graphics]* 2

1.1 *Typical emissions from SI engines as a function of the equivalence ratio.* [21] 4
1.2 *Conceptual schematics of conventional CI conbustion.*[7] 5
1.3 *Diagram showing the equivalence ratio-temperature ranges for soot and NO_x formation and the regions for conventional diesel, SI, HCCI, and diesel LTC engines.*[8] 6

2.1 *Peugeot DW 10 and its characteristics.* 8
2.2 *Scheme of the experimental setup.* 9
2.3 *Delphi Diesel Injector.* 9
2.4 *Horiba 7100 exhaust gas analyzer.* 10
2.5 *Fast Acquisition interface.* 10
2.6 *Part of Slow Acquisition interface.* 11
2.7 *Combustion efficiency with a single injection.* 13
2.8 *CA50 with a single injection* 14
2.9 *CA90-CA10 with single injection* 14
2.10 *IMEP with a single injection* 15
2.11 *Indicated efficiency with single injection* 15
2.12 *Max in Cylinder pressure rate with a single injection.* 15
2.13 *CO emissions with a single injection.* 15
2.14 *NOx emissions with a single injection.* 16
2.15 *HC emissions with a single injection.* 16
2.16 *CA50 with double injection.* 18
2.17 *Combustion duration with double injection.* 18
2.18 *Max In Cylinder Pressure.* 18
2.19 *IMEP with double injection.* 19
2.20 *Indicated Efficiency with double injection.* 19
2.21 *Combustion Efficiency.* 19
2.22 *CO emissions with double injection.* 19
2.23 *NOx emissions with double injection.* 20
2.24 *HC emissions with double injection.* 20
2.25 *NOx comparison.* 22
2.26 *CO comparison.* 22
2.27 *HC comparison.* 22

2.28 *HC zoom.* 22
2.29 *Indicated Efficiency Comparison.* 23
2.30 *Single injection mean heat release rate with various SOI.* 24
2.31 *Double injection mean heat release rate with SOI2=5[CAD].* 24
2.32 *Max in cylinder pressure comparison.* 24
2.33 *Indicated efficiency comparison.* 24
2.34 *NOx comparison.* 25
2.35 *HC comparison.* 25
2.36 *CO emissions.* 25
2.37 *In-cylinder pressures and heat release rates as a function of the nitric oxide and ozone concentrations when simultaneously seeding the intake of the engine.[23]* 26

3.1 *Corona discharge cell. [40]* 29
3.2 *UV ozone generator scheme.[38]* 29
3.3 *Rate of product of O_3, O and O_2 species (left axis) and in-cylinder pressure (right axis) as function of CAD. In-cylinder gas temperature is represented at the top axis for 10 ppm of ozone concentration.* 30
3.4 *Steel tube CAD.* 31
3.5 *Ozone injector.* 31
3.6 *Mass Flow Controller.* 32
3.7 *Primary heater.* 32
3.8 *CAD drawing of secondary heater to be placed around the tube.* 32
3.9 *Anseros COM-AD-01 ozone generator.* 33
3.10 *Anseros MP6060 ozone analyzer.* 33
3.11 *Experimental set-up* 34
3.12 *Pipe scheme.* 35
3.13 *Injectors.* 35
3.14 *Comparison between different air flow rates and temperatures,a variation in either leads to a different flow speed.* 36
3.15 *O_3-in oriented towards flow inlet.* 36
3.16 *Ozone concentration O_3-in towards flow outlet at room temperature and atmospheric pressure for various flow rates.* 37
3.17 *Ozone concentration O_3-in flat at room temperature and atmospheric pressure for various flow rates.* 37
3.18 *Ozone concentration O_3-in flat at different temperatures with a 250 Nl/min flow.* 37
3.19 *Ozone concentration O_3-in flat at different temperatures with a 650 Nl/min flow.* 37
3.20 *Solidworks 3D model of ozone injector pipe.* 38
3.21 *Turbulence generators.* 39
3.22 *Turbulence intensity of the flow with a washer as turbulence generator.* 39
3.23 *Definitive configuration of the ozone injector.* 40
3.24 *Tube insulation.* 41
3.25 *Intermediate configuration with nitric oxide addition.* 41
3.26 *Definitive configuration.* 42

3.27 *Ozone concentration with $T = 20\ °C$ and every NO/O_3 ratio tested.* . . 44
3.28 *Ozone concentration with $T = 200\ °C$ and every NO/O_3 ratio tested.* . 45
3.29 *Comparison between ozone concentration with $T = 20\ °C$ and $T = 200\ °C$.* 45
3.30 *Comparison between ozone concentration with different air temperature and NO/O_3 ratio of 0.5 and 0.25* 46
3.31 *Different concentration of ozone when injecting NO.* 48
3.32 *Simulated ozone concentration without nitric oxide adduction, variable temperature.* 49
3.33 *Comparison between simulations at different temperatures: (a) $T = 20\ °C$, (b) $T = 100\ °C$, (c) $T = 150\ °C$, (d) $T = 200\ °C$.* 50
3.34 *Pipe scheme with indication of the time portions.* 51
3.35 *Adduction pipe simulation.* 52
3.36 *Comparison between simulation and experimental data, with $T = 200\ °C$.* 53

4.1 *Labview interface to control ozone production.* 55
4.2 *Scheme of the experimental setup.* 56
4.3 *Tadm vs ozone.* 57
4.4 *Combustion Efficiency vs ozone.* 58
4.5 *Max in Cylinder pressure gradient.* 58
4.6 *Tadm vs Max Mean T cylinder.* 59
4.7 *Comparison between different approaches at the same experiment.* . . . 60
4.8 *HC emissions with ozone seeded intake.* 60
4.9 *NO_x emissions with ozone seeded intake.* 60
4.10 *Max temperature with ozone seeded intake.* 61
4.11 *Influence of ozone on CA50.* 62
4.12 *Influence of ozone on IMEP.* 63
4.13 *Influence of ozone on HC emissions.* 63

5.1 *Ozone generator prototype.* 66